

# LOCAL SCOUR AT STRUCTURES

**Subhasish Dey, *Chair Professor***



Department of Civil Engineering  
Indian Institute of Technology  
Kharagpur, West Bengal  
INDIA

# **LOCAL SCOUR AT STRUCTURES (Part I)**



- *Scour* is a phenomenon of lowering of level of riverbeds by erosive action of flowing stream
- Amount of reduction in level of riverbeds below an assumed natural level is termed as *scour depth*
- *Scour* is classified as *general scour* and *local scour*
- *General scour* occurs as a result of change in characteristics of the river
- *Local scour* develops near structures, due to the modification of flow field as a result of obstruction to the flow

- *General scour* is categorized as *short-term scour* and *long-term scour* based on time taken for scour development
- *Short-term scour* develops during a single or several closely spaced floods. It occurs due to
  - Convergence of flow
  - A shift in channel thalweg or braids within channel
  - Bed-form migration
- *Long-term scour* takes considerably long time, normally several years. It is caused by
  - Natural changes in catchments (channel straightening, volcanic activities, climate change etc)
  - Human activities (channel alterations, streambed mining, dam / reservoir construction, and land-use changes)

- *Local scour* is classified as *clear-water scour* and *live-bed scour*
- *Clear-water scour* occurs when the sediment is removed from the scour hole but not supplied by the approaching stream
  - Equilibrium scour depth is attained when the fluid induced force can no longer dislodge the sediment particles from the scour hole
- *Live-bed scour* occurs when the scour hole is continuously fed with the sediment by the approaching stream
  - Equilibrium scour depth is attained over a period of time, when the rate of removal of sediment out of the scour hole equals the rate of supply of sediment into the scour hole

## Scour within Channel Contractions

- *Channel contraction* is the reduction in the width of waterways by constructing parallel sidewalls
- The reduction in flow area due to channel contraction increases the flow velocity and thereby enhances the bed shear stress
- As a result, the sediment bed within the channel contraction is scoured. Such local scour is called *contraction scour*
- **Straub** (1934) was the pioneer to present a simplified one-dimensional theory
- His theory was extended and modified by **Ashida** (1963), **Laursen** (1963), **Komura** (1966), **Gill** (1981), **Webby** (1984) and **Lim** (1993)
- **Dey and Raikar** (2005, 2006) studied the scour in long contractions in gravel-beds and proposed analytical models for the estimation of scour depth under both clear-water and live-bed scour conditions

- Channel contraction are designated as long or short depending on the ratio of the length of contraction  $L$  to the approaching channel width  $b_1$
- According to **Komura** (1966) and **Dey and Raikar** (2005), a contraction becomes long when  $L/b_1 > 1$ , whereas **Webby** (1984) considered it as  $L/b_1 > 2$
- **Smith** (1967) proposed the angle of upstream and downstream transitions as  $12.5^\circ$  for a smooth transition to the contracted zone
- Figs. 6.1(a) and 6.1(b) show a schematic of channel contraction and photograph of the scoured bed

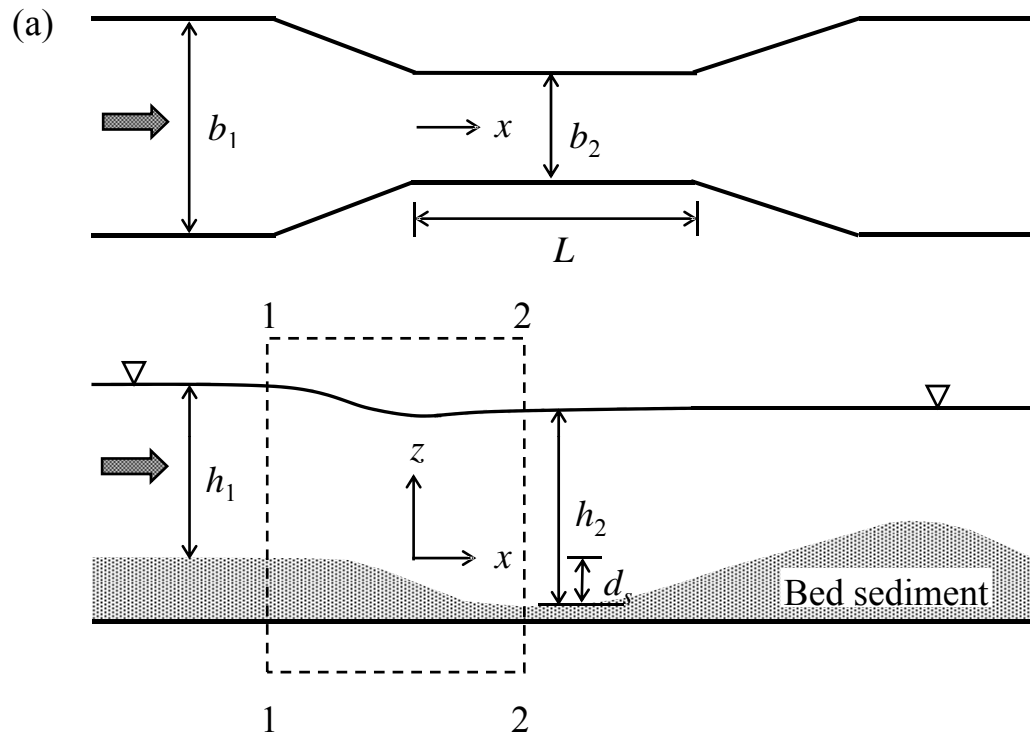


Fig. 6.1 (a) Schematic of rectangular channel contraction at equilibrium scour condition and (b) photograph showing a scoured bed

## ***Flow Field within Scoured Zone of Channel Contraction***

- **Raikar and Dey (2004)** detected the flow field within the scoured zone of channel contractions by an acoustic Doppler velocimeter (ADV)
- The velocity vectors within a channel contraction given in Fig. 6.2 shows the passage of flow within the scour hole

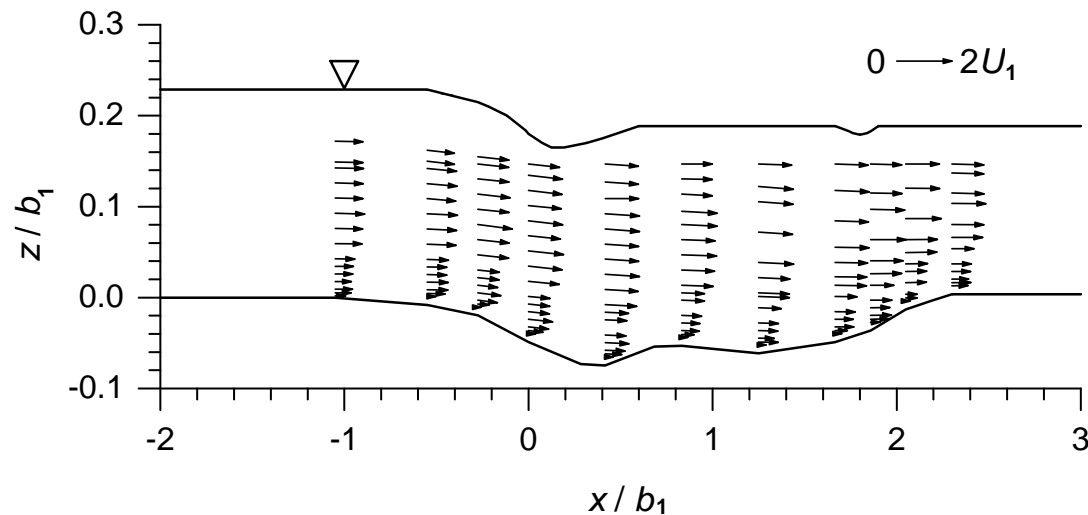


Fig. 6.2 Flow field within scoured zone of a channel contraction at equilibrium

## ***Influence of Various Parameters on Scour Depth***

- Parameters that influence the scour within channel contractions are:
  - Parameters relating to contraction: Channel opening ratio and channel shape
  - Parameters relating to the bed sediment: Median particle size, particle size distribution, angle of repose and cohesiveness
  - Parameters relating to the approaching flow condition: Approaching flow velocity, approaching flow depth, shear velocity and roughness
  - Parameters relating to the fluid: Mass density, viscosity, gravitational acceleration and temperature (may not be important in scour problems)



- Functional relationship showing the influence of various parameters on equilibrium scour depth  $d_s$  in a long rectangular contraction can be given by:

$$d_s = f_1(U_1, h_1, \rho, \rho_s, g, \nu, d_{50}, b_1, b_2, \sigma_g) \quad (6.1)$$

where  $U_1$  = approaching flow velocity;  $h_1$  = approaching flow depth;  $\rho$  = mass density of water;  $\rho_s$  = mass density of sediment;  $g$  = gravitational acceleration;  $\nu$  = kinematic viscosity of water;  $d_{50}$  = median sediment size;  $b_2$  = contracted width of channel; and  $\sigma_g$  = geometric standard deviation of the particle size distribution

- In sediment-water interaction, the parameters  $g$ ,  $\rho$  and  $\rho_s$  are combined into a parameter  $\Delta g$  (**Dey and Debnath 2001; Dey and Raikar 2005**); where  $\Delta = s - 1$ ; and  $s$  = relative density of sediment, that is  $\rho_s/\rho$

- It is reasonable to use the parameter channel opening ratio  $\hat{b}$  ( $= b_2/b_1$ ) to account for the combined effect of  $b_1$  and  $b_2$
- The influence of kinematic viscosity  $\nu$  is insignificant for a turbulent flow over rough beds (**Yalin** 1977)
- Using the Buckingham  $\pi$ -theorem with  $U_1$  and  $b_1$  as repeating variables, Eq. (6.1) can be written as

$$\tilde{d}_s = f_2(\tilde{d}, F_0, \tilde{h}, \hat{b}, \sigma_g) \quad (6.2)$$

where  $\tilde{d}_s = d_s/b_1$ ;  $\tilde{d} = d_{50}/b_1$ ;  $F_0 = U_1/(\Delta g d_{50})^{0.5}$ , that is the densimetric Froude number; and  $\tilde{h} = h_1/b_1$ .

- Figs. 6.3(a) - 6.3(d) show the variation of the nondimensional equilibrium scour depth  $\tilde{d}_s$  with  $\tilde{d}$ ,  $\tilde{h}$ ,  $F_0$  and  $\hat{b}$  for uniform sediments

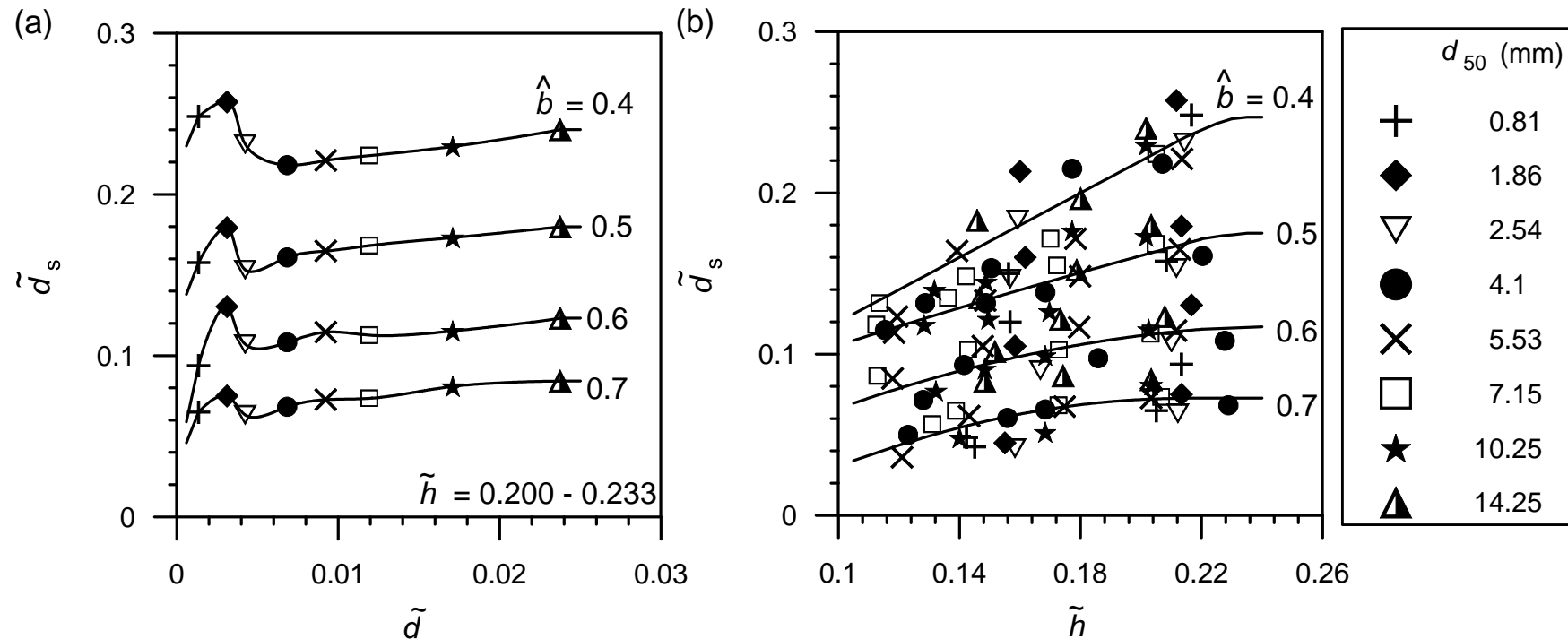


Fig. 6.3 Variations of (a)  $\tilde{d}_s$  with  $\tilde{d}$ ; (b)  $\tilde{d}_s$  with  $\tilde{h}$   
(after **Dey and Raikar 2005**)

- The scour depth increases with an increase in sediment size for gravels [Fig. 6.3(a)]. But the curves of scour depth versus sediment size have considerable sag at the transition of sand and gravel
- The scour depth increases with an increase in approaching flow depth at lower depths, while it becomes independent of approaching flow depth at higher flow depths [Fig. 6.3(b)]

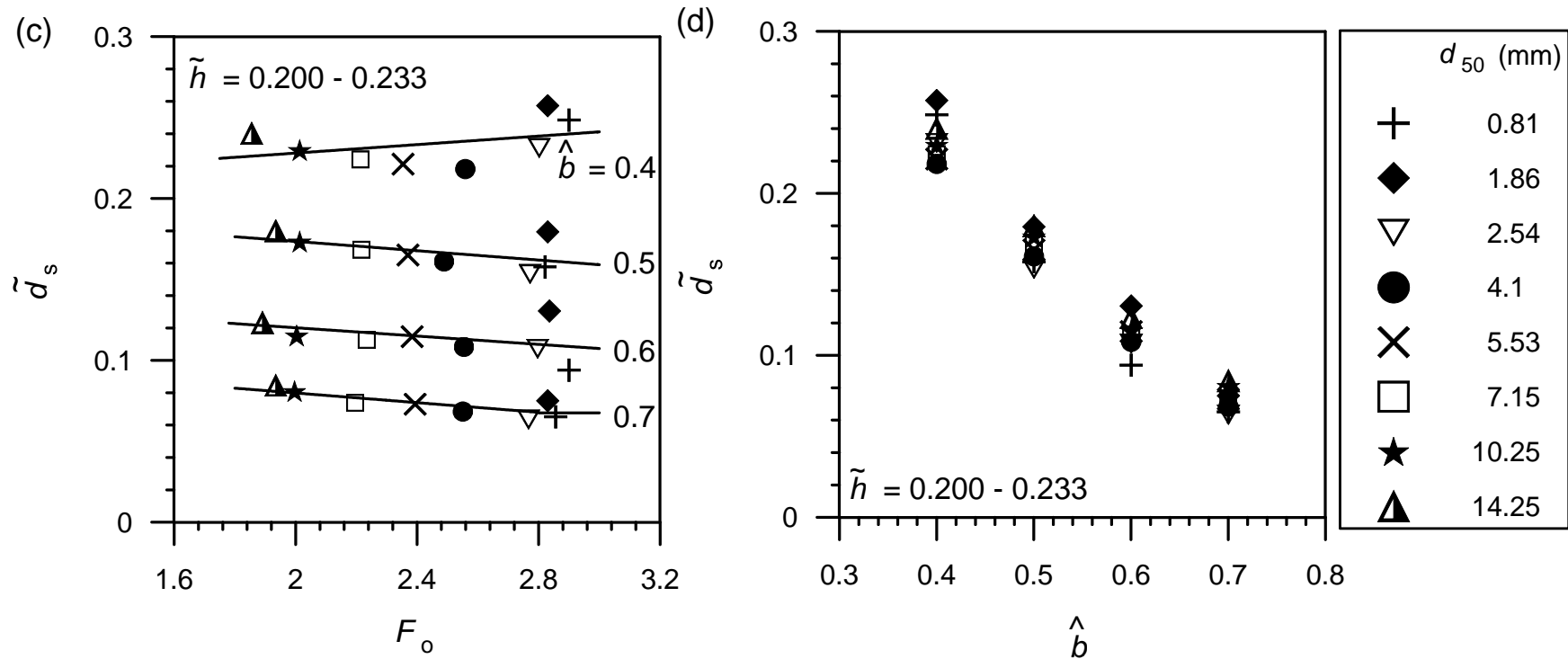


Fig. 6.3 Variations of (c)  $\tilde{d}_s$  with  $F_o$ ; (d)  $\tilde{d}_s$  with  $\hat{b}$   
 (after **Dey and Raikar 2005**)

- The scour depth reduces gradually with an increase in densimetric Froude number for larger opening ratios, whereas the trend is opposite for small opening ratios [Fig. 6.3(c)]
- The scour depth increases with a decrease in channel opening ratio [Fig. 6.3(d)]

- For nonuniform sediments ( $\sigma_g > 1.4$ ), the scour depth is reduced due to the formation of armor-layer in the scour hole
- Equilibrium scour depth  $d_s(\sigma_g)$  in nonuniform sediments can be given as

$$\tilde{d}_s(\sigma_g) = K_\sigma \tilde{d}_s \quad (6.3)$$

where  $K_\sigma$  = coefficient due to sediment gradation, defined as the ratio of equilibrium scour depth in nonuniform sediment to that in uniform sediment

- The variation of  $K_\sigma$  with  $\sigma_g$  is given in Fig. 6.4

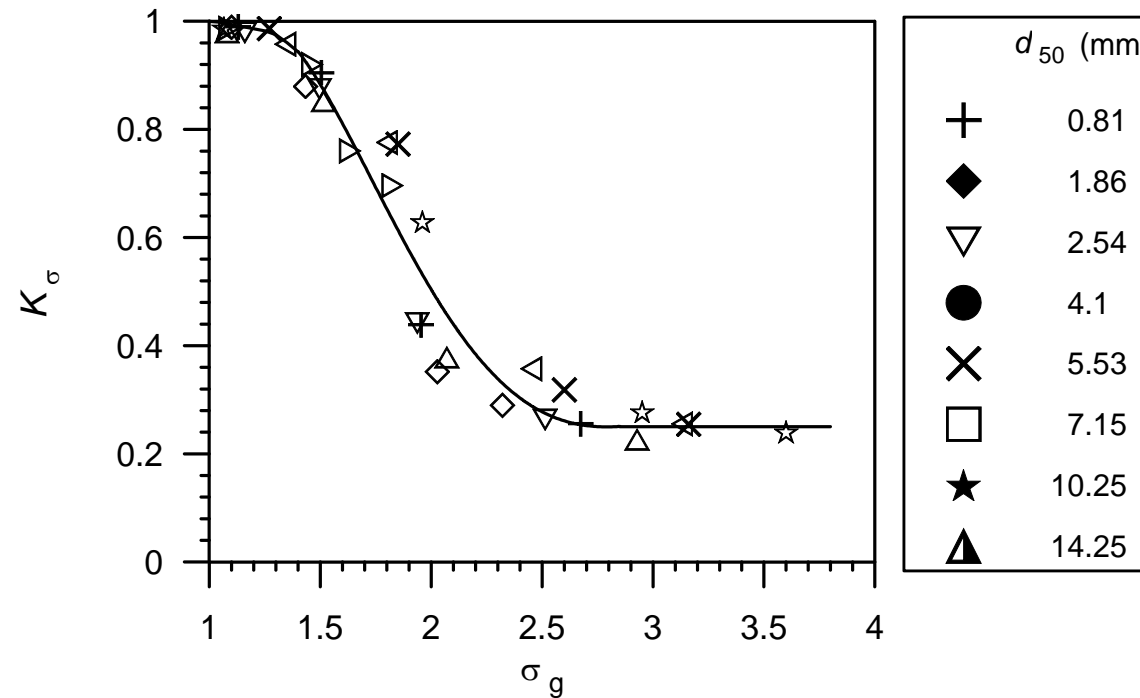


Fig. 6.4 Variations of  $K_\sigma$  as a function of  $\sigma_g$  (after Dey and Raikar 2005)

- The scour depth in nonuniform sediment with  $\sigma_g = 3$  is drastically reduced to 25% of scour depth in uniform sediment
- The reduction of scour depth for  $\sigma_g > 3$  is not influenced by the nonuniformity of sediments

## ***Laursen's Model***

**Laursen** (1963) developed a model for scour depth within a rectangular channel contraction

- The discharge in the channel is given by

$$Q = U_1 h_1 b_1 = U_2 h_2 b_2 \quad (6.4)$$

where  $h_2$  = flow depth in contracted zone; and  $U_2$  = flow velocity in contracted zone

- The scour depth  $d_s$  is given by

$$d_s = (h_2 - h_1) + (1 + K) \left( \frac{U_2^2}{2g} - \frac{U_1^2}{2g} \right) \quad (6.5)$$

where  $K$  = head loss coefficient, defined as

$$K = \frac{2gh_f}{U_2^2 - U_1^2} \quad (6.6)$$

where  $h_f$  = head loss through transition

- Eq. (6.5) can then be written in nondimensional form as

$$\hat{d}_s = \frac{h_2}{h_1} - 1 + \left( \frac{1+K}{2} \right) F_1^2 \left[ \left( \frac{b_1}{b_2} \right)^2 \left( \frac{h_1}{h_2} \right)^2 - 1 \right] \quad (6.7)$$

where  $\hat{d}_s = d_s/h_1$ ; and  $F_1 = U_1^2/gh_1$ , that is the approaching flow Froude number

- When scour depth in contracted zone reaches equilibrium, the bed shear stress becomes equal to tractive force, that is  $\tau_c = 0.628d_{50}$  (in Pa); where  $d_{50}$  in mm
- The bed shear stress, in the uncontracted zone can be estimated using the Manning equation and the Strickler's relationship for  $n$  (= Manning roughness coefficient) as

$$\tau_{01} = \frac{U_1^2 d_{50}^{0.33}}{30h_1^{0.33}} \quad (6.8)$$



- Taking the ratio of shear or tractive force in the contracted and uncontracted zones yields

$$\frac{\tau_{01}}{\tau_c} = \frac{U_1^2}{120d_{50}^{0.67}h_1^{0.33}} \quad (6.9)$$

- Similar expression can also be written for the bed shear stress in the contracted zone.
- The flow depth ratio  $h_2/h_1$  can be obtained as

$$\frac{\tau_{01}}{\tau_{02}} = \left(\frac{U_1}{U_2}\right)^2 \left(\frac{h_2}{h_1}\right)^{1/3} = \frac{\tau_{01}}{\tau_c} \quad (6.10)$$

- Using Eqs. (6.4) and (6.10), one can write

$$\frac{h_2}{h_1} = \left(\frac{\tau_{01}}{\tau_c}\right)^{3/7} \left(\frac{b_1}{b_2}\right)^{6/7} \quad (6.11)$$

- Substituting Eq. (6.11) into Eq. (6.7), results

$$\hat{d}_s = \left( \frac{\tau_{01}}{\tau_c} \right)^{3/7} \left( \frac{b_1}{b_2} \right)^{6/7} - 1 + 1.87(1 + K) \left( \frac{d_{50}}{h_1} \right)^{0.67} \left[ \frac{(b_1/b_2)^{2/7}}{(\tau_{01}/\tau_c)^{6/7}} - 1 \right] \left( \frac{\tau_{01}}{\tau_c} \right) \quad (6.12)$$

- Neglecting the difference in the velocity heads and the loss through the transition, Eq. (6.12) reduces to

$$\hat{d}_s = \left( \frac{\tau_{01}}{\tau_c} \right)^{3/7} \left( \frac{b_1}{b_2} \right)^{6/7} - 1 \quad (6.13)$$

## *Dey and Raikar's Model*

**Dey and Raikar (2005)** proposed an analytical model for clear-water scour within channel contraction

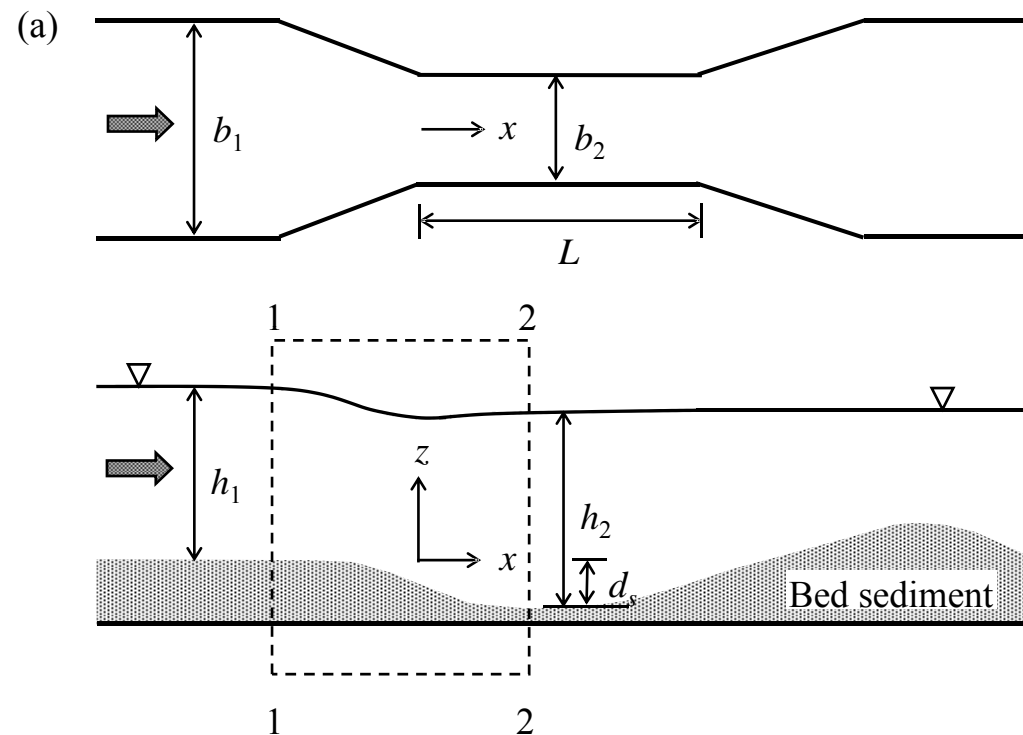


Fig. 6.1 (a) Schematic of rectangular channel contraction at equilibrium scour condition

- Applying the energy equation between sections 1 and 2 for the flow situation at equilibrium scour condition, one obtains

$$h_1 + \frac{U_1^2}{2g} = h_2 + \frac{U_2^2}{2g} - d_s + h_f \quad (6.14)$$

where  $h_f$  = head loss. It is negligible if the contraction is gradual and smooth (**Graf** 2003)

## Clear-Water Scour Model

### Determination of Scour Depth with Sidewall Correction:

- In clear-water scour, the equilibrium scour depth  $d_s$  reaches in a long contraction, when the flow velocity  $U_2$  in the contracted zone becomes equaling critical velocity  $U_c$  for sediments

- The flow velocity  $U_2|_{U_2=U_c}$  in the contracted zone can be determined from the well-known equation of bed shear stress as a function of dynamic pressure. It is

$$U_2|_{U_2=U_c} = u_{*c} \sqrt{\frac{8}{f_b}} \quad (6.15)$$

where  $u_{*c}$  = critical shear velocity for sediment; and  $f_b$  = friction factor associated with the bed

- The Colebrook-White equation used to evaluate  $f_b$  is given as

$$\frac{1}{\sqrt{f_b}} = -0.86 \ln \left( \frac{\varepsilon P_b}{14.8 A_b} + \frac{2.51}{R_b \sqrt{f_b}} \right) \quad (6.16)$$

where  $\varepsilon$  = equivalent roughness height ( $= 2d_{50}$ );  $A_b$  = flow area associated with the bed;  $P_b$  = wetted perimeter associated with the bed ( $= b_2$ ); and  $R_b$  = flow Reynolds number associated with the bed, that is

$$R_b = \frac{4 U_2|_{U_2=U_c} A_b}{\nu P_b}$$

- In the contracted zone, the bed is rough consisting of sediment particles and the sidewalls are smooth
- The friction factor associated with the wall  $f_w$  is considerably different from  $f_b$
- **Vanoni's** (1975) method of sidewall correction is applied for the contracted zone of the channel, as was done by **Dey** (2003a, b)
- The solution for  $f_b$  was obtained from the following equations

$$f_b = 0.316R_b \left( \frac{4U_2|_{U_2=U_c} A}{\nu P_w} - \frac{R_b P_b}{P_w} \right)^{-1.25} \quad (6.17)$$

$$\frac{1}{\sqrt{f_b}} = -0.86 \ln \left( \frac{\varepsilon U_2|_{U_2=U_c}}{3.7 \nu R_b} + \frac{2.51}{R_b \sqrt{f_b}} \right) \quad (6.18)$$

where  $A$  = total flow area of contracted zone ( $= h_2 b_2$ ); and  $P_w$  = wetted perimeter associated with the wall ( $= 2h_2$ )

- In clear-water scour, continuity equation [Eq. (6.4)] becomes

$$U_1 h_1 b_1 = U_2 \Big|_{U_2=U_c} h_2 b_2 \quad (6.19)$$

- For given data of  $U_1$ ,  $h_1$ ,  $b_1$ ,  $b_2$  and  $d_{50}$ , the unknowns  $U_2 \Big|_{U_2=U_c}$ ,  $h_2$ ,  $R_b$  and  $f_b$  can be determined numerically solving Eqs. (6.15) and (6.17) - (6.19)
- Eq. (6.14) is used to determine equilibrium scour depth  $d_s$  given as

$$d_s = h_2 + \frac{U_2 \Big|_{U_2=U_c}^2}{2g} - h_1 - \frac{U_1^2}{2g} \quad (6.20)$$

- Comparison of nondimensional equilibrium scour depths  $\hat{d}_s$  computed from the analysis with the experimental data of clear-water scour is shown in Fig. 6.5(a)

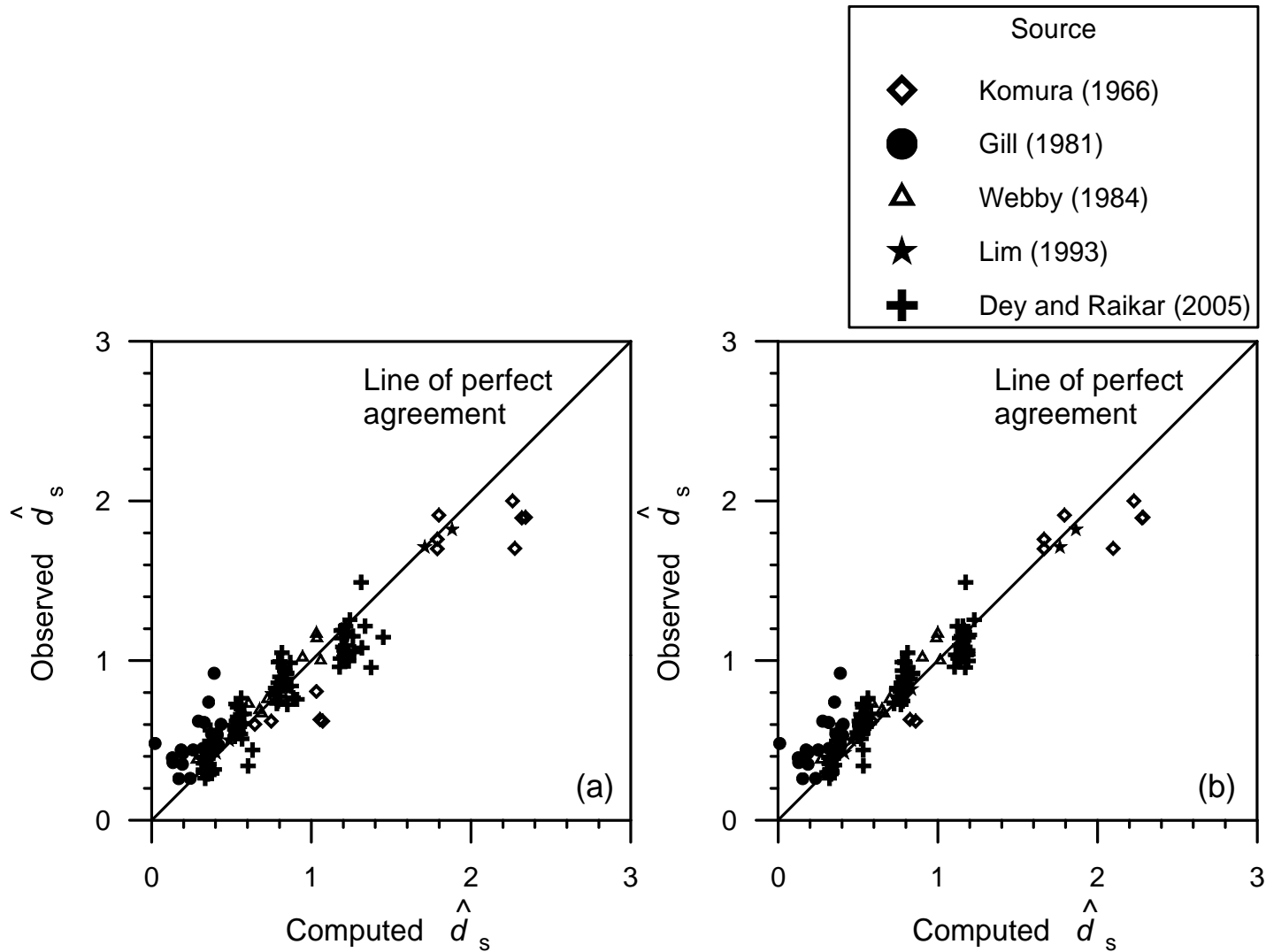


Fig. 6.5 Comparison between the measured and computed scour depths  $\hat{d}_s$  : (a) using clear-water scour model with sidewall correction and (b) using clear-water scour model without sidewall correction (after Dey and Raikar 2005)



### Determination of Scour Depth without Sidewall Correction:

- In this approach, the average flow velocity in the contracted zone  $U_2|_{U_2=U_c}$  for equilibrium scour is determined using the equation of the semi-logarithmic average velocity as

$$\frac{U_2|_{U_2=U_c}}{u_{*c}} = 5.75 \log \frac{h_2}{2d_{50}} + 6 \quad (6.21)$$

- For given data of  $U_1$ ,  $h_1$ ,  $b_1$ ,  $b_2$  and  $d_{50}$ , the unknowns  $U_2|_{U_2=U_c}$  and  $h_2$  can be obtained numerically solving Eqs. (6.19) and (6.21)
- The equilibrium scour depth  $d_s$  is determined from Eq. (6.20)
- Comparison of nondimensional equilibrium scour depths  $\hat{d}_s$  computed from this method with the experimental data of clear-water scour is shown in Fig. 6.5(b)

## Live-Bed Scour Model

**Dey and Raikar** (2006) proposed a live-bed scour model for the estimation of scour depth within channel contraction

- In live-bed scour, the equilibrium scour depth  $d_s$  reaches, when the sediment supplied by the approaching flow into the contracted zone is balanced by the sediment transported out of the contracted zone
- At equilibrium, the sediment continuity equation between sections 1 and 2 of Fig. 6.1(a) is

$$\xi|_{u_* = u_{*1}} b_1 = \xi|_{u_* = u_{*2}} b_2 \quad (6.22)$$

where  $\xi$  = bed-load transport rate of sediment

- Using **Engelund and Fredsøe** (1976) formula for  $\xi$

$$\xi = 1.55 \pi d_{50} u_* \left( 1 - 0.7 \frac{u_{*c}}{u_*} \right) \left[ 1 + \left( \frac{0.085 \pi \Delta g d_{50}}{u_*^2 - u_{*c}^2} \right)^4 \right]^{0.25} \quad (6.23)$$

- Assuming the semi-logarithmic average velocity for approaching flow, the shear velocity  $u_{*1}$  at section 1 is obtained as

$$u_{*1} = U_1 \left( 5.75 \log \frac{h_1}{2d_{50}} + 6 \right)^{-1} \quad (6.24)$$

- Incorporating semi-logarithmic average velocity in Eq. (6.4), yields

$$\frac{b_1}{b_2} \cdot \frac{h_1}{h_2} = \frac{u_{*2}}{U_1} \left( 5.75 \log \frac{h_2}{2d_{50}} + 6 \right) \quad (6.25)$$

where  $u_{*2}$  = shear velocity in the contracted zone

- For given data of  $U_1$ ,  $h_1$ ,  $b_1$ ,  $b_2$  and  $d_{50}$ , the unknowns  $U_2$  and  $h_2$  can be determined numerically solving Eqs. (6.22), (6.23) and (6.25)
- Eq. (6.14) is used to determine equilibrium scour depth  $d_s$  given as

$$d_s = h_2 + \frac{U_2^2}{2g} - h_1 - \frac{U_1^2}{2g} \quad (6.26)$$

- Comparison of nondimensional equilibrium scour depths  $\hat{d}_s$  computed using the model with the live-bed scour data is shown in Fig. 6.6

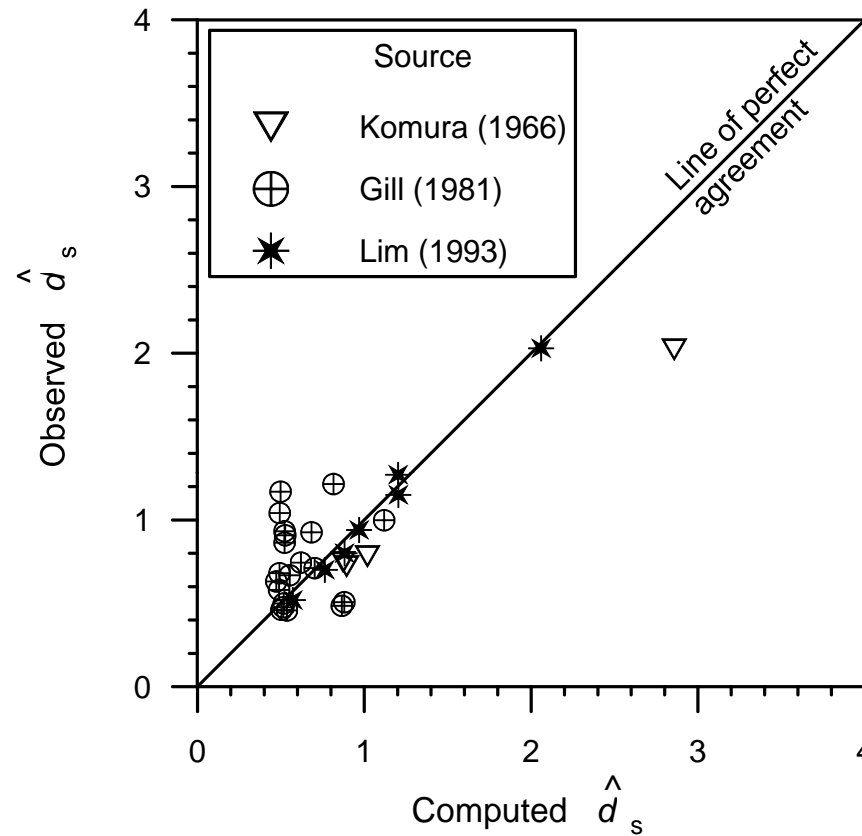


Fig. 6.6 Comparison between the equilibrium scour depths  $\hat{d}_s$  computed using live-bed scour model and the experimental data (after **Dey and Raikar 2006**)

- In case of live-bed scour, the equilibrium scour depth fluctuates due to the passage of bed-forms over a period of time
- The present analysis does not take into account the bed-forms, the resulting equilibrium scour depth is the mean value of the instantaneous equilibrium scour depths over a period of time

## ***Comparative Study of Different Predictors of Scour Depth***

- From the laboratory experimental studies, a number of analytical and empirical equations (Table 1) have been developed to estimate the maximum equilibrium scour depth (that is design scour depth) both under clear-water and live-bed scour conditions
- In general, these equations are based on a limited range of data

Table 1. Equations of Maximum Equilibrium Scour Depth within Channel Contractions Proposed by Different Investigators

Investigator	Proposed equation	Regime
<b>Laursen (1963)</b>	$\hat{d}_{sm} = \hat{b}^{-0.857} - 1$	Clear-water
<b>Komura (1966)</b>	$\hat{d}_{sm} = 1.6F_{rc}^{0.2}\hat{b}^{-0.67}\sigma_g^{-0.5} - 1$ where $F_{rc} = U_1 _{U_1=U_c}/(gh_1)^{0.5}$	Clear-water
	$\hat{d}_{sm} = 1.22F_{rc}^{0.2}\hat{b}^{-0.67}\sigma_g^{-0.2} - 1$	Live-bed
<b>Gill (1981)</b>	$\hat{d}_{sm} = 1.58\hat{b}^{-0.857} - 1$	Clear-water and live-bed
<b>Lim (1993)</b>	$\hat{d}_{sm} = 1.854F_0^{0.75}\hat{b}^{-0.75}\hat{d}^{0.25} - 1$	Clear-water and live-bed
<b>Dey and Raikar (2005)</b>	$\hat{d}_{sm} = 0.368F_{1ec}^{0.55}\hat{d}^{-0.19}\hat{b}^{-1.26}$ where $F_{1ec} = U_{1ec}/(\Delta gh_1)^{0.5}$ ; and $U_{1ec}$ = excess critical approaching flow velocity	Clear-water

Note: In order to get maximum  $\hat{d}_{sm}$ , equations of  $\hat{d}_{sm}$  are expressed for  $U_1/U_c \rightarrow 1$  or  $u_{*1}/u_{*c} \rightarrow 1$ . For uniform sediments,  $\sigma_g$  is considered to be unity

## Predictors under Clear-Water Scour Condition

- The comparisons between the observed scour depths and computed scour depths using different existing equations (Table 1) for clear-water scour are shown in Fig. 6.7
- **Laursen** (1963) equation underestimates observed scour depths to some extent being not safe for the design purpose, as a large number of data lie above the line of perfect agreement
- The equation of **Gill** (1981) is very conservative (uneconomical), as all the scour data lie well below the line of perfect agreement (maximum 6 times the observed data)
- The equations recommended by **Komura** (1966), **Lim** (1993) and **Dey and Raikar** (2005) provide a reasonable estimation of scour depth in long contractions, as they envelop almost all data and over predict less than **Gill's** (1981) equation



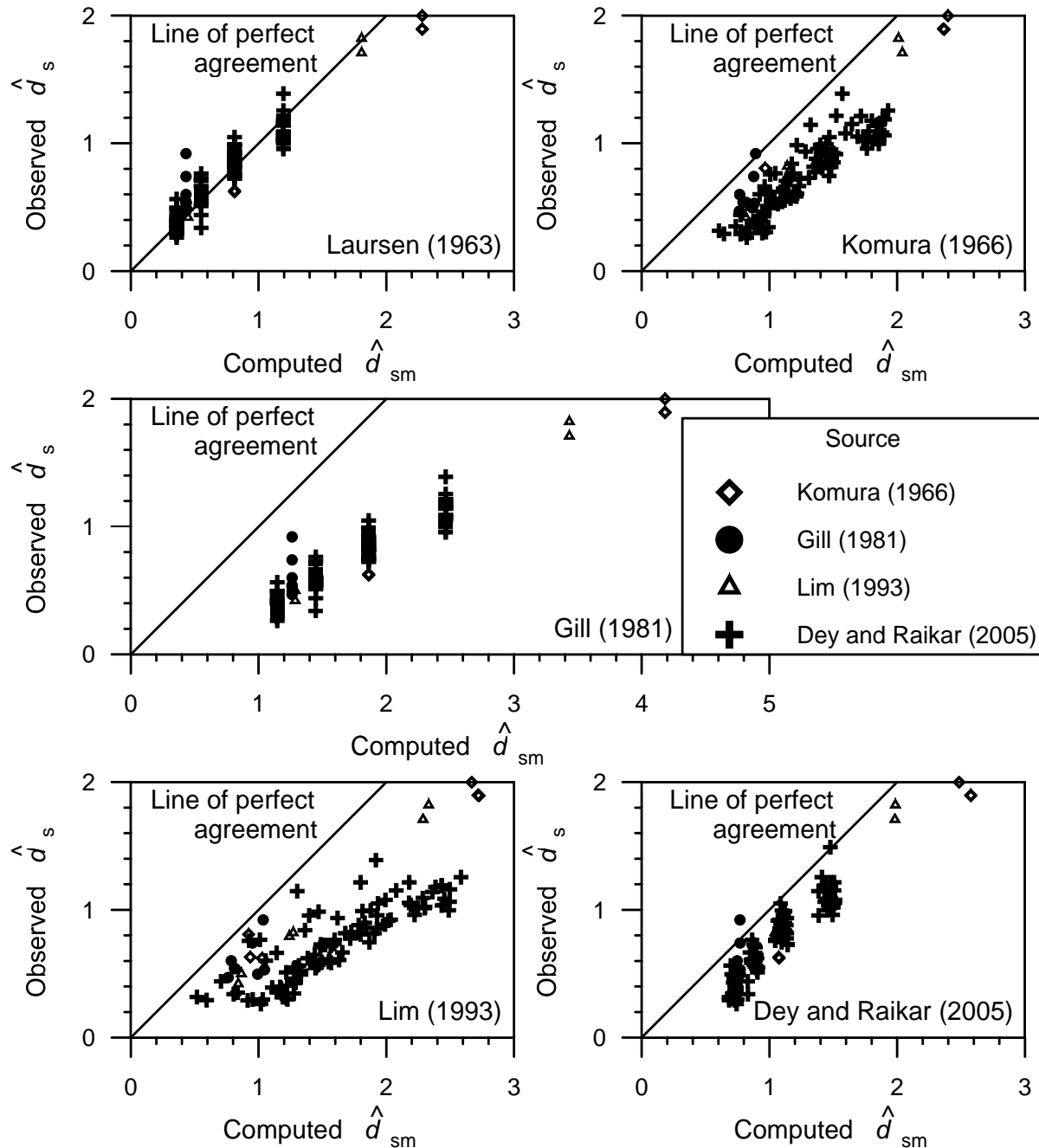


Fig. 6.7 Comparisons of the equations of maximum equilibrium scour depth  $\hat{d}_{sm}$  proposed by different investigators with the experimental data for clear-water scour

## Predictors under Live-Bed Scour Condition

- The comparisons between the observed scour depths and the computed scour depths using different existing equations (Table 1) for live-bed scour are shown in Fig. 6.8
- Equation proposed by **Komura** (1966) underestimates observed scour depths and is unsafe for the design purpose, because almost all data lie above the line of perfect agreement
- **Gill's** (1981) equation is uneconomical, as all the scour data lie well below the line of perfect agreement
- The equation recommended by **Lim** (1993) provides a satisfactory estimation of scour depth in long contractions, as most of data lie along the line of perfect agreement

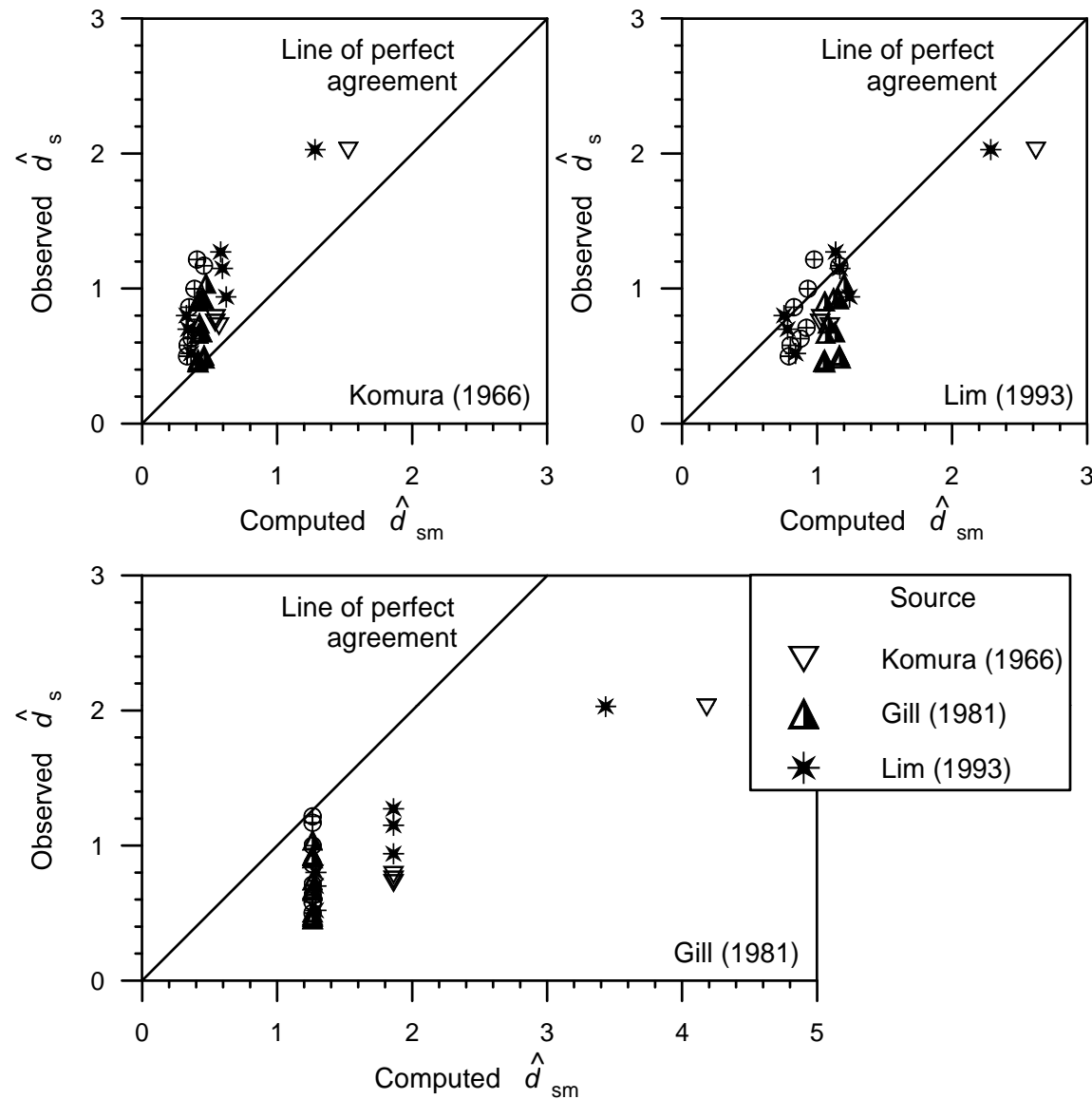


Fig. 6.7 Comparisons of the equations of maximum equilibrium scour depth  $\hat{d}_{sm}$  proposed by different investigators with the experimental data for clear-water scour

## Example

- Estimate the maximum equilibrium scour depth within a long contraction for the following data:
  - Approaching channel width,  $b_1 = 70$  m
  - Channel width at contracted zone,  $b_2 = 46$  m
  - Median size of sediment,  $d_{50} = 2.6$  mm
  - Geometric standard deviation of sediment,  $\sigma_g = 2.84$
  - Approaching flow depth,  $h_1 = 1.8$  m
  - Approaching flow velocity,  $U_1 = 1.76$  m/s

- For  $d_{50} = 2.6$  mm, the critical shear velocity  $u_{*c}$  is calculated from Eq. (2.30a) – (2.30e) as 0.0429 m/s
- From Eq. (6.21) replacing  $U_2|_{U_2=U_c}$  by  $U_1|_{U_1=U_c}$  and  $h_2$  by  $h_1$ , the average critical flow velocity  $U_1|_{U_1=U_c}$  corresponding to  $h_1 = 1.8$  m is obtained as 0.884 m/s. Hence, with  $U_{1ec}$  as  $U_1 - U_1|_{U_1=U_c}$ ,  $F_{1ec} = U_{1ec}/(\Delta gh_1)^{0.5} = 0.164$
- Using  $\hat{b} = b_2/b_1 = 0.657$  and  $\hat{d} = d_{50}/h_1 = 0.00144$  in **Dey and Raikar's** (2005) equation given in Table 1, the value of  $\hat{d}_{sm}$  is 0.8
- Therefore, the maximum equilibrium scour depth  $d_{sm}$  for uniform sediment is 1.44 m
- For nonuniform sediment, with  $\sigma_g = 2.84$  for which  $K_\sigma = 0.31$  (obtained from Fig. 6.4), the maximum equilibrium scour depth  $d_{sm}$  is estimated as 0.447 m

## Scour Downstream of a Structure

- The flow discharge in channels and rivers are regulated by hydraulic structures
  - Examples: weirs, stilling basins, diversion work and sills, dams
  - Uses: flood control, power generation, etc.
- The water released from these structures impinges on the free surface of the tailwater as a jet called *plunging jet*
- The freely falling jet may have considerable potential to scour the downstream bed of the structures and such scour is known as *jet scour*
- Jet scour develops very rapidly, which causes danger to the stability of the channel bed and damage to the hydraulic structures
- Fig. 6.9 shows various hydraulic structures, which come under the group of this study

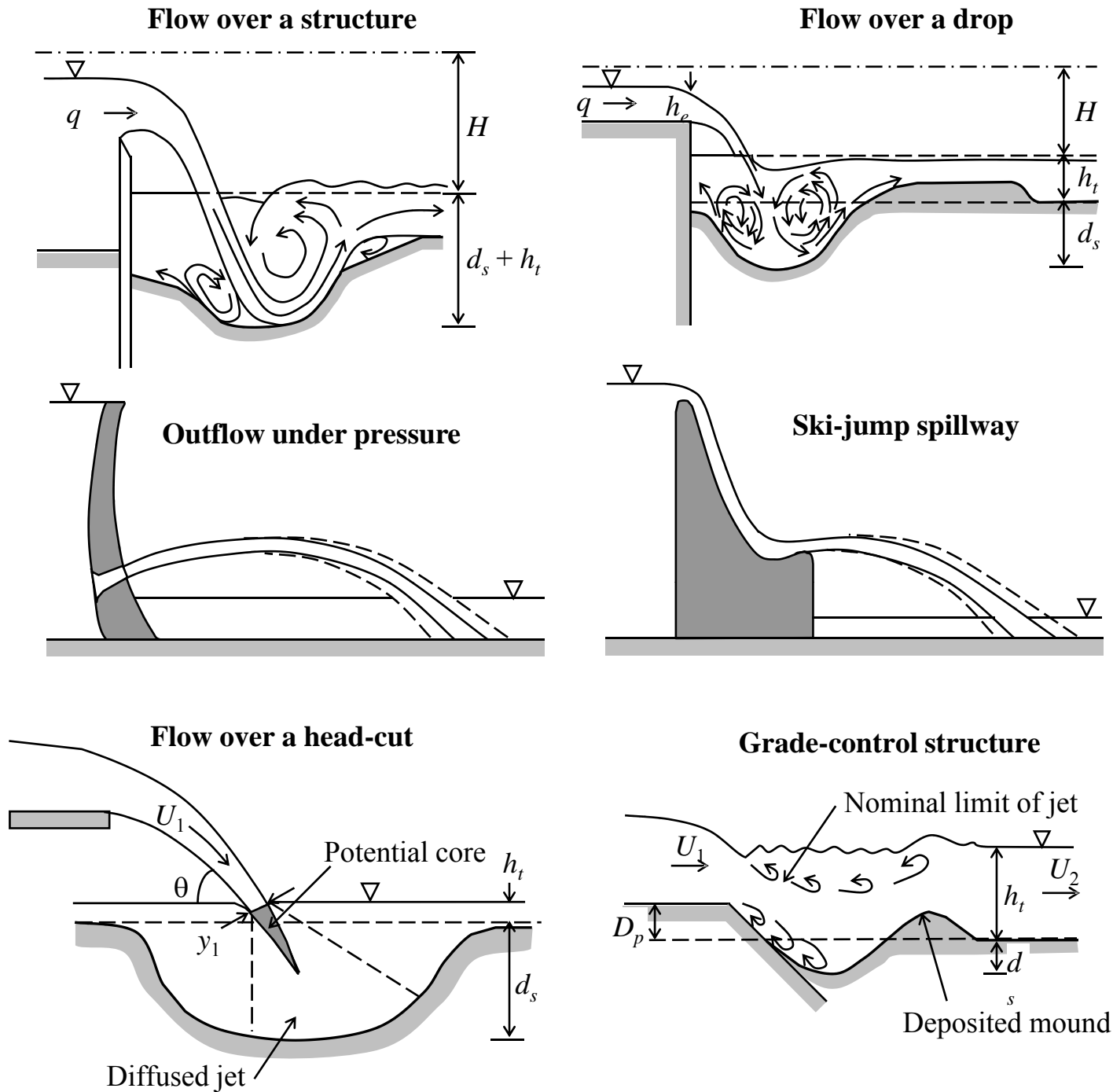


Fig. 6.9 Schematic of flow over different hydraulic structures

- **Schoklitsch** (1932) was the pioneer to study such type of scour
- He proposed an empirical relationship for the scour depth as

$$d_s = \frac{4.75q^{0.57} H^{0.2}}{d_{90}^{0.32}} - h_t \quad (6.27)$$

where  $q$  = discharge per unit width;  $H$  = height between upstream and downstream water levels;  $d_{90}$  = 90% finer sediment; and  $h_t$  = tailwater depth

- **Kotoulas** (1967) developed a relationship for the equilibrium scour depth downstream of a structure, based on the dimensional analysis and using experimental data as

$$d_s = \frac{1.9}{g^{0.35}} \left( \frac{H^{0.35} q^{0.7}}{d_{95}^{0.4}} \right) - h_t \quad (6.28)$$

where  $d_{95}$  = 95% finer sediment



- **Bormann and Julien** (1991) put forward an expression for the scour downstream of grade-control structures based on two-dimensional jet diffusion and particle stability as

$$d_s = \frac{k_b q^{0.6} U_1 \sin \theta}{(2\Delta g)^{0.8} d_{90}^{0.4}} - D_p \quad (6.29)$$

where  $k_b$  = coefficient =  $3.24[\sin\varphi/\sin(\varphi + \theta)]^{0.8}$ ;  $U_1 = (2gH)^{0.5}$ , that is the jet velocity entering tailwater;  $D_p$  = drop height of grade-control structure;  $\theta$  = jet angle near surface; and  $\varphi$  = angle of repose of bed sediment

- **Fahlbusch** (1994) derived the relationship to predict the equilibrium scour depth downstream of a dam as

$$d_s = \frac{20}{\lambda} \sqrt{\frac{qU_1 \sin \theta}{g}} - h_t \quad (6.30)$$

where  $\lambda$  = scour factor that depends on  $d_{90}$ , obtained from Fig. (6.10)

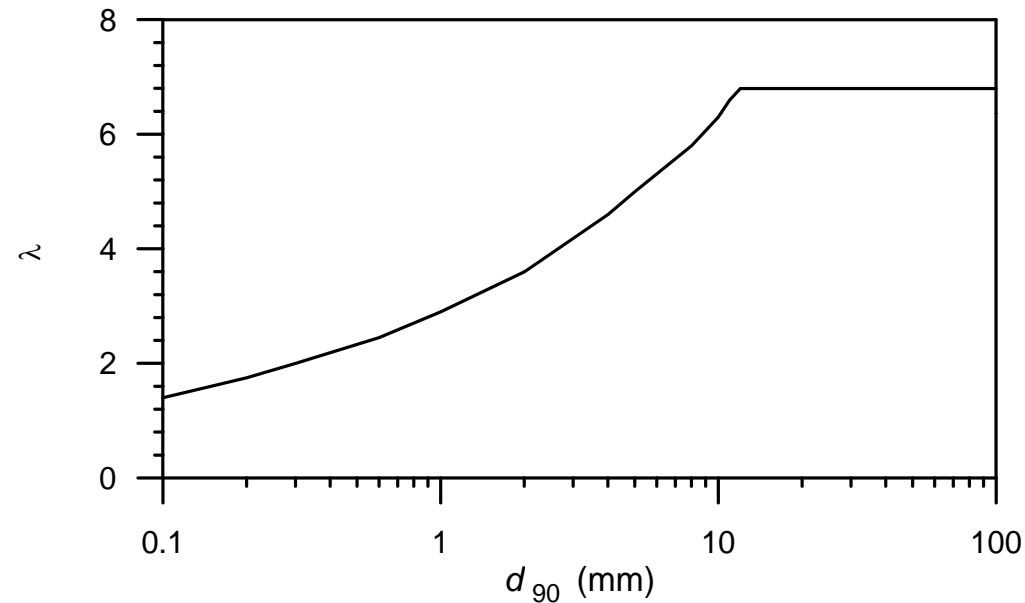


Fig. 6.10 Scour factor  $\lambda$  as a function of  $d_{90}$  (after **Fahlbusch** 1994)

- **Stein et al.** (1993) developed an analytical equation to predict the equilibrium scour depth downstream of a head-cut. It is

$$d_s = \frac{C_d^2 C_f \rho U_1^2 y_1}{\tau_c} \sin \theta \quad (6.31)$$

where  $C_d$  = diffusion coefficient;  $C_f$  = friction coefficient;  $y_1$  = initial jet thickness; and  $\tau_c$  = critical shear stress of bed sediment

- Out of these equations, the scour depth relationship proposed by **Schoklitsch** (1932) yields excellent results (**Hoffmans and Verheij** 1997)

## ***Scour Downstream of Two-Dimensional Culverts***

- Two-dimensional culverts refer to jet flow under hydraulic structures having considerable width
  - Examples: free jets, submerged jets
- Two-dimensional jets can even be vertical or inclined
- Fig. 6.11 depicts different types of horizontal jets

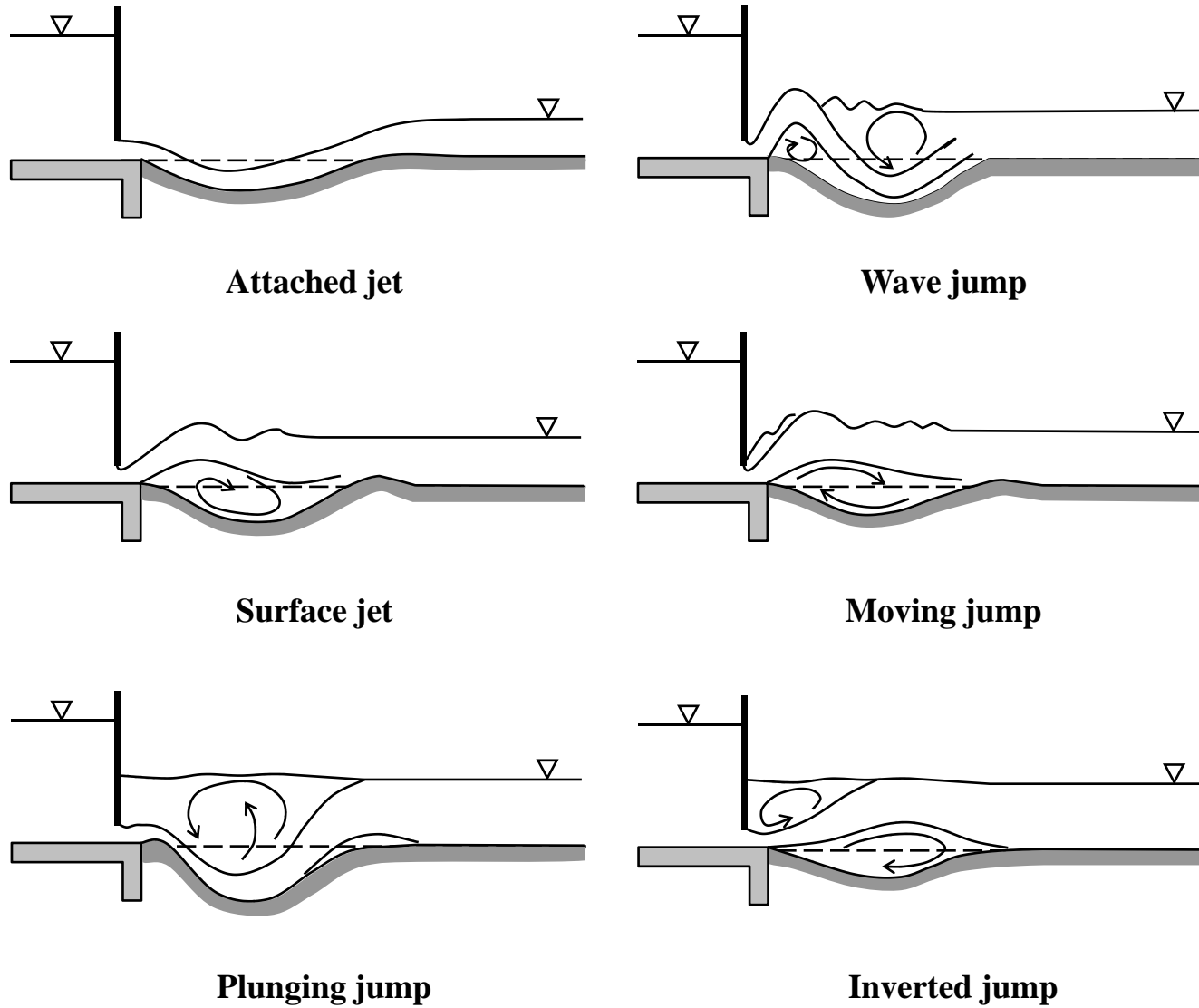


Fig. 6.11 Two-dimensional horizontal jets

- The flow through circular, square and other shaped outlets is considered as three-dimensional culvert flow, as the scour hole developed downstream of these culverts is three-dimensional
- These culverts are designed as cross-drains across the roadway embankments
- These outlets discharge water where the tailwater depth is usually less than the diameter or the width of the outlet
- Sometimes, three-dimensional scour pattern also occur in which the tailwater depth is relatively high
- In case of larger tailwater depths, a submerged hydraulic jump is formed and the turbulence is very high resulting in severe scouring than unsubmerged jet scour

- **Rajarithnam and Berry (1977)** proposed a relationship for the equilibrium scour depth downstream of a circular culvert under submerged condition as

$$d_s = 0.4D(F_0 - 2) \qquad 2 < F_0 < 14 \qquad (6.32)$$

where  $D$  = pipe diameter of circular culvert;  $F_0 = U_1/(\Delta g d_{50})^{0.5}$ , that is the densimetric Froude number; and  $U_1$  = jet velocity

- **Ruff et al. (1982)** put forward the expression for the scour depth downstream of circular culvert. It is

$$d_s = 2.07D(Q/\sqrt{gD^5})^{0.45} \qquad (6.33)$$

where  $Q$  = discharge through the culvert

- **Breusers and Raudkivi (1991)** obtained the relationship for the scour depth downstream of a circular culvert, using the assumption that the maximum flow velocity in the jet never exceeds the critical flow velocity as

$$d_s = 0.08DU_1 / u_{*c} \quad (6.34)$$

where  $u_{*c}$  = critical shear velocity for bed sediment

- **Hoffmans (1997)** developed a simple equation for the estimation of maximum scour depth based on the momentum principle as

$$d_s = \frac{7}{\lambda} \left[ \frac{Q(U_1 - U_2)}{g} \right]^{1/3} \quad (6.35)$$

- Eqs. (6.32) – (6.35) can only be used for the initial approximation of the magnitude of the equilibrium scour depth
- The actual scour depths are to be determined by physical model studies



## Scour Downstream of an Apron due to Submerged Jets

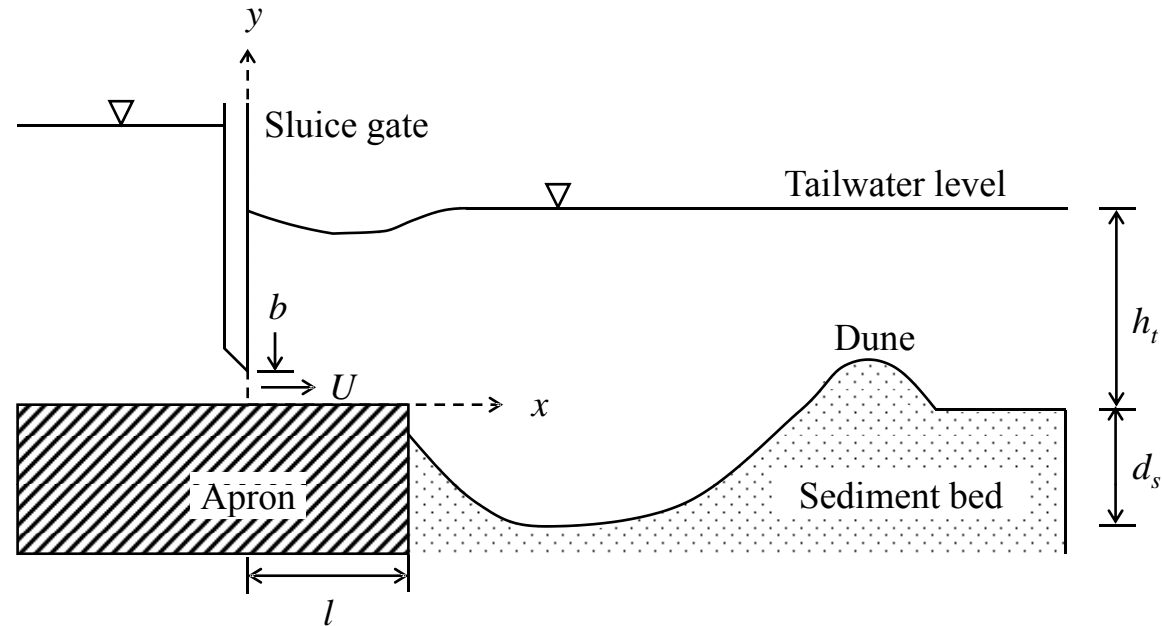


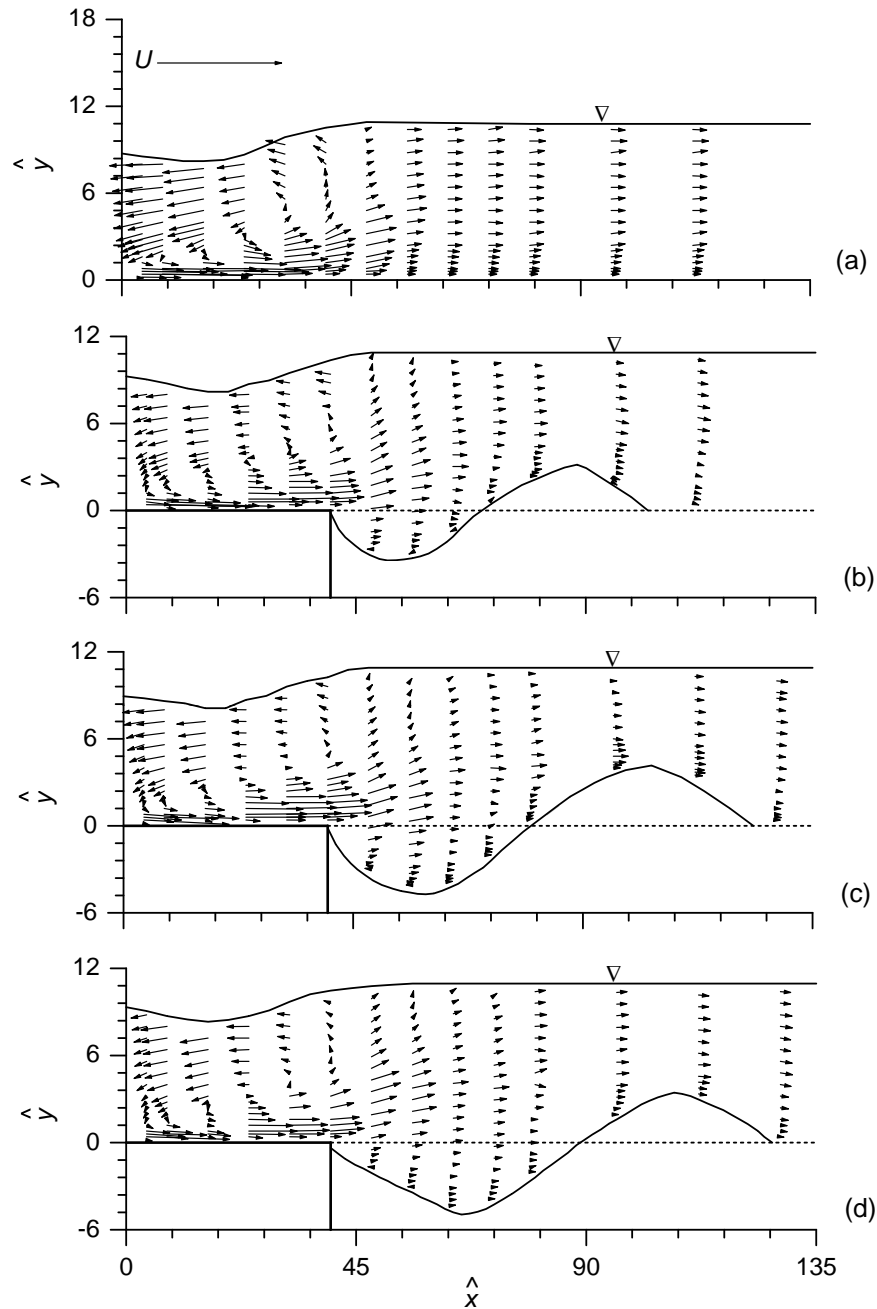
Fig. 6.12 Schematic of scour hole downstream of an apron due to submerged jet

- Scour downstream of an apron is complex in nature owing to the abrupt change of the flow characteristics on the sediment bed with time
- Scour initiates at the downstream edge of the apron when the bed shear stress exerted by the submerged jet exceeds the critical bed shear stress for the bed sediments
- The evolution of the vertical dimension of scour hole is faster than the longitudinal one
- In the initial stage, the suspension of sediments is the only means of sediment transport
- With the development of the vertical dimension of scour hole, the mode of sediment transport changes to a combination of suspended- and bed-loads

- As the flow separation takes place at the edge of the apron having a reattachment of flow at the deepest point of the scour hole, the movement of the sediment particles is divided into two parts
  - Some part of sediments moves along the downstream slope of the scour hole and ultimately goes out of the scour hole
  - The other part is moved back towards the upstream along the upstream slope of the scour hole by the reversed flow
- The down-slope sliding and rolling movement of sediments takes place when the reversed flow becomes feeble with the development of scour hole
- The upstream portion of the scour hole achieves a steep slope

## *Flow Field in Developing Scour Hole*

- Figs. 6.13(a) - 6.13(d) represent the normalized velocity vectors in submerged jets over the initial flat sediment bed, intermediate scour holes and equilibrium scour hole downstream of an apron [see **Sarkar** (2005)] in  $\hat{x}\hat{y}$  -plane; where  $\hat{x}$  is  $x/b$ ;  $\hat{y}$  is  $y/b$ ; and  $b$  is the sluice opening
- The magnitude and the direction of velocity vectors are  $(\hat{u}^2 + \hat{v}^2)^{0.5}$  and  $\arctan(\hat{v}/\hat{u})$ , respectively, where  $\hat{u}$  is  $u/U$ ; and  $\hat{v}$  is  $v/U$ ; and  $U$  is the issuing jet velocity



(a) (b) (c) (d)

Fig. 6.13 Normalized velocity vectors for (a) flat bed condition; (b) intermediate scour hole with  $0.3d_{se}$ ; (c) intermediate scour hole with  $0.8d_{se}$  and (d) equilibrium scour depth with  $d_{se} = 0.062$  m

- Figs. 6.13(a) – 6.13(d) illustrate the characteristics of the decay of jet including a vortical flow in the fully developed zone over the apron and the sediment beds (initial flat bed, intermediate scour holes and equilibrium scour hole)
- The growth rate of the boundary layer over the apron is slower than that over the scoured bed due to an increase in flow depth within the scour hole
- To be more explicit, the growth rate of the boundary layer within an intermediate scour hole is less than that within equilibrium scour hole
- Consequently, the rate of decay of the submerged jets is higher within the scour hole in general and with increased scour hole dimensions in particular

- The reversal nature of the velocity indicates a strong vortical flow (that is the surface roller)
- The submerged jet travels above the original bed level in the scoured zone and is attenuating in nature
- On the other hand, below the original bed level in the scoured zone, the jet velocities diminish with an increase in scour hole dimension

## Effects of Different Parameters on Scour Depth

- Fig. 6.14 shows the variation of nondimensional equilibrium scour depth  $\tilde{d}_{se}$  ( $= d_{se}/b$ ) with sediment size - sluice opening ratio  $\tilde{d}$  ( $= d_{50}/b$ ) for different apron lengths  $l$  and jet Froude numbers  $F_u$  [ $= U/(gb)^{0.5}$ ]

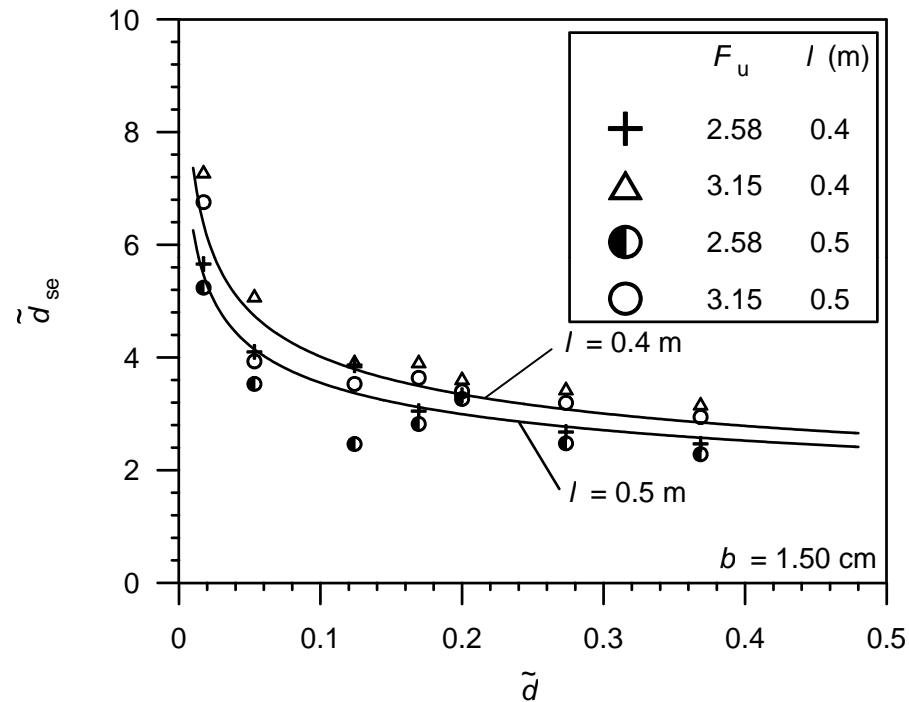


Fig. 6.14 Variation of  $\tilde{d}_{se}$  with  $\tilde{d}$  for different  $l$  and  $F_u$  (after **Dey and Sarkar 2006**)



- The equilibrium scour depth  $\tilde{d}_{se}$  decreases with an increase in  $\tilde{d}$  which implies that  $d_{se}$  is less for relatively coarse sediment
- With the development of scour hole, the bed shear stress acting on the scour hole reduces
- For coarser sediments, which need relatively more critical bed shear stress to initiate motion, the equilibrium scour reaches at a lesser scour depth  $d_{se}$
- $\tilde{d}_{se}$  decreases sharply for  $\tilde{d} < 0.1$ , and then, the rate of reduction of  $\tilde{d}_{se}$  falls down, becoming independent of  $\tilde{d}$  for  $\tilde{d} > 0.3$
- $\tilde{d}_{se}$  increases with a decrease in  $l$
- The submerged jet loses its erosive power through the decaying process over the apron before encountering the sediment bed
- A reduction of  $l$  increases the erosive power of the jet, which exerts greater bed shear stress over the sediment bed resulting in an increase of  $d_{se}$

- Fig. 6.15 shows the dependency of  $\tilde{d}_{se}$  on densimetric Froude number  $F_0$  for different  $l$  and  $d_{50}$

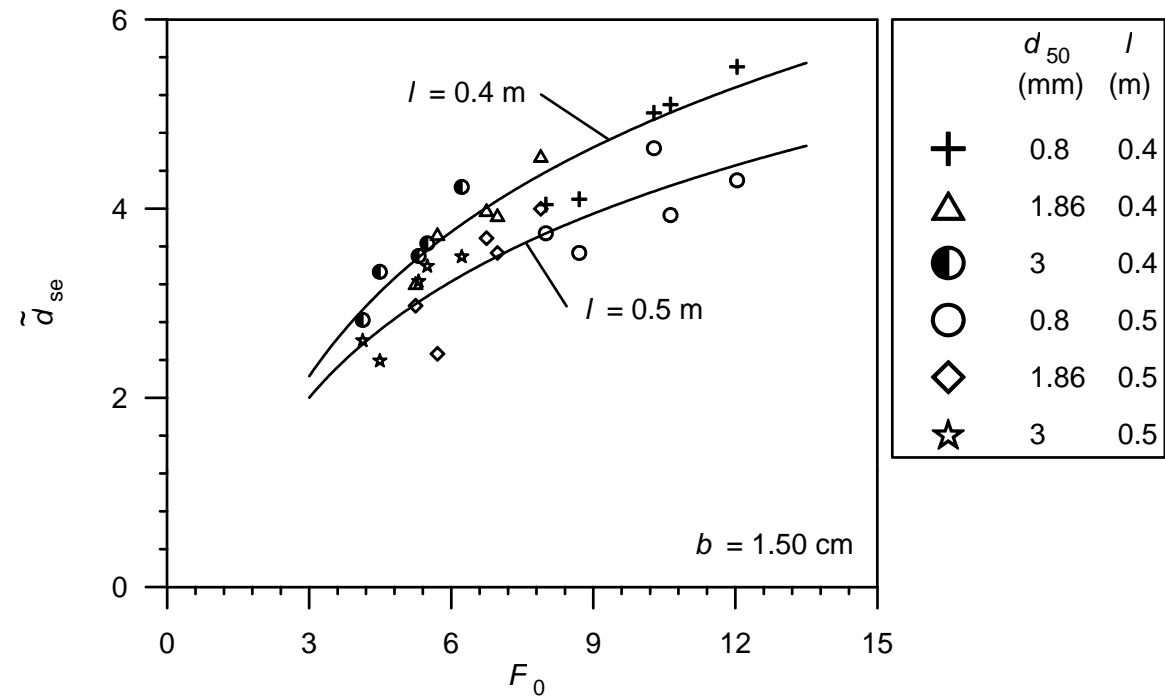


Fig. 6.15 Variation of  $\tilde{d}_{se}$  with  $F_0$  for different  $l$  and  $d_{50}$  (after **Dey and Sarkar 2006**)

- $\tilde{d}_{se}$  increases with an increase in  $F_0$
- As  $F_0 \sim U$  and  $F_0 \sim d_{50}^{-0.5}$ ,  $\tilde{d}_{se}$  increases with an increase in  $U$  and with a decrease in  $d_{50}$
- Rate of increase of  $\tilde{d}_{se}$  is more for lower  $F_0$ , whereas for higher  $F_0$  ( $F_0 > 12$ ), it drops down becoming almost independent of  $F$
- Also, for a given  $F_0$ ,  $\tilde{d}_{se}$  decreases with an increase in  $l$

- Fig. 6.16 depicts  $\tilde{d}_{se}$  as a function of tailwater depth - sluice opening ratio  $\tilde{h}$  ( $= h/l$ ) for different  $l$  and  $F_0$

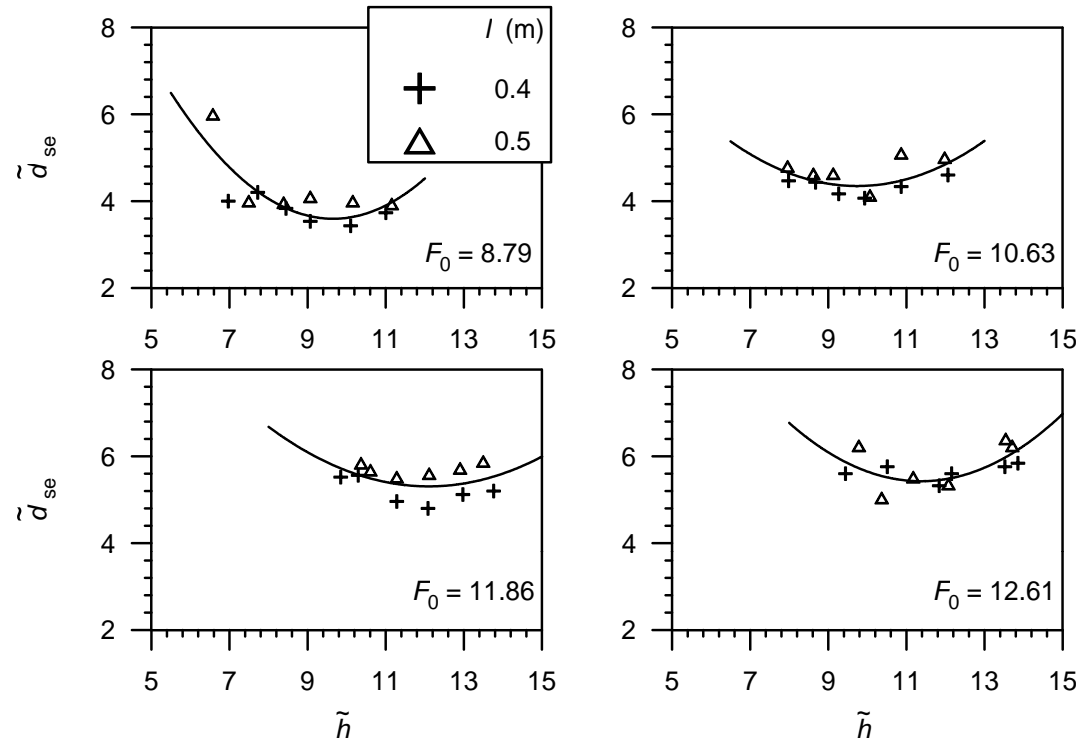


Fig. 6.16 Variation of  $\tilde{d}_{se}$  with  $\tilde{h}$  for different  $l$  and  $F_0$  (after **Dey and Sarkar 2006**)

- Variation of  $\tilde{d}_{se}$  with  $\tilde{h}$  is sagging in nature
- A critical value of tailwater depth exists corresponding to a minimum value of  $\tilde{d}_{se}$

- Fig. 6.17 shows the variation of coefficient  $K_\sigma$  with geometric standard deviation of particle size distribution  $\sigma_g$  for well-graded nonuniform sediments

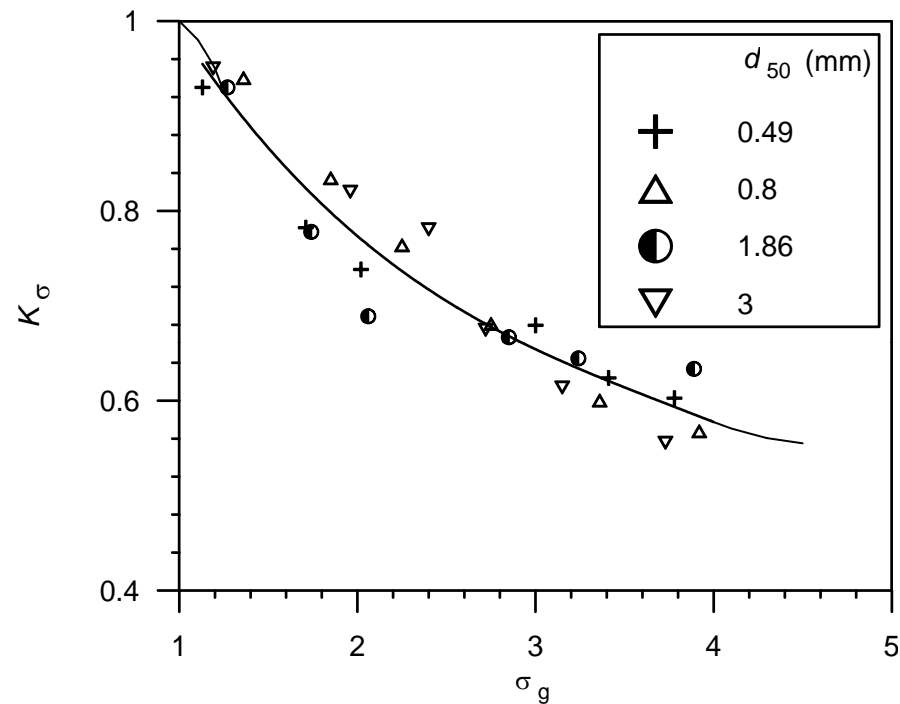


Fig. 6.17 Coefficient  $K_\sigma$  as a function of  $\sigma_g$  (after **Dey and Sarkar 2006**)

- The sediment gradation has a pronounced influence on the scour depth
- In nonuniform sediment ( $\sigma_g > 1.4$ ), a process of armoring in the scour hole commences resulting in an exposure of coarser particles due to washing out the finer fraction
- The armor-layer causes a gradual increase in the effective critical bed shear stress that restricts the development of scour hole
- From Fig. 6.17, it is apparent that for nonuniform sediment having  $\sigma_g = 4$ , the scour depth is drastically reduced to 54% of the scour depth in uniform sediment

- **Dey and Sarkar (2006)** proposed an equation of nondimensional maximum scour depth downstream of an apron due to submerged jets issuing from a sluice opening. It is

$$\tilde{d}_{se} = 2.59 F_0^{0.94} \tilde{l}^{-0.37} \tilde{h}^{0.16} \tilde{d}^{0.25} \quad (6.36)$$

where  $\tilde{l} = l/b$

- The range of applicability of the above equation is  $6.57 \leq \tilde{h} \leq 13.85$  and  $\tilde{l} > 26$

# **LOCAL SCOUR AT STRUCTURES (Part II)**



## Scour below Horizontal Pipes

- Pipelines are laid on riverbeds to transport gas and crude oil and also to dispose of the wastewater
- Scour occurs below the pipeline under the action of flow, which may cause the suspension of pipeline along its length

### Initiation of Scour:

- When a pipeline laid on an erodible bed with little embedment is subjected to strong flow, the pressure difference is set up between the two sides of the pipe
- The pressure difference induces the seepage flow below the pipeline and as a result the sediment bed below the pipeline, which is called *initiation of scour*

- The critical condition for the initiation of scour was studied by many investigators (**Sumer and Fredsøe** 2002)
- Fig. 6.18(a) shows the pressure difference setup below a pipe
- With an increase in flow velocity, a critical point is reached at which the rate of seepage flow increases more rapidly than the order of the driving pressure difference
- At the same time the surface of the sand in the immediate downstream of the pipe rises
- The mixture of sediment and water breaks through the space underneath the pipe and this process is called *pipng*

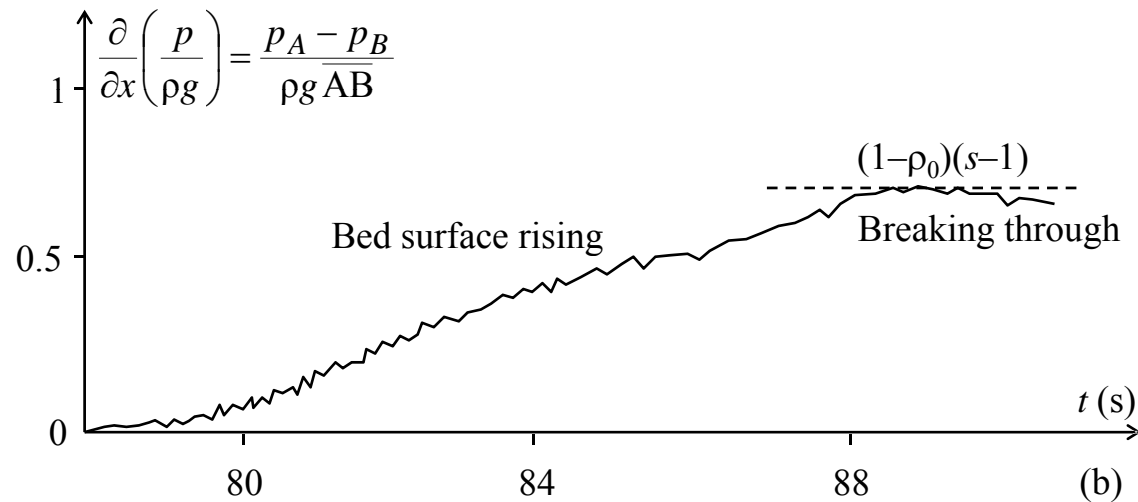
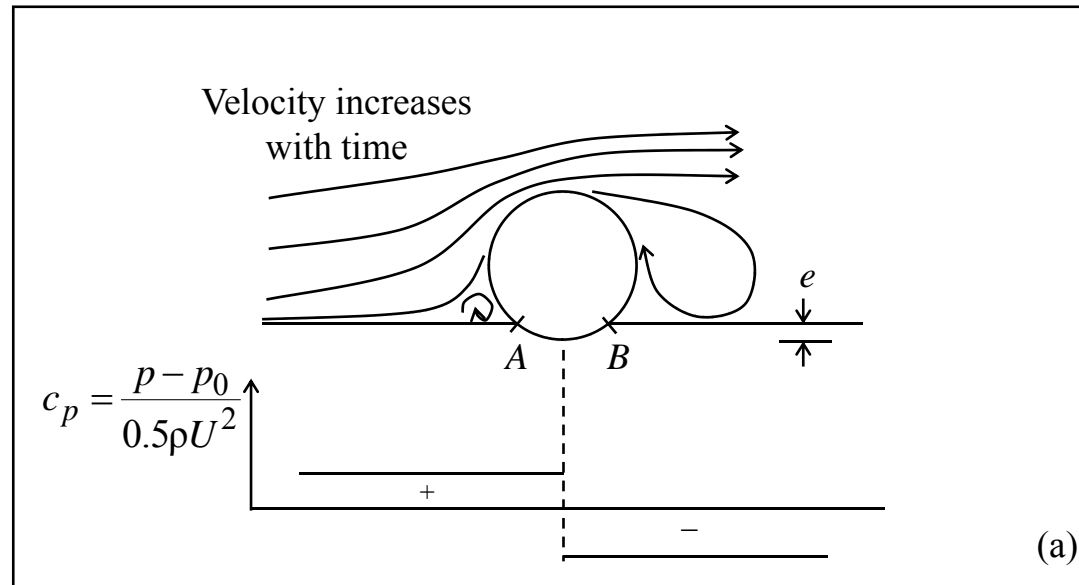


Fig. 6.18 (a) Pressure distribution and (b) time series of pressure gradient below a pipeline (after **Sumer et al.** 2001)

- At equilibrium, the forces acting on an element of sediment bed of volume  $\Delta x \times 1 \times 1$  are:
- The seepage (driving) force  $P$  given by

$$P = \frac{\partial p}{\partial x} \Delta x \quad (6.37)$$

where  $p$  = pressure intensity; and  $x$  = distance along the perimeter of the pipe

- The submerged weight  $W$  of the sediment is

$$W = \rho g (s - 1)(1 - \rho_0) \Delta x \quad (6.38)$$

where  $\rho_0$  = porosity of sediment

- At equilibrium

$$P \geq W \quad (6.39)$$

- Using Eqs. (6.37) and (6.38) into Eq. (6.39), yields

$$\frac{\partial}{\partial x} \left( \frac{p}{\rho g} \right) \geq (s-1)(1-\rho_0) \quad (6.40)$$

- Time series of pressure gradient  $\partial(p/\rho g)/\partial x$  measured by **Sumer et al.** (2001) is presented in Fig. 6.18(b)
- Observations made by **Sumer and Fredsøe** (2002) are
  - As the flow velocity increases, the pressure gradient is enhanced (because  $p$  is proportional to  $U^2$ )
  - With an increase in pressure gradient, a critical condition is reached at which the sediment in the immediate downstream of the pipe begins to rise

- This stage continues for a short period (about 5 s), and subsequently, a mixture of sediment and water breaks through
  - At this instant, the pressure gradient exceeds the floatation gradient  $(s - 1)(1 - \rho_0)$  and the sediment is continuously removed
- The initiation of scour does not occur all along the length of the pipe simultaneously, but occurs locally
  - Eq. (6.40) can be written in the nondimensional form as

$$\left[ \frac{\partial \hat{p}}{\partial \hat{x}} \cdot \frac{U^2}{gD(s-1)(1-\rho_0)} + C \right]_{cr} \geq 1 \quad (6.41)$$

where  $\hat{p} = p/\rho U^2$ ;  $\hat{x} = x/D$ ;  $U$  = flow velocity at the top of the pipe;  $D$  = diameter of pipe; and  $C$  = a nondimensional term that accounts for the effect of the vortices developed in front of the pipe and in the lee wake

- The terms  $\partial\hat{p}/\partial\hat{x}$  and  $C$  are functions of the burial depth - pipe diameter ratio ( $e/D$ )

- Eq. (6.41) becomes

$$\hat{U}_{cr} \geq f\left(\frac{e}{D}\right) \quad (6.42)$$

where  $\hat{U} = U^2/[gD(s-1)(1-\rho_0)]$

- Eq. (6.42) is called the *critterion for the initiation of scour*
- The function  $f(e/D)$  is determined experimentally, which not only depends on  $e/D$  ratio, but also on pipe Reynolds number  $R = UD/\nu$  and relative roughness  $\hat{k} (= k_s/D$ , where  $k_s$  = surface roughness of pipe)
- The influence of  $\hat{k}$  is negligible when there is no significant change in flow regime (from subcritical to supercritical or from supercritical to transcritical) around the pipe
- Fig. 6.19 shows the variation of criterion for the initiation of scour with  $e/D$ -ratio

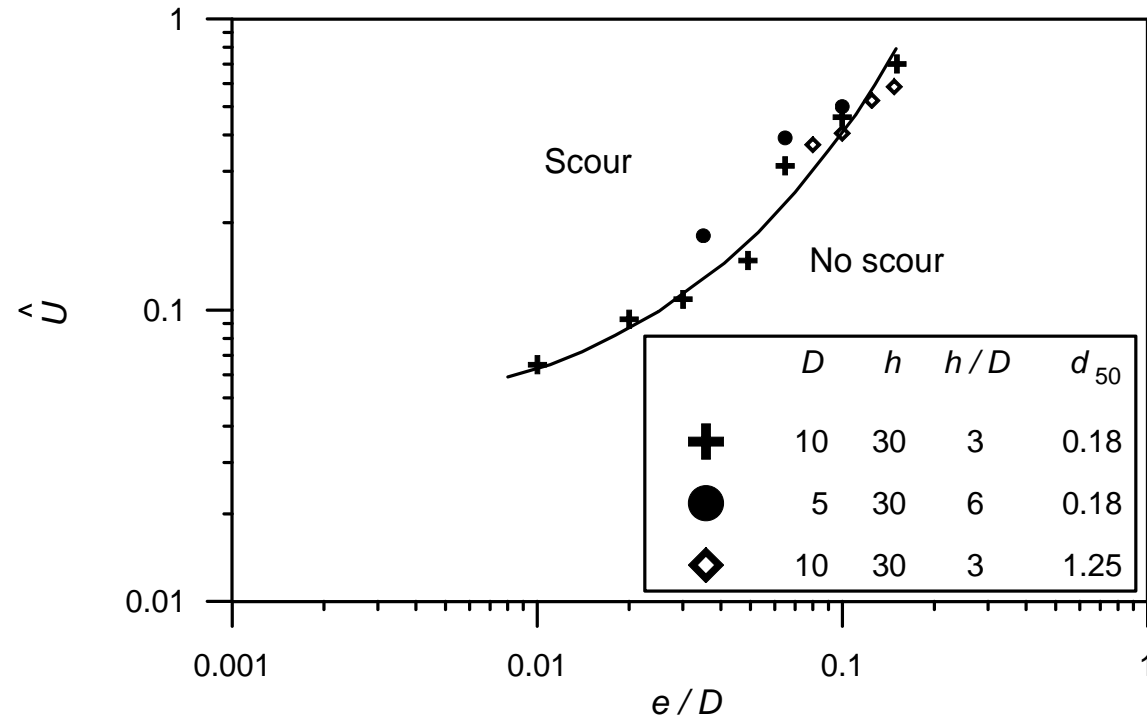


Fig. 6.19 Initiation of scour under flow (after **Sumer et al.** 2001)

- After the piping process, a small gap  $\delta$  ( $\delta \ll D$ ) is developed between the pipe and the bed
- A considerable amount of water is diverted through this gap leading to flow concentration in the gap, which enhances the shear stress acting on the bed just below the pipeline



- Increase in bed shear stress is of the order of magnitude equal to three times the bed shear stress in the approaching flow
- As a result, a large amount of sediment is scoured below the pipeline
- The sediment-water mixture flows in the form of violent jet and such scour process is known as *tunnel erosion* (see Fig. 6.20)
- With an increase in gap size, the gap velocity decreases and the tunnel erosion ceases and this stage is followed by *lee-wake erosion*

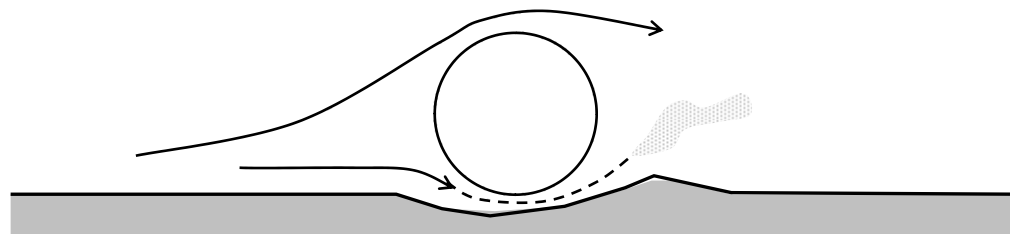


Fig. 6.20 Tunnel erosion below a pipeline

- As a result of tunnel erosion, a dune is formed on the downstream end of the pipe, which gradually migrates further downstream, and finally disappears as the scour progresses
- At this stage, the scour is governed by the lee-wake erosion, which occurs due to the vortex shedding on the downstream end of the pipe (Fig. 6.21)

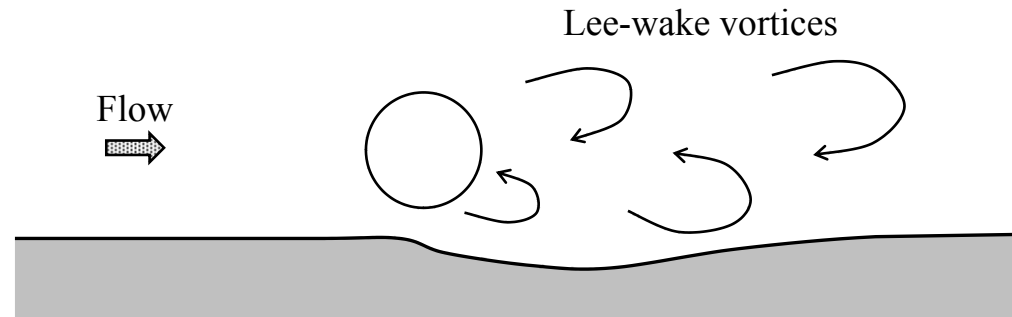


Fig. 6.21 Lee-wake erosion and vortices shedding downstream of a pipe

- When the gap between the pipe and bed reaches a certain value at the end of the tunnel erosion, the vortex shedding begins
- The vortices that shed from the bed of the pipe sweep the sediment as they get convected downstream
- The Shields parameter  $\Theta$  increases approximately by 4 times indicating the greater scour potential at the lee side of the pipe
- The vortex shedding is established within the first 15 minutes
- Subsequently, the scour downstream end of the pipe occurs under the action of the systematic wake flow, that is an agglomeration of separation of vortices that shed from the pipe and steadily convected downstream
- The equilibrium is attained when the bed shear stress below the pipe reaches the value equal to the approaching bed shear stress
- Fig. 6.22 illustrates the development of scour with time (typical) below a pipe with no initial gap and subjected to a steady flow

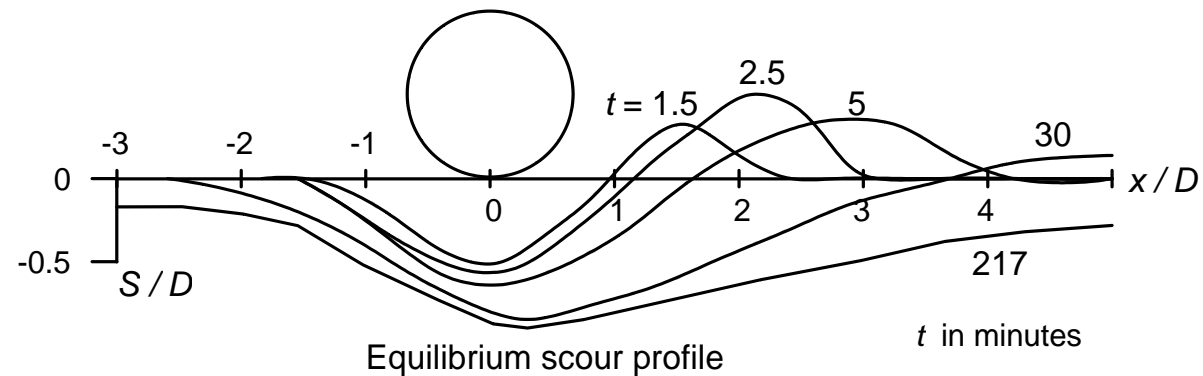


Fig. 6.22 Scour development (after **Mao** 1986)

- Initially, the scour breaks out underneath the pipe locally, and it propagates along the length of the pipeline in both the direction
- The scour hole is interrupted by stretches, called span shoulders, where the pipe gets supported
- After a reasonable developed stage, the scour in the middle part of a scour hole can be considered as two-dimensional

## Scour Depth

- **Kjeldson et al.** (1973) were the initiators to establish an empirical relationship for an equilibrium scour depth under live-bed scour condition. It is

$$S = 0.972 \left( \frac{U^2}{2g} \right)^{0.2} D^{0.8} \quad (6.43)$$

- Eq. (6.43) can be expressed in nondimensional form as

$$\frac{S}{D} \sim \Theta^{0.2} \quad (6.44)$$

- By dimensional analysis, the functional form for the nondimensional scour depth is

$$\frac{S}{D} = f(\hat{k}, R, \Theta) \quad (6.45)$$

- The influence of  $\hat{k}$  and  $R$  exist on the downstream flow of the pipe

- For hydraulically rough pipes, the pipe Reynolds number  $R$  does not affect the wake flow, while for hydraulically smooth pipes,  $R$  has influence on the downstream vortex shedding
- Fig. 6.23 presents the data plot of **Kjeldsen et al. (1973)**, **Lucassen (1984)**, **Mao (1986)** and **Kristiansen (1988)** on scour depth

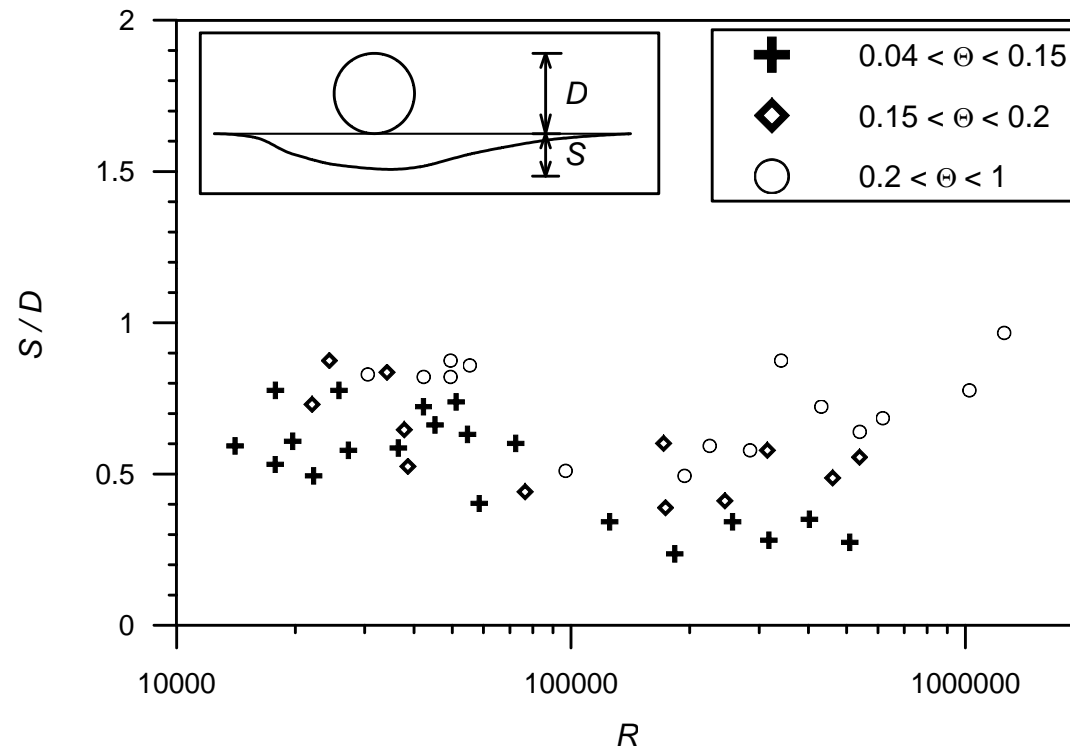


Fig. 6.23 Data of equilibrium scour depth for live-bed scour condition (after **Sumer and Fredsøe 1990**)

- There is a feeble influence of  $R$  on the scour depth
- The influence of the Shields parameter  $\Theta$  on scour depth  $S$  depends on the scour condition
  - In clear-water scour, the effect of  $\Theta$  on  $S$  is more pronounced
  - In live-bed scour,  $S$  has very little variation with  $\Theta$
- **Chao and Hennessy** (1972) proposed a method to evaluate the maximum scour depth below pipelines from the following equation

$$U_{bot} = U \left[ \frac{2(2H/D)^2 - (2H/D) - 1}{2(2H/D)^2 - 3(2H/D) + 1} \right] \quad (6.46)$$

where  $U_{bot}$  = average velocity in the scour hole below a pipeline; and  $H$  = scour depth measured from the pipe center

- **Ibrahim and Nalluri's (1986)** empirical equations for the estimation of scour depth below pipelines are

$$\frac{S}{D} = 4.706 \left( \frac{U}{U_c} \right)^{0.89} F^{1.43} + 0.06 \quad \text{for clear-water scour} \quad (6.47)$$

$$\frac{S}{D} = 0.084 \left( \frac{U}{U_c} \right)^{-0.03} F^{-0.16} + 1.33 \quad \text{for live-bed scour} \quad (6.48)$$

where  $F = U/(gh)^{0.5}$ ;  $h$  = flow depth; and  $U_c$  = critical velocity for sediments

- The Dutch research group (**Bijker and Leeuwestein 1984**) proposed the following empirical equation of the scour depth below a submarine pipeline, which includes the moderate effect of sediment size on scour depth

$$S = 0.929 \left( \frac{U^2}{2g} \right)^{0.26} D^{0.78} d_{50}^{-0.04} \quad (6.49)$$



- **Alix et al.** (1999) found that the pipe Reynolds number  $R$  has negligible influence on the scour depth, while the Froude number is an important parameter that influences the scour depth
- The equation proposed by **Alix et al.** (1999) for the scour depth is

$$S / D = 2F \operatorname{sech}(1.7e/D) \quad (6.50)$$

- **Chiew** (1991) proposed the following iterative method to predict the scour depth below pipelines
  - For a given value of  $h/D$ , determine the unit discharge through the gap  $q_{bot}$  from Fig. 6.24, where  $q_o$  = unit discharge of the approaching flow
  - Assume a scour depth  $S$  and estimate the average velocity below the pipeline  $U_{bot}$  by

$$U_{bot} = q_{bot} / S \quad (6.51)$$

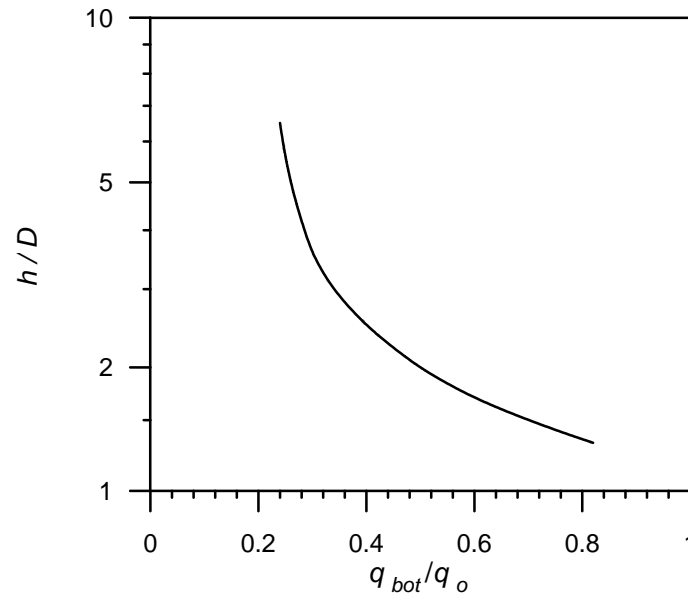


Fig. 6.24 Variation of  $h/D$  with  $q_{bot}/q_o$  (after **Chiew** 1991)

- Compute the bed shear stress in the scour hole  $\tau_{bot}$  using

$$\tau_{bot} = f\rho U_{bot}^2 / 8 \quad (6.52)$$

where  $\rho$  = mass density of water; and  $f$  = friction factor to be estimated from the Moody diagram for a relative roughness ( $= d_{50}/S$ ) and a Reynolds number ( $= U_{bot}S/\nu$ )

- Compare  $\tau_{bot}$  with the critical shear stress  $\tau_c$  obtained from the Shields diagram. Continue the iteration until  $\tau_{bot} = \tau_c$

## Example

- Compute the maximum scour depth below a 100 mm diameter submarine pipe laid on a sediment bed of  $d_{50} = 0.6$  mm, subjected to steady flow of 0.35 m/s with flow depth 0.4 m. Take  $\nu = 0.85 \times 10^{-6}$  m<sup>2</sup>/s
- For  $h/D = 0.4/0.1 = 4$ ,  $q_{bot}/q_o$  is obtained from Fig. 6.24 as 0.29
- Hence,  $q_{bot} = 0.29(0.35 \times 0.4) = 0.0406$  m<sup>3</sup>/s
- Assuming  $S = 120$  mm,  $U_{bot} = 0.0406/0.12 = 0.338$  m/s
- For a relative roughness  $= 0.6/120 = 0.005$  and a Reynolds number  $= 0.338 \times 0.12 / (0.85 \times 10^{-6}) = 4.8 \times 10^4$ , the friction factor  $f$  obtained from the Moody diagram is 0.032

- The bed shear stress in the scour hole below pipeline,  
 $\tau_{bot} = 0.032 \times 1000 \times 0.338^2 / 8 = 0.457 \text{ Pa}$
- From the Shields diagram, for  $d_{50} = 0.6 \text{ mm}$ ,  $\tau_c$  is estimated as  
 $0.324 \text{ Pa}$
- Therefore,  $\tau_{bot} > \tau_c$
- With iterative procedure, the value of  $S$  that satisfy the condition of  
 $\tau_{bot} = \tau_c$  is  $141 \text{ mm}$
- Therefore, the maximum scour depth is  $141 \text{ mm}$

## Scour at Bridge Piers

- The obstruction of the flowing stream by a bridge pier causes a three-dimensional separation of flow forming a vortex flow field around the pier (**Dey et al.** 1995; **Dey** 1995)
- To be more explicit, the flow separates at the upstream face of the pier as it travels by the side of the pier, creating a vortex trail, termed horseshoe vortex, which moves downstream
- As a result of which local scour takes place around the pier due to the removal of bed sediments
- Review of the important experiments and field studies was given by **Breusers et al.** (1977), **Dargahi** (1982), **Breusers and Raudkivi** (1991), **Dey** (1997a, b), **Melville and Coleman** (2000), **Richardson and Davis** (2001), and **Sumer and Fredsøe** (2002)

# Flow Field around Bridge Piers

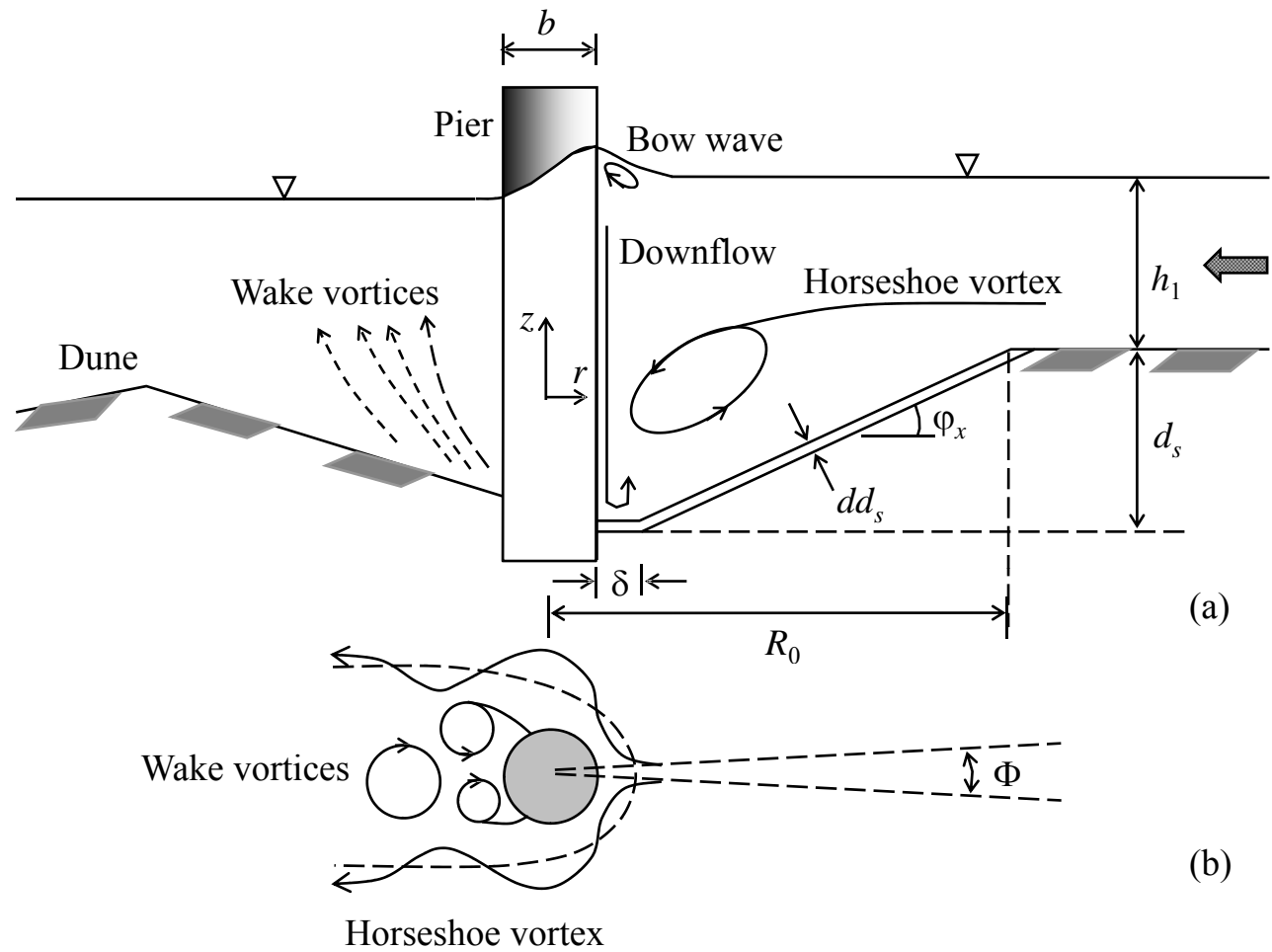


Fig. 6.25 Definition sketch showing components of flow field around a pier

- The flow field around a pier is coupled with a complex three-dimensional separation of the approaching flow upstream and a periodical vortex shedding downstream of the pier
- Complexity increases with the development of the scour hole
- The existence of the pier in the flowing stream induces a downward negative pressure gradient normal to the approaching flow
- The boundary layer at the pier upstream gets through this pressure gradient set up by the pier, separating the flow and forming the *horseshoe vortex*
- In addition, the other flow components developed are the *downflow*, *wake vortex* and *bow wave*

- **Melville** (1975), **Dey et al.** (1995), **Ahmed and Rajaratnam** (1998) and **Graf and Istiarto** (2002) measured the flow field within the scour hole around a circular pier
- **Raikar** (2006) studied the characteristics of turbulent horseshoe vortex flow within the developing scour holes at cylindrical piers and presented the evolution of the horseshoe vortex during the development of a scour hole through the vector diagrams
- Fig. 6.26 shows the time-averaged velocity vectors at different azimuthal planes ( $0^\circ$ ,  $45^\circ$  and  $90^\circ$  with reference to the upstream axis of symmetry) for intermediate and equilibrium scour holes at a circular pier



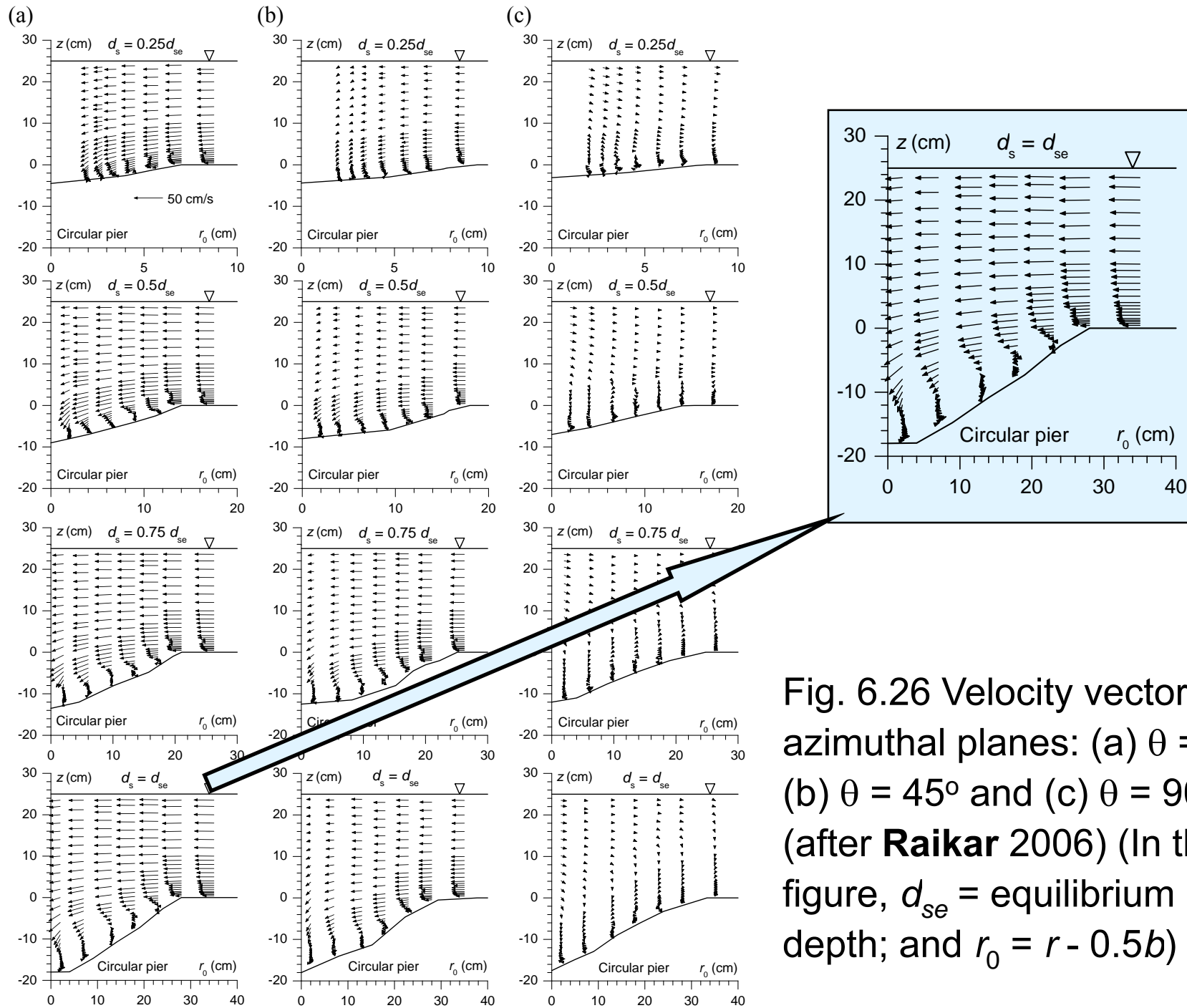


Fig. 6.26 Velocity vectors at azimuthal planes: (a)  $\theta = 0^\circ$ ; (b)  $\theta = 45^\circ$  and (c)  $\theta = 90^\circ$  (after Raikar 2006) (In the figure,  $d_{se}$  = equilibrium scour depth; and  $r_0 = r - 0.5b$ )

## ***Parameters Influencing Scour Depth at Piers***

- Scour at piers is influenced by various parameters (**Breusers et al. 1977**), which are grouped as follows:
  - Parameters relating to the pier: Size, shape, spacing, number and orientation with respect to the approaching flow direction
  - Parameters relating to the bed sediment: Median size, particle size distribution, mass density, angle of repose and cohesiveness
  - Parameters relating to the approaching flow condition: Approaching flow velocity, approaching flow depth, shear velocity and roughness
  - Parameters relating to the fluid: Mass density, viscosity, gravitational acceleration and temperature (may not be important in scour problems)

- Parameters relating to the time: Time of scouring for an evolving scour hole
  - Parameters relating to the unsteadiness: Passage of flood wave in rivers and waves in marine environment
- The relationship showing the influence of various parameters on the equilibrium scour depth  $d_s$  at piers can be given in functional form as follows:

$$d_s = f_1(U_1, h_1, \rho, \rho_s, g, \nu, b, d_{50}, \sigma_g, t) \quad (6.53)$$

where  $b$  = pier width; and  $t$  = time of scour

## Effect of Pier Width Relative to Sediment Size on Scour Depth

- Fig. 6.27 shows the variation of nondimensional equilibrium scour depth  $\hat{d}_s (= d_s/b)$  as a function of  $\tilde{b} (= b/d_{50})$  for clear-water scour condition

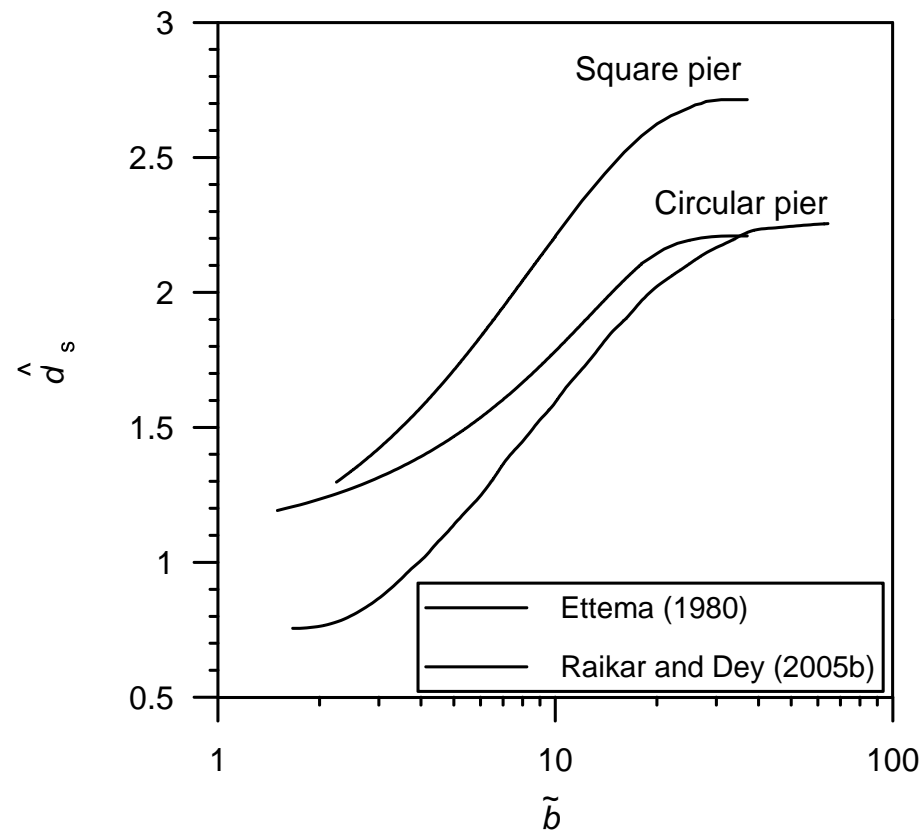


Fig. 6.27 Variation of  $\hat{d}_s$  with  $\tilde{b}$  for  $U_1/U_c \approx 1$

- The equilibrium scour depth  $\hat{d}_s$  relative to pier width being greater for larger pier width and smaller sediment size
- This is due to an enhanced scour potential of the vortex flow consisting of the horseshoe vortex and the downflow (**Dey et al. 1995; Dey 1995**), which are proportional to the pier width  $b$  (**Breusers 1965**)
- Also, the horseshoe vortex is stronger to excavate large volume of sediments, when the sediment size is relatively fine developing greater scour depth  $d_s$
- Coarser sediments make the bed more porous to allow the downflow to penetrate and dissipate its energy in the sediment bed
- For square piers, the scour depth is greater than that for circular pier, because the strengths of the downflow and horseshoe vortex are greater in the case of the square pier (**Tseng et al. 2000**)

## Effect of Approaching Flow Depth Relative to Pier Width on Scour Depth

- The dependency of  $\hat{d}_s$  at circular piers for clear-water scour condition on the ratio of approaching flow depth to pier width  $\hat{h}$  ( $= h_1/b$ ) for different  $\tilde{b}$  and  $d_{50} = 4.1$  mm is presented in Fig. 6.28 (**Raikar 2006**)

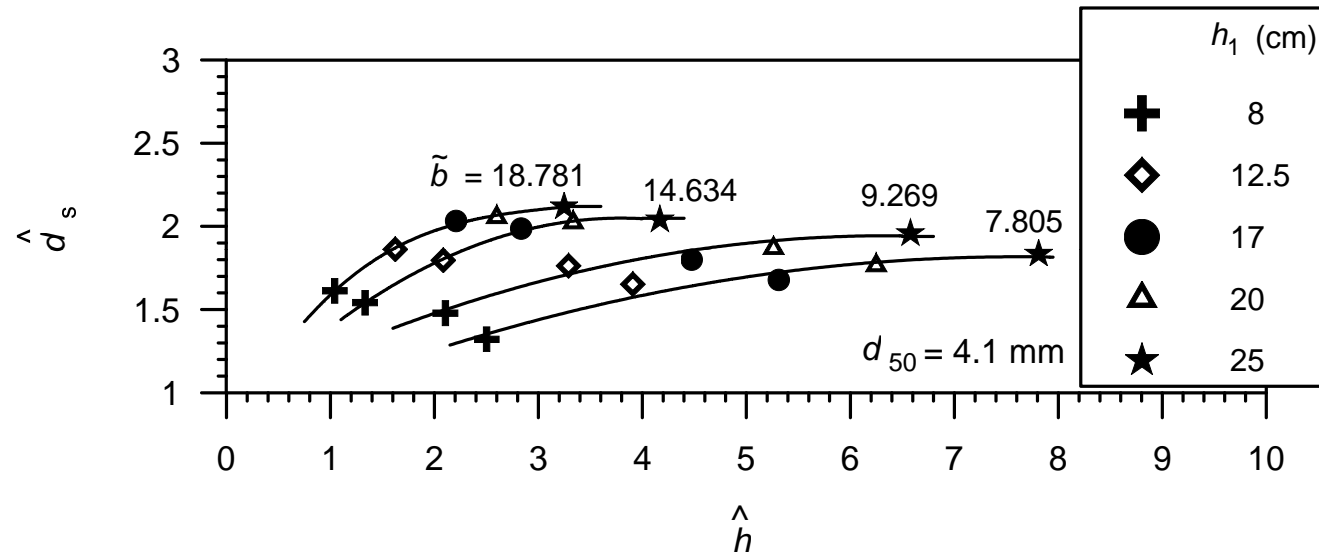


Fig. 6.28 Dependency of  $\hat{d}_s$  on  $\hat{h}$  for circular piers under  $U_1/U_c \approx 1$  (after **Raikar 2006**)

- At small  $\hat{h}$ , the nondimensional equilibrium scour depth  $\hat{d}_s$  increases sharply with an increase in  $\hat{h}$
- As  $\hat{h}$  increases,  $\hat{d}_s$  becomes almost independent of  $\hat{h}$
- For larger  $\tilde{b}$ , the range of influence of flow depth is relatively small
- That is for large pier width, scour depth  $d_s$  is independent of flow depth at  $\hat{h} = 3$ , whereas for small pier width,  $\hat{h}$  is approximately 7
- There is a little increase of horseshoe vortex strength due to an increase in flow depth beyond three and seven times of pier width for large and small pier widths, respectively

- In case of pier scour in sands, most of the investigators stated that the influence of flow depth is insignificant for  $\hat{h} > 1 - 3$  (**Raudkivi and Ettema 1983; Raudkivi 1986**)
- Also, for the same value of  $h_1$  (in the plots, same symbols are used),  $\hat{d}_s$  increases with an increase in  $\tilde{b}$
- For shallow flow depths, the surface roller, termed bow wave, having a sense of rotation opposite to the horseshoe vortex, reduces the horseshoe vortex strength, resulting in a reduced scour depth



## Effect of Nonuniform Sediment Gradation on Scour Depth

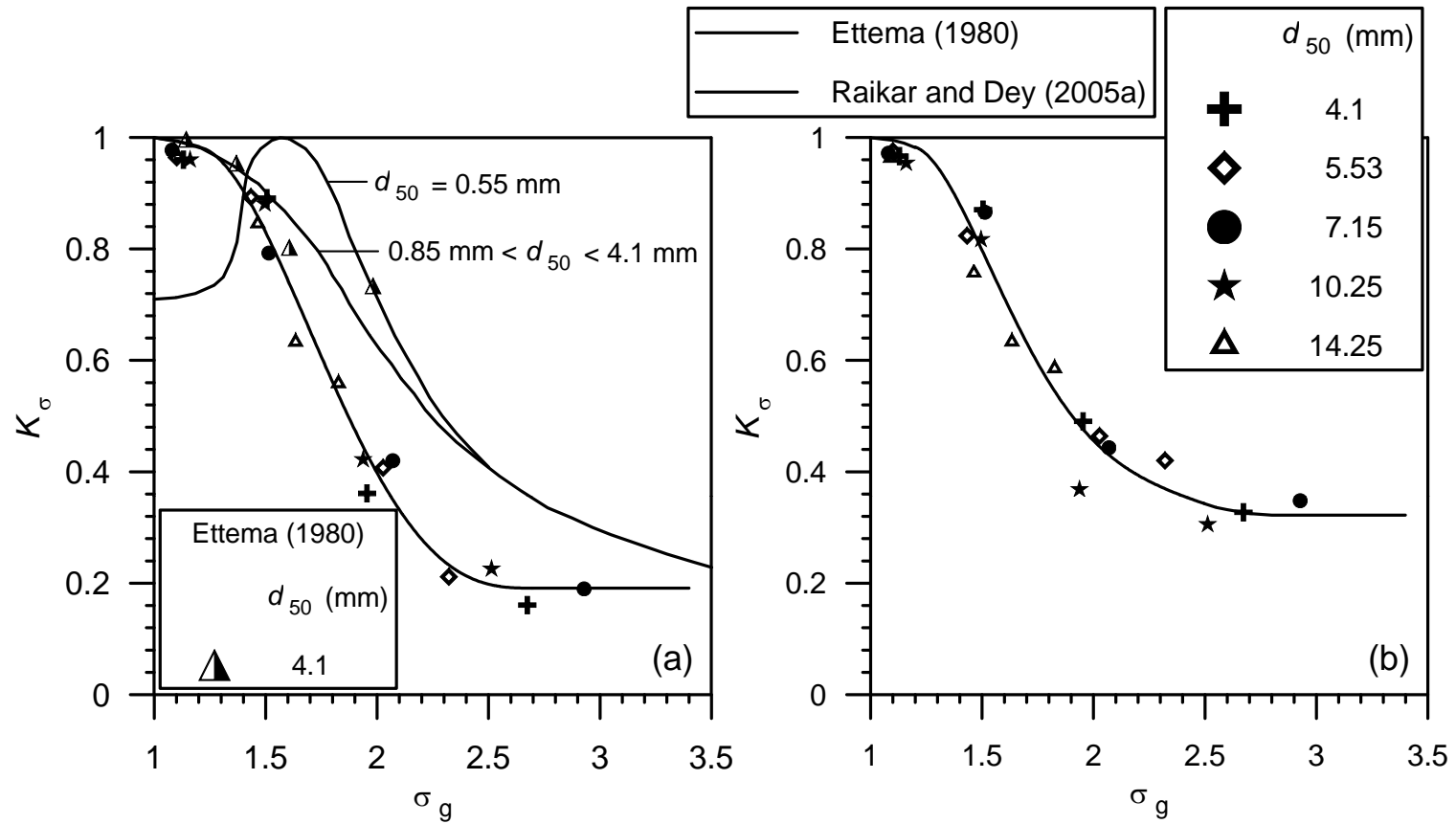


Fig. 6.29 Variation of  $K_\sigma$  with  $\sigma_g$  for  $U_1/U_c \approx 1$ : (a) circular piers and (b) square piers

- In nonuniform sediments ( $\sigma_g > 1.4$ ), a process of armoring in the scour hole commences resulting in an exposure of coarser particles due to washing out of the finer fraction
- The armor-layer thus formed gradually increases the effective critical bed shear stress, which inhibits the further growth of scour hole
- Hence, the nonuniform sediments consistently produce lower scour depths than that of the uniform sediments
- The dependencies of  $K_\sigma$  on  $\sigma_g$  for circular and square piers are shown in Figs. 6.29(a) and 6.29(b)
- It is evident from the mean curves for scour at circular piers that the difference between **Ettema's** (1980) curve for sands and **Raikar and Dey's** (2005a) curve for gravels is considerable
- For a given  $\sigma_g$ , coefficient  $K_\sigma$  for square piers is greater than that for circular piers due to stronger horseshoe vortex for square piers

## Time-Variation of Scour Depth

- The time-variation of scour depth at piers embedded in gravels studied by **Raikar and Dey** (2005a) is presented below:

### Scour Depth in Uniform Gravels:

- According to **Sumer et al.** (1993), the instantaneous scour depth at a pier  $d_{st}$  at time  $t$  can be represented in functional form as

$$d_{st} = d_s [1 - \exp(-t/T)] \quad (6.54)$$

where  $T$  = time scale

- $T$  represents the time period during which scour depth develops substantially
- Time scale  $T$  can be determined from the scour depth  $d_{st}$  versus time  $t$  diagram by estimating the slope of the tangent to the  $d_{st}(t)$  curve at  $t = 0$ , as shown schematically in Fig. 6.30(a)

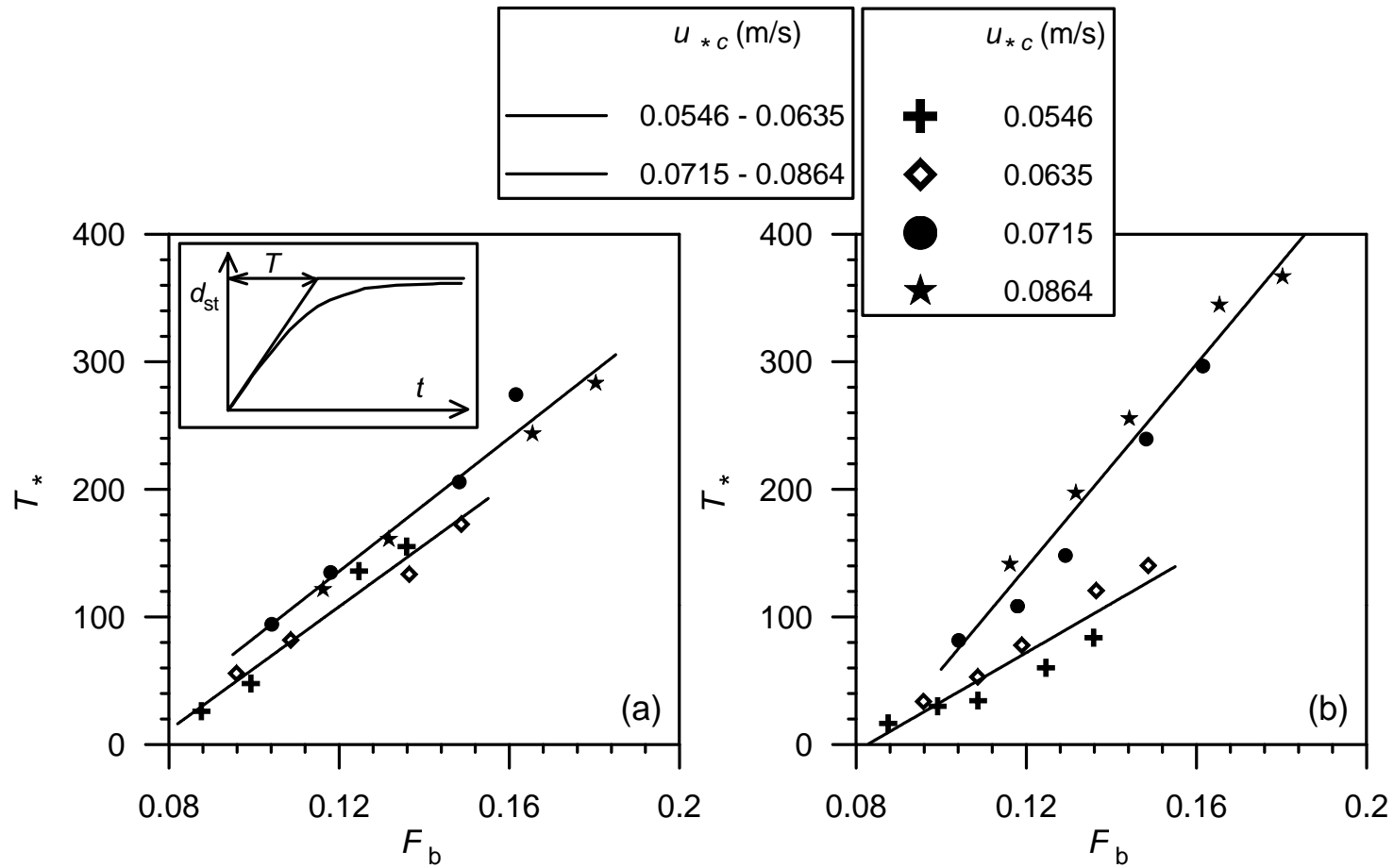


Fig. 6.30 Variation of  $T^*$  with  $F_b$  for different gravel sizes  $d_{50}$  under  $U_1/U_c \approx 1$ : (a) circular pier and (b) square pier (after **Raikar and Dey 2005a**)

- The time scale can be expressed in nondimensional form as  $T_* [= T(\Delta g d_{50}^3)^{0.5}/b^2]$
- For pier scour, the nondimensional time scale  $T_*$  can be written in the following functional form:

$$T_* = T_*(F_b, d_{50}) \quad (6.55)$$

where  $F_b$  = pier Froude number, that is  $U_1/(gb)^{0.5}$

- For circular and square piers, the variations of nondimensional time scale  $T_*$  with pier Froude number  $F_b$  for different sizes of gravels are given in Figs. 6.30(a) and 6.30(b)
- $T_*$  increases with increase in  $F_b$  and  $u_{*c}$

## Scour Depth in Nonuniform Gravels:

- In nonuniform gravels ( $\sigma_g > 1.4$ ),  $T_*$  is represented as a function of  $\sigma_g$  for different  $u_{*c}$
- $T_*$  decrease with an increase in  $\sigma_g$  and  $u_{*c}$
- Due to the formation of an armor-layer at the base of the scour hole, the rate of development of scour hole reduces
- Hence, the time to reach equilibrium in nonuniform gravels is lesser than that in uniform gravels
- The nondimensional time scale  $T_*(\sigma_g)$  for nonuniform gravels can be represented as a function of  $T_*$  for uniform gravels as

$$T_*(\sigma_g) = K_T T_* \quad (6.56)$$

where  $K_T$  = coefficient for time scale depending on the gradation of gravels

- The dependencies of  $K_T$  on  $\sigma_g$  for circular and square piers are shown in Figs. 6.31(a) and 6.31(b)

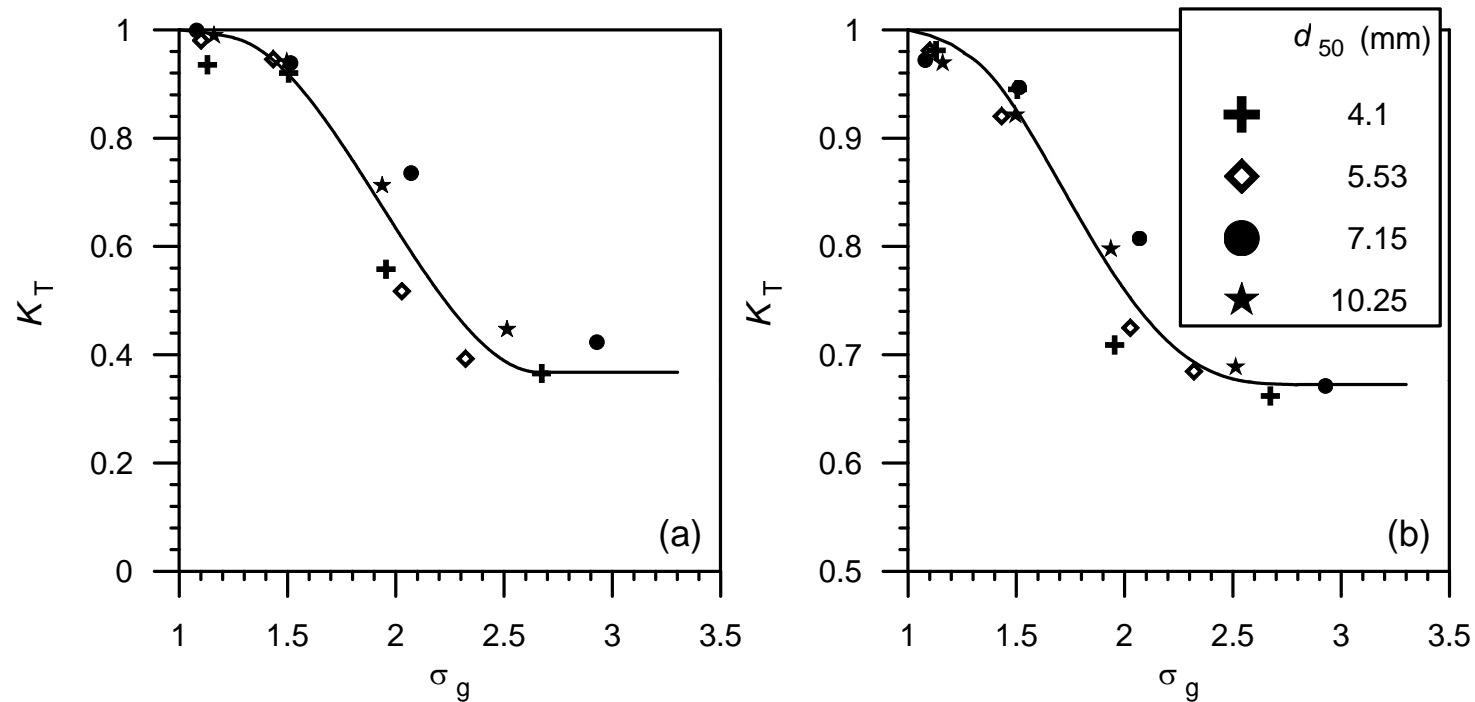


Fig. 6.31 Variation of  $K_T$  as a function of  $\sigma_g$  for  $U_1/U_c \approx 1$ : (a) circular piers and (b) square piers (after **Raikar and Dey 2005a**)

## ***Modeling of Time-Variation of Scour Depth***

- **Dey** (1999) proposed an analytical model to estimate the time-variation of scour depth in an evolving scour hole at cylindrical piers under clear-water and live-bed scour condition with uniform and nonuniform sediments
- The hydrodynamic forces (namely drag and lift forces) acting on the sediment particles owing to the vortex flow remove the bed particles and decrease with an increase in scour depth
- The conical shape of the scour hole upstream makes an angle  $\phi_x$  with the original bed except for the semicircular flat region having a width  $\delta$  [Fig. 6.25(a)]
- The angle  $\phi_x$ , termed ***dynamic angle of repose***, was measured to be about 15% greater than the angle of repose of the bed sediment in still water (**Dey et al. 1995; Melville and Raudkivi 1977**)



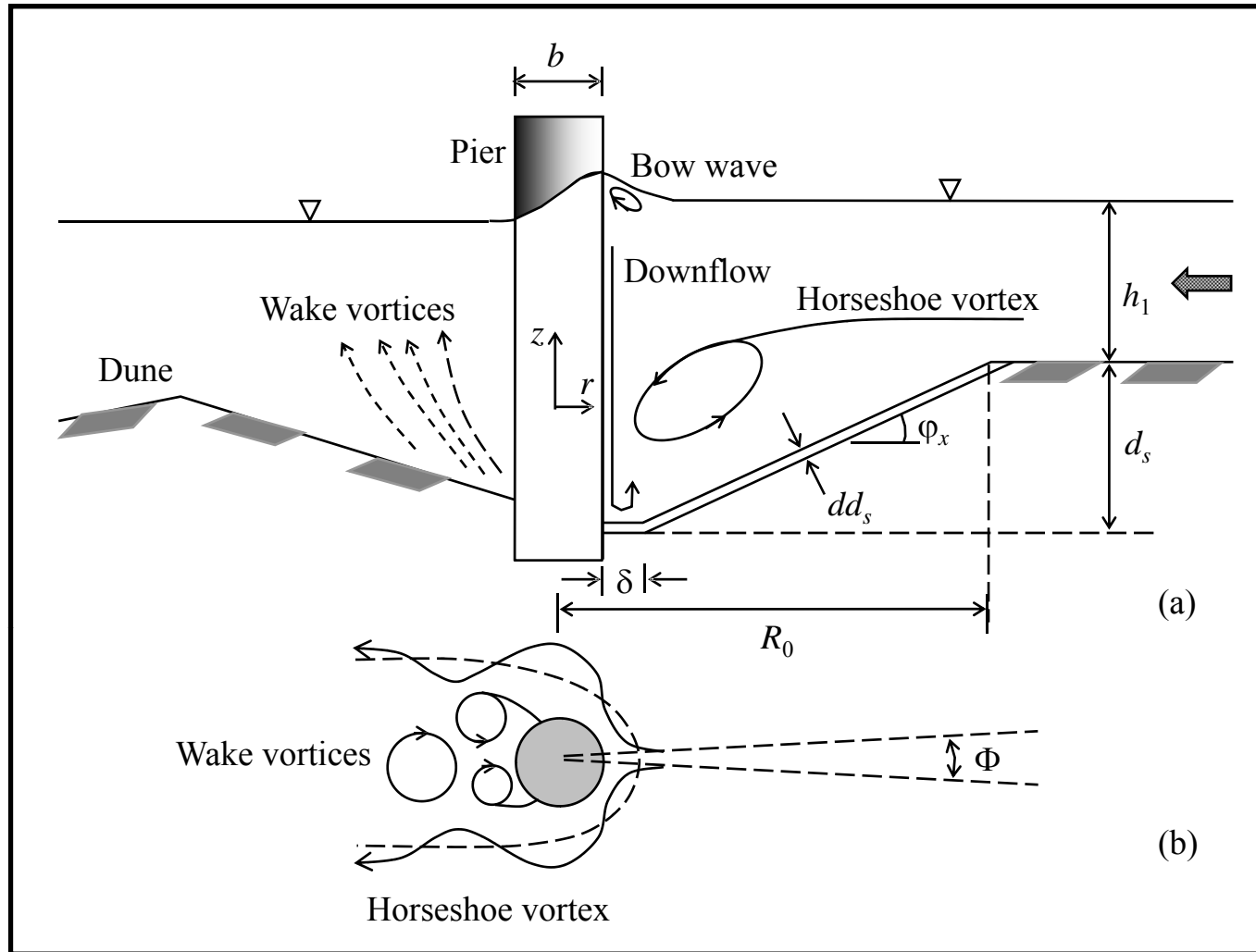


Fig. 6.25 Definition sketch showing components of flow field around a pier

- The sediment particles are mainly dislodged from the pier base by the action of the vortex and are carried downstream by the sides of the pier
- The semicircular region is also fed with the sediment particles of the conical portion of scour hole upstream, as it collapses; and subsequently, those particles are picked up (**Dey** 1991)
- The depletion of the bed sediment in the scour hole takes place layer by layer
- In live-bed scour, the approaching sediment load is also added to the hole

- The mathematical model of scouring process at a pier is derived from the following concepts:
  - The horseshoe vortex at the pier base upstream is the basic cause of scouring (**Melville** 1975)
  - Sediment particles are picked up from the flat semicircular region upstream where the maximum scour depth appears (**Dey** 1991)
  - The scour profiles are geometrically similar with time as scouring progresses (**Dey** 1991)
  - The rate of change of sediment mass in the scour hole equals the difference between the sediment mass removal rate from the scour hole and the sediment mass inflow rate by the approaching flow into the scour hole

- Figs. 6.25(a) – 6.25(b) present the sectional elevation and the top view of a typical scour hole at a cylindrical pier in time  $t$ , as was idealized by **Dey et al.** (1995)
- Considering a small angle  $\Phi$  to the axis of symmetry of the scour hole upstream
- The mass of sediment picked up from the flat semi-circular region during a small interval of time  $dt$  is

$$dm_1 = 0.5\delta(\delta + b)\beta E dt \quad (6.57)$$

where  $\beta$  = factor; and  $E$  = sediment pick-up rate at the base of the pier in time  $t$

- The effective pick-up rate of sediment, that leaves the scour hole, is actually considered to be  $\beta E$
- $\beta$  is introduced for the reason that the number of sediment particles leaving the scour hole decreases with the scour depth

- The characteristic kinetic energy of sediment particles is assumed proportional to  $\tau_b d_e^3$  (where  $\tau_b$  is the bed shear stress in the scour hole at the pier base and  $d_e$  is the effective size of sediment)
- The potential energy of the sediment particles, corresponding to the scour depth  $d_{st}$  from the point of view of similarity of the scour profiles, is proportional to  $\rho \Delta g d_e^3 d_{st}$  (where  $d_{st}$  = scour depth in time  $t$ )
- The fraction of the sediment that leaves the hole is proportional to  $\beta$  which is, in turn, proportional to the ratio of the kinetic energy to potential energy that is  $\tau_b / (\rho \Delta g d_{st})$
- The width of the flat semicircular region  $\delta$  can be expressed as a fraction of the radial length of the scour hole from the pier boundary at the original bed level upstream

$$\delta = \varepsilon(R_0 - 0.5b) \quad (6.58)$$

where  $\varepsilon$  = geometric factor; and  $R_0$  = radius of the scour hole at the original bed level upstream in time  $t$ . Thus,  $R_0$  is given by

$$R_0 = \left[ \frac{d_{st}}{(1-\varepsilon)} \right] \cot \varphi_x + 0.5b \quad (6.59)$$

- Using Eqs. (6.58) and (6.59) into Eq. (6.57), yields

$$dm_1 = 0.58 \frac{\varepsilon}{1-\varepsilon} d_{st} \cot \varphi_x \left( \frac{\varepsilon}{1-\varepsilon} d_{st} \cot \varphi_x + b \right) \times \beta E dt \quad (6.60)$$

- In Eq. (6.60), the sediment pick-up rate  $E$  at the base of the pier due to scouring, determined using the formula of **van Rijn** (1984), is given as

$$E = 0.00033 \rho_s (\Delta g d_e)^{0.5} d_{*e}^{0.3} T_s^{1.5} \quad (6.61)$$

where  $d_{*e}$  = particle parameter, that is  $d_e(\Delta g/\nu^2)^{1/3}$ ;  $T_s$  = transport-stage parameter due to scour, that is  $(\tau_b - \tau_{bc})/\tau_{bc}$ ;  $\tau_{bc}$  = critical shear stress in the scour hole ( $= \xi \tau_{cre}$ );  $\tau_{cre}$  = critical shear stress on a plane bed for the particle size of  $d_e$ ; and  $\xi$  = factor depending on turbulence agitation and oscillation of horseshoe vortex

- According to **Kothyari et al.** (1992a), the effective size of sediment  $d_e$ , an equivalent mean size of the uniform sediment where scouring rate is same as that of the nonuniform sediment, can be determined as

$$d_e = 0.925d_{50}\sigma_g^{0.67} \quad \text{nonuniform sediment} \quad (6.62a)$$

$$d_e = d_{50} \quad \text{uniform sediment} \quad (6.62b)$$

- The local bed shear stress  $\tau_b$  at the pier base is determined from the empirical formula given by **Kothyari et al.**(1992a) as

$$\tau_b = 4\tau \left[ \left( \frac{2}{\pi} \right) \left( \frac{d_{st}}{d_v} \right)^2 \cos \varphi_x + 1 \right]^{-0.57} \quad (6.63)$$

where  $\tau$  = bed shear stress of approaching flow; and  $d_v$  = diameter of the horseshoe vortex at the beginning of scour

- **Kothyari et al.** (1992a) proposed an empirical equation as  $d_v = 0.28h_1^{0.15}b^{0.85}$

- Critical shear stress,  $\tau_{cr}$  that is given in the Shields diagram can be determined from the empirical formula proposed by **van Rijn** (1984) as

$$\tau_{cre} = \Delta\rho g d_e \Theta_{cr} \quad (6.64)$$

where  $\Theta_{cr}$  = nondimensional critical shear stress or Shields parameter, that is  $\tau_{cre}/(\Delta\rho g d_e)$

- In live-bed scour, when the bed shear stress of approaching flow  $\tau$  exceeds its critical value for the initiation of sediment motion, the sediment particles start moving being picked up from the upstream bed at a rate of  $E_u$
- The sediment mass that is entering into the scour hole, deposits over the flat semicircular region of the scour hole by the downward flow
- The deposition of the approaching sediment load does not take place uniformly over the entire scour hole due to the downward motion of the fluid towards the flat semicircular region



- The flow field inside the scour hole has an upward motion along the slant bed where the sediment deposition is not possible (**Dey** 1995)
- The mass rate of sediment deposition in the scour hole is always less than that of sediment pick-up from the scour hole during scouring
- The equilibrium prevails over a period of time when sediment deposition and pick-up rates are equal
- The mass of sediment deposited over the flat semicircular region of the scour hole, in an interval of time  $dt$ , is

$$dm_2 = 0.5 \operatorname{sgn}(T_u) \Phi \delta(\delta + b) E_u dt \quad (6.65)$$

where  $E_u$  = sediment pick-up rate by the approaching flow at the plane bed upstream

- The function  $\text{sgn}(T_u)$  is

$$\text{sgn}(T_u) = 1 \quad \text{for } T_u > 0 \text{ (live-bed scour)} \quad (6.66a)$$

$$\text{sgn}(T_u) = 0 \quad \text{for } T_u \leq 0 \text{ (clear-water scour)} \quad (6.66b)$$

where  $T_u = (\tau - \tau_{cr})/\tau_{cr}$ ; and  $\tau_{cr} =$  critical shear stress on the plane bed for the particle size of  $d_{50}$

- $\tau_{cr}$  can be determined from Eq. (6.64) using  $d_{50}$  in place of  $d_e$
- The function  $\text{sgn}(T_u)$  implies that there is no sediment supply ( $dm_2 = 0$ ) into the scour hole under a clear-water scour condition
- Using Eqs. (6.58) and (6.59), Eq. (6.65) is rewritten as

$$dm_2 = 0.5 \text{sgn}(T_u) \Phi \frac{\varepsilon}{1-\varepsilon} d_{st} \cot \varphi_x \left( \frac{\varepsilon}{1-\varepsilon} d_{st} + b \right) \times E_u dt \quad (6.67)$$

- The sediment mass, picked up by the approaching flow under a live-bed scour condition, has a direct contribution towards a decrease in rate of change of scour depth in the process of its deposition in the hole

- The formula given by **van Rijn** (1984) is also used to estimate  $E_u$  as

$$E_u = 0.00033\rho_s(\Delta g d_{50})^{0.5} d_{*50}^{0.3} T_s^{1.5} \quad (6.68)$$

where  $d_{*50} = d_{50}(\Delta g/v^2)^{1/3}$

- Applying the geometrical similarity of scour profiles with time, the depletion of the sediment mass due to an increase in scour depth  $dd_{st}$  in time  $dt$  is given by

$$dm_3 = 0.5(1 - \rho_0)\rho_s \Phi\{\delta(\delta + b) + \sec \phi_x[(R^2 - 0.25b^2) - \delta(\delta + b)]\} dd_{st} \quad (6.69)$$

where  $\rho_0$  = porosity of sediment

- Substituting Eqs. (6.58) and (6.59) into Eq. (6.69), yields

$$dm_3 = 0.5(1 - \rho_0)\rho_s \Phi \frac{d_{st}}{1 - \varepsilon} \left[ \varepsilon \cot \varphi_x \left( \frac{\varepsilon}{1 - \varepsilon} d_{st} \cot \varphi_x + b \right) + \frac{(1 + \varepsilon)d_{st} \cot \varphi_x (1 - \varepsilon)b}{\sin \varphi_x} \right] dd_{st} \quad (6.70)$$

- The fundamental equation to describe the scouring process can be obtained from the concept of conservation of the mass of sediment as

$$dm_1 = dm_2 + dm_3 \quad (6.71)$$

- Eqs. (6.60), (6.67) and (6.70) are used in Eq. (6.71) to obtain the following differential equation in nondimensional form:

$$\begin{aligned} (1 - \rho_0) \left[ \varepsilon \cot \varphi_x \left( \frac{\varepsilon}{1 - \varepsilon} \hat{d}_{st} \cot \varphi_x + 1 \right) + \frac{(1 + \varepsilon)\hat{d}_{st} \cot \varphi_x + 1 - \varepsilon}{\sin \varphi_x} \right] \frac{d\hat{d}_{st}}{d\hat{t}} \\ = \varepsilon \cot \varphi_x \left( \frac{\varepsilon}{1 - \varepsilon} \hat{d}_{st} \cot \varphi_x + 1 \right) \times [\beta \hat{D}^{0.5} \varphi_p - \text{sgn}(T_u) \varphi_{pu}] \tilde{b} \end{aligned} \quad (6.72)$$

where  $\hat{t} = td_{50}(\Delta gd_{50})^{0.5}/b^2$ ;  $\hat{d}_{st} = d_{st}/b$ ;  $\hat{D} = d_e/d_{50}$ ;  $\varphi_p$  = sediment pick-up function due to scouring, that is  $E/[\rho_s(\Delta gd_e)^{0.5}]$ ; and  $\varphi_{pu}$  = sediment pick-up function for the upstream bed that is  $E_u/[\rho_s(\Delta gd_{50})^{0.5}]$

- The geometric factor  $\varepsilon$  was taken as 0.1 (**Dey** 1991)
- $\rho_0$  and  $\varphi_x$  were assumed as 0.4 and 37 degree
- Eq. (6.72) is a first-order differential equation, which can be solved by the Runge-Kutta method to determine the dependency  $\hat{d}_{st}$  on  $\hat{t}$
- Figs. 6.32(a) - 6.32(c) presents the validation of the model using the experimental data of **Raudkivi and Ettema** (1983) and **Kothyari et al.** (1992b)

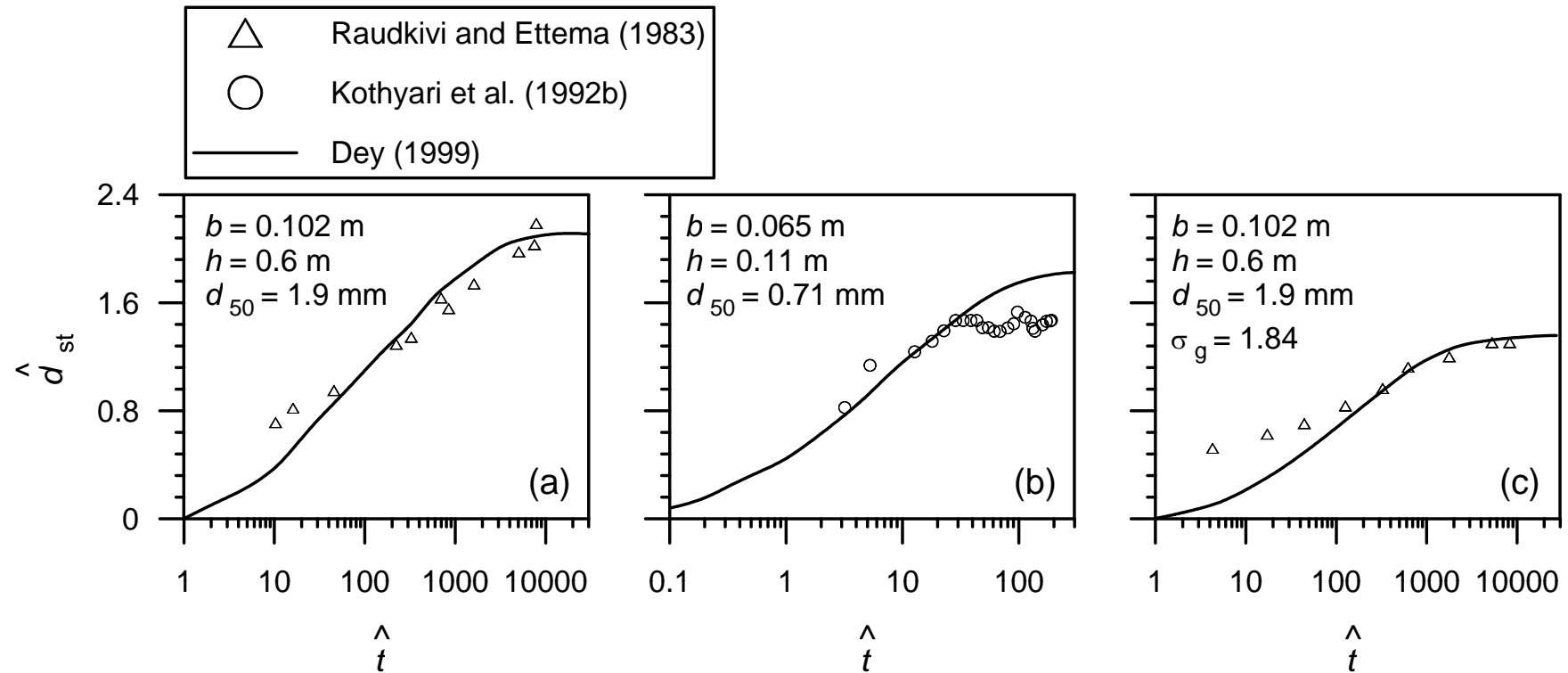


Fig. 6.32 Dependency of  $\hat{d}_{st}$  on  $\hat{t}$ : (a) uniform sediments under clear-water scour; (b) uniform sediments under live-bed scour and (c) nonuniform sediments under clear-water scour (after **Dey** 1999)

## Equilibrium Scour Conditions and Maximum Scour Depth:

- The traditional concept of equilibrium for clear-water scour, when the  $\tau_b \rightarrow \tau_{cr}$  cannot be applied to strongly three-dimensional (turbulent) vortex flow situations
- The sediment particles are dislodged by the fluid-induced forces under the combined effect of bed shear stress, turbulent agitation and oscillation of the horseshoe vortex (**Melville 1997; Dey and Kar 1995**)
- **Melville and Raudkivi (1977)** and **Dey and Bose (1994)** estimated that  $\tau_b < \tau_{cr}$  in the scour hole when the equilibrium was reached
- Hence, an equilibrium condition in pier scour can be defined when  $\tau_b \rightarrow \xi \tau_{cr}$  with  $\xi = 0.7$  (**Dey and Bose 1994**)

- In live-bed scour, when the rate of sediment pick-up out of the scour hole is balanced by the incoming sediment transport rate due to the approaching flow, an equilibrium condition prevails over a period of time
- However, the maximum scour depth can be estimated from Eq. (6.72) for either condition of scour
- The value of  $\beta = 0.97$  was found to give satisfactory agreement between the results obtained using the model and the experimental data reported by various investigators
- For maximum scour depth, incorporating  $d\hat{d}_{st} / d\hat{t} = 0$ , into Eq. (6.72), the following formula for maximum scour depth at piers is obtained as

$$\hat{d}_s = 0.393 \left( \frac{h_1}{b} \right)^{0.15} \left\{ 21.28 \left[ \frac{\tau_0 / \tau_{cr}}{1 + 1.02 \operatorname{sgn}(T_u)^{0.67} \hat{D}^{0.53} T_u} \right]^{1.754} - 1 \right\}^{0.5} \quad (6.73)$$



- The comparison of nondimensional equilibrium scour depths  $\hat{d}_s$  computed from the **Dey's** (1999) model with the laboratory experimental and field data reported by various investigators is shown in Fig. 6.33

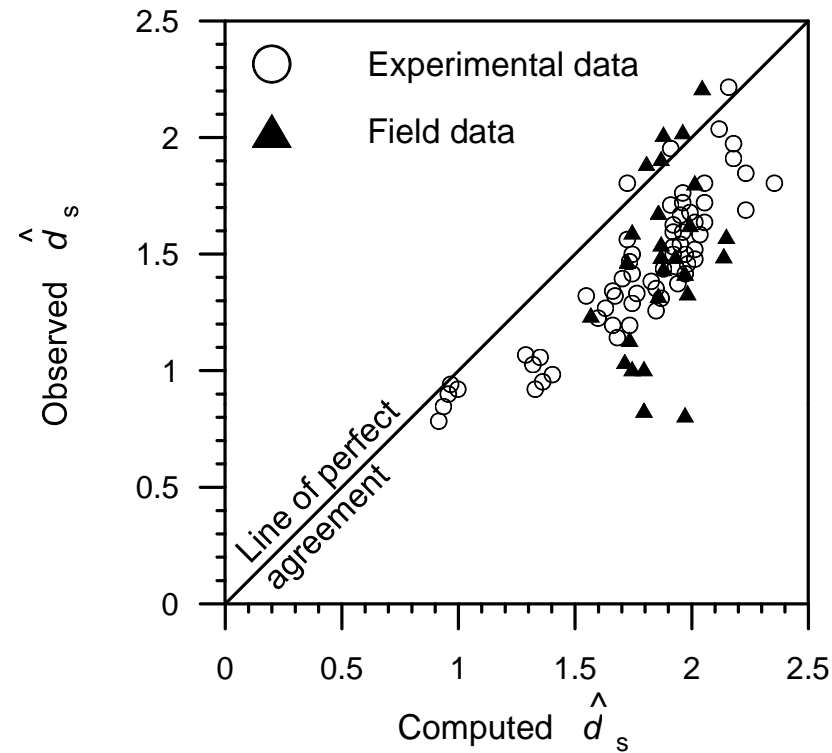


Fig. 6.33 Comparison between the equilibrium scour depths  $\hat{d}_s$  computed using the model and the experimental and field data (after **Dey** 1999)

## ***Equations of Equilibrium Scour Depth***

- A large number of empirical equations are proposed for the estimation of maximum scour depth at piers based on the model studies in laboratory experimental flumes (**Dey 1997a; Melville and Coleman 2000**)
- These equations are derived from a limited range of data and are applicable to the conditions similar to those for which they are valid
- The adequacy of these equations for the design purposes is difficult due to limited field measurements
- Design equations proposed by **Melville and Coleman (2000)** and **HEC18 (Richardson and Davis 2001)** seem to be good

- **Melville and Coleman's** (2000) design equation for the estimation of maximum scour depth  $d_s$  at piers as a product of  $K$ -factors is given by

$$d_s = K_h K_I K_d K_s K_\alpha K_t \quad (6.74)$$

where  $K_h$  = flow depth - foundation size factor;  $K_I$  = flow intensity factor;  $K_d$  = sediment size factor;  $K_s$  = pier shape factor;  $K_\alpha$  = pier alignment factor; and  $K_t$  = time factor. The relationships for these  $K$ -factors are as follows:

- The *flow depth - foundation size factor*  $K_h$  is the value of  $\hat{d}_s$  at a particular value of  $\hat{h}$ . It is obtained by the envelope curves for pier scour data as

$$K_h(b < 0.7h_1) = 2.4b \quad (6.75a)$$

$$K_h(0.7h_1 \leq b < 5) = 2(h_1 b)^{0.5} \quad (6.75b)$$

$$K_h(b \geq 5h_1) = 4.5h_1 \quad (6.75c)$$

- The *flow intensity factor*  $K_I$  is the ratio of scour depth at a particular flow velocity to that at the critical velocity for the bed sediment
- $K_I$  represents the effect of flow intensity on scour depth and it also accounts for the nonuniformity of sediments. It is given by

$$K_I = \frac{U_1 - (U_{ca} - U_c)}{U_c} \quad \text{for} \quad \frac{U_1 - (U_{ca} - U_c)}{U_c} < 1 \quad (6.76a)$$

$$K_I = 1 \quad \text{for} \quad \frac{U_1 - (U_{ca} - U_c)}{U_c} \geq 1 \quad (6.76b)$$

where  $U_{ca}$  = critical velocity for armor-layer particles

- The *sediment size factor*  $K_d$  is the ratio of  $\hat{d}_s$  at a particular value of  $\tilde{b}$  to that of  $\tilde{b}$ , where  $\hat{d}_s$  becomes a maximum and beyond which there is no effect of  $\tilde{b}$  on  $\hat{d}_s$ . It is obtained by envelope curves for pier scour data as

$$K_d(\tilde{b} \leq 25) = 0.57 \log(2.24\tilde{b}) \quad (6.77a)$$

$$K_d(\tilde{b} > 25) = 1 \quad (6.77b)$$

- For the piers embedded in gravel-beds, **Raikar and Dey (2005b)** proposed new sediment size factors. They are

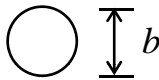

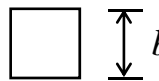

$$K_d(\tilde{b} \leq 10) = 0.25 \ln \tilde{b} + 0.363 \quad (6.78a)$$

$$K_d(10 < \tilde{b} \leq 25) = 0.076 \ln \tilde{b} + 0.75 \quad (6.78b)$$

$$K_d(\tilde{b} > 25) = 1 \quad (6.78c)$$

- The *shape factor*  $K_s$  is defined as the ratio of the scour depth for a particular pier shape to that for the circular piers. The shape factors  $K_s$  for different piers are given in Table 2

Table 2. Shape Factors  $K_s$  for Piers

Pier model	Pier shape	$K_s$
	Circular	1
	Round nosed	1
	Square nosed	1.1
	Sharp nosed	0.9

- The *alignment factor*  $K_\alpha$  is the ratio of the scour depth at an oblique pier to that at an aligned pier
- In case of non-circular piers, the scour depth increases with an increase in the effective projected width of the piers
- The multiplying factor  $K_\alpha$  for rectangular pier can be obtained by:

$$K_\alpha = (b_p / b)^{0.65} \quad (6.79)$$

where  $b_p$  = projected width of rectangular pier normal to the approaching flow (=  $L\sin\alpha + b\cos\alpha$ );  $\alpha$  = pier orientation relative to approaching flow; and  $L$  = pier length

- The curves for alignment factors proposed by **Laursen and Toch** (1956) are shown in Fig. 6.34

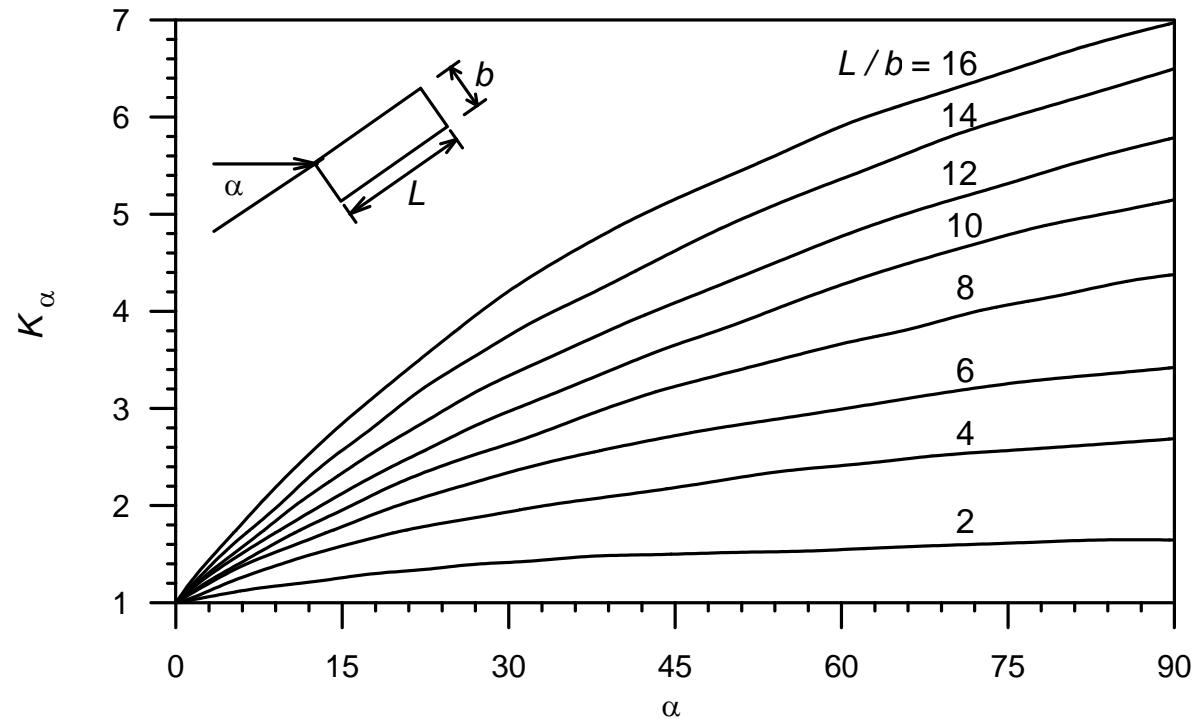


Fig. 6.34 Alignment factor  $K_\alpha$  (after Laursen and Toch 1956)



- The *time factor*  $K_t$  is the ratio of scour depth at a particular time  $t$  to the equilibrium scour depth. Its value depends on the scour condition
- For live-bed scour,  $K_t$  is unity
- For clear-water scour,  $K_t$  is given by

$$K_t = \exp \left\{ -0.03 \left| \frac{U_c}{U_1} \ln \left( \frac{t}{t_e} \right) \right|^{1.6} \right\} \quad (6.80)$$

where  $t_e$  = time to reach equilibrium scour depth

- At threshold condition ( $U_1 = U_c$ ),  $t_e$  being maximum, when  $h_1 > 6b$ , is given as

$$t_e (\text{days}) = 28.96 \frac{b}{U_1} \quad (6.81)$$

where  $b$  and  $U_1$  are in m and m/s, respectively

- According to **HEC18 (Richardson and Davis 2001)**, the scour depth at a pier in both clear-water and live-bed scour conditions is given by

$$\hat{d}_s = 2K_s K_\alpha K_{bed} K_a \left( \frac{h_1}{b} \right)^{0.35} F_1^{0.43} \quad (6.82)$$

where  $K_{bed}$  = factor for bed condition (Table 3);  $F_1 = U_1 / (gh_1)^{0.5}$ ; and  $K_a$  = factor for armoring of bed sediment

- The factors  $K_\alpha$  and  $K_a$  are furnished in Tables 4 and 5, respectively

Table 3. Factors  $K_{bed}$  for Bed Condition

Bed condition	Dune height $H$ (m)	$K_{bed}$
Clear-water scour	N/A	1.1
Plane bed and antidune flow	N/A	1.1
Small dunes	$3 > H > 0.6$	1.1
Medium dunes	$9 > H > 3$	1.1 - 1.2
Large dunes	$H \geq 9$	1.3

Table 4. Alignment Factors  $K_\alpha$  for Piers

$\alpha$ (degree)	$L/b = 4$	$L/b = 8$	$L/b = 12$
0	1	1	1
15	1.5	2	2.5
30	2	2.75	3.5
45	2.3	3.3	4.3
90	2.5	3.9	5

Table 5. Armor Factors  $K_a$

Minimum bed sediment size	$K_a$
$d_{50} \geq 0.06$ m	0.7

## Example

- Estimate the maximum equilibrium scour depth at bridge pier for the following data:
  - Square nosed rectangular pier having  $b = 2$  m,  $L = 12$  m inclined at 15 degree to the approaching flow direction
  - Approaching flow velocity,  $U_1 = 1.2$  m/s
  - Approaching flow depth,  $h_1 = 2$  m
  - Median size of bed sediment,  $d_{50} = 2$  mm
  - Geometric standard deviation of sediment,  $\sigma_g = 1.24$
  
- For  $d_{50} = 2$  mm, the critical shear velocity  $u_{*c}$  is calculated from Eq. (2.30a) – (2.30e) as 0.0362 m/s
  
- Using the equation of semi-logarithmic average velocity [ $U_c/u_{*c} = 5.75\log(0.5h_1/d_{50}) + 6$ ], the critical flow velocity  $U_c$  for  $h_1 = 2$  m is obtained as 0.78 m/s

- The  $K$ -factors are determined using Eqs. (6.75) – (6.80) as:
  1. For  $b/h_1 = 2/2 = 1$  (0.7 to 5),  $K_h = 2(2 \times 2)^{0.5} = 4$  m
  2. For  $U_1/U_c = 1.2/0.78 = 1.54 > 1$  (that is live-bed scour),  $K_l = 1$  and  $K_t = 1$
  3. For  $\tilde{b} = b/d_{50} = 2/(2 \times 10^{-3}) = 1000 > 25$ ,  $K_d = 1$
  4. For square nosed pier,  $K_s = 1.1$  (from Table 2)
  5. From Fig. 6.34,  $K_\alpha = 1.8$  for  $L/b = 12/2 = 6$  and  $\theta = 15^\circ$
  6.  $K_\sigma = 1$  for  $\sigma_g = 1.24 (< 1.4, \text{ that is uniform sediment})$
- Using **Melville and Coleman's** (2000) equation [Eq. (6.74)], the maximum scour depth at pier in uniform sediments is:  $d_s = K_h K_l K_d K_s K_\sigma K_t = 4 \times 1 \times 1 \times 1.1 \times 1.8 \times 1 = 7.92$  m

## **LOCAL SCOUR AT STRUCTURES (Part III)**

## Scour at Bridge Abutments

- Scour at bridge abutments is also equally responsible for failure of bridges as scour at piers
- A study of the US Federal Highway Administration in 1973 concluded that of 383 bridge failures, 25% involved pier damage and 72% involved abutment damage (**Richardson et al.** 1993)
- **Macky** (1990) mentioned that about 50% of total expenditure was made towards the bridge damage repairing and maintenance, out of which 70% was spent towards the abutment scour
- Abutment scour has been studied extensively by various researchers (see review given by **Barbhuiya and Dey** 2004)



## ***Flow Field around Bridge Abutments***

- The flow field at an abutment is complex
- The complexity increases with the development of the scour hole involving separation of flow to develop three-dimensional vortex flow
- **Ahmed and Rajaratnam** (2000) studied the flow fields at abutment placed on a planar or unscoured bed
- **Kwan** (1988) and **Kwan and Melville** (1994) used the hydrogen bubble technique to measure the three-dimensional flow field in a scour hole at a wing-wall abutment
- They identified a primary vortex, which is similar to the horseshoe vortex at piers, along with the downflow being the principal cause of scour at abutments
- Fig. 6.35 shows the major flow components at a wing-wall abutment identified by **Kwan** (1988)

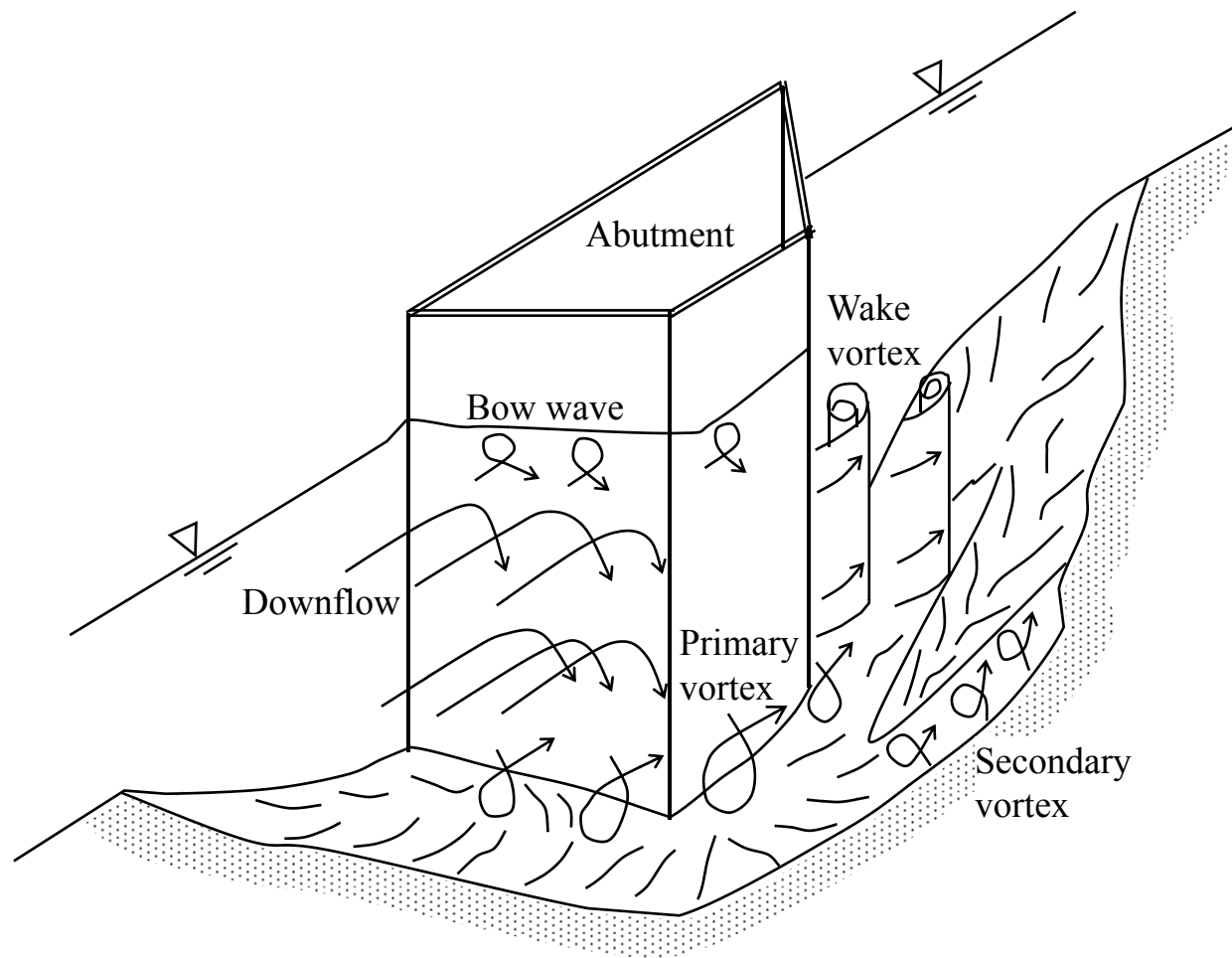


Fig. 6.35 Schematic of flow field at an abutment after **Kwan** (1988)

- **Barbhuiya** (2003) investigated the three-dimensional turbulent flow fields at vertical-wall, 45° wing-wall and semicircular abutments, placed vertically on a flat rigid bed and in stabilized erodible scoured bed, using the acoustic Doppler velocimeter (ADV)
- The normalized velocity vectors at different azimuthal sections (Fig. 6.36) of a 45° wing-wall abutment with a scour hole are shown in Fig. 6.37 (**Dey and Barbhuiya 2006**)
- In Fig. 6.37,  $\hat{x} = x/l$ ;  $\hat{r} = r/l$ ;  $x$  = streamwise distance;  $r$  = radial distance; and  $l$  = abutment length transverse to flow

# 45° wing-wall abutment

(after Dey and Barbhuiya 2006)

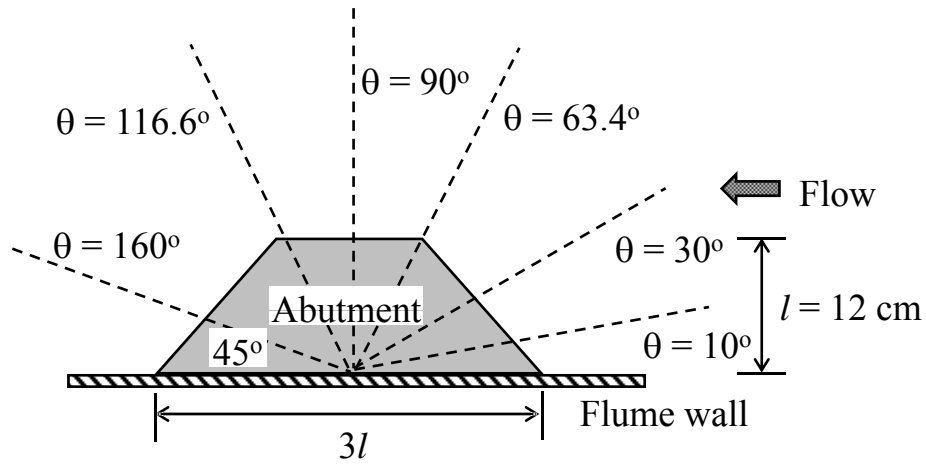


Fig. 6.36 Sections of flow measurements

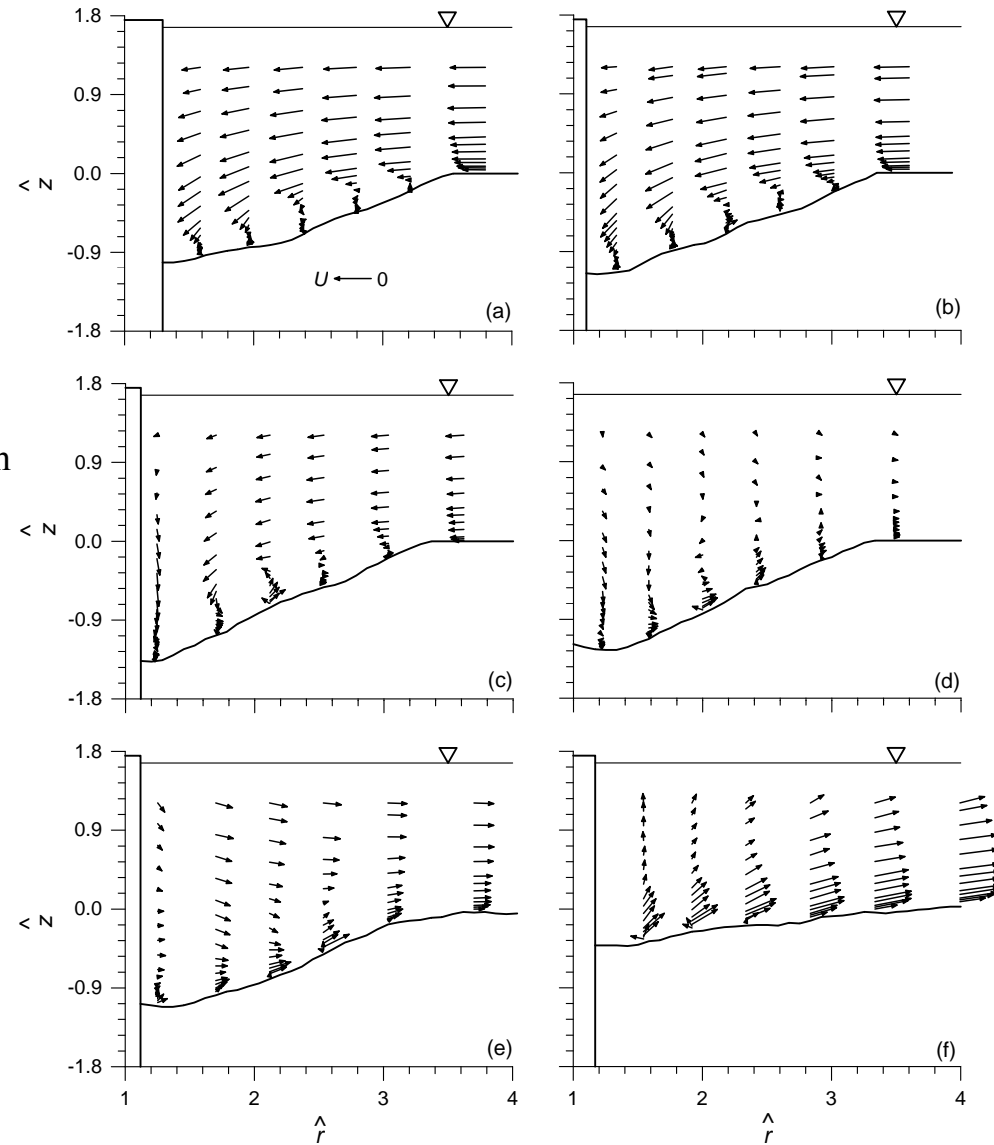


Fig. 6.37 Normalized velocity vectors at azimuthal sections: (a)  $\theta = 10^\circ$ ; (b)  $\theta = 30^\circ$ ; (c)  $\theta = 63.4^\circ$ ; (d)  $\theta = 90^\circ$ ; (e)  $\theta = 116.6^\circ$  and (f)  $\theta = 160^\circ$

## ***Parameters Influencing Scour Depth at Abutments***

- Parameters involved in the scour phenomenon at abutments can be grouped as follows:
  - Parameters relating to the abutment: Size, shape, spacing, number and orientation with respect to the approaching flow direction
  - Parameters relating to the bed sediment: Median size, particle size distribution, mass density, angle of repose and cohesiveness
  - Parameters relating to the approaching flow condition: Approaching flow velocity, approaching flow depth, shear velocity and roughness
  - Parameters relating to the fluid: Mass density, viscosity, gravitational acceleration and temperature (may not be important in scour problems)

- Parameters relating to the geometry of channel: Width, cross-sectional shape and slope
  - Parameters relating to the time: Time of scouring for an evolving scour hole
  - Parameters relating to the unsteadiness: Passage of flood wave in rivers and waves in marine environment
- The relationship showing the influence of various parameters on the equilibrium scour depth  $d_s$  at abutments can be given in functional form as follows:

$$d_s = f_1(U_1, h_1, \rho, \rho_s, g, \nu, l, d_{50}, \sigma_g, t) \quad (6.83)$$

The dependency of scour depth on various parameters studied by **Dey and Barbhuiya (2004a)** is presented

## Effect of Abutment Length - Sediment Diameter Ratio on Scour Depth

- The variation of nondimensional equilibrium scour depth  $\hat{d}_s (= d_s/l)$  at abutments in sand-beds as a function of  $\tilde{l} (= l/d_{50})$  under clear-water scour condition is given in Fig. 6.38(a)

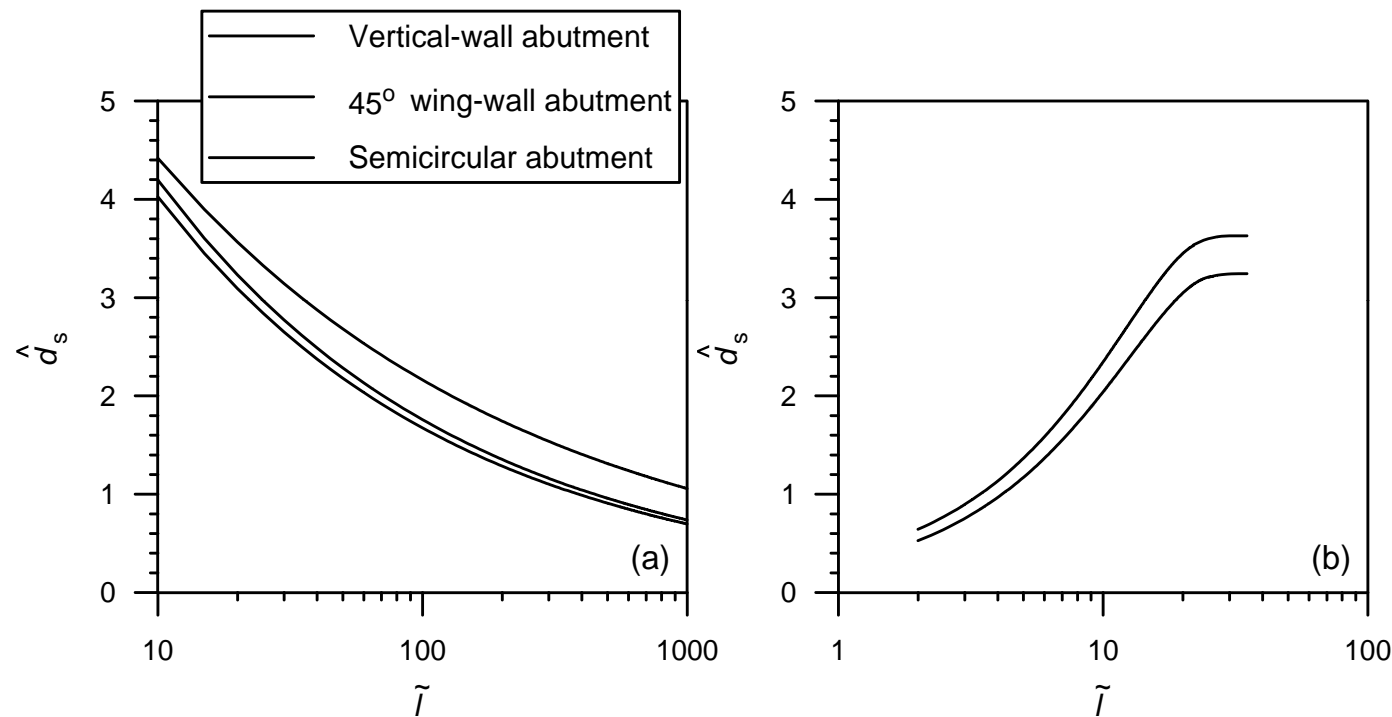


Fig. 6.38 Variation of  $\hat{d}_s$  with  $\tilde{l}$  for  $U_1/U_c \approx 1$ : (a) in sand-beds (after **Dey and Barbhuiya 2004a**) and (b) in gravel-beds (after **Raikar and Dey 2005b**)

- The equilibrium scour depth  $\hat{d}_s$  decreases with an increase in  $\tilde{l}$
- The trend is almost opposite to pier scour
- $\hat{d}_s$  is greater for smaller abutment length and coarser sediment size
- The substantial increase of approaching flow velocity  $U_1$  to maintain the clear-water scour condition for a coarser sediment size increases the strength of the primary vortex and the downflow to a great extent, resulting in a vortex flow with an enhanced scour potential
- $\hat{d}_s$  is independent of  $\tilde{l}$  for larger abutment length and finer sediment size
- For a given  $\tilde{l}$ , the magnitude of  $\hat{d}_s$  for vertical-wall abutment is greater than that for other types of abutments
- The variation of  $\hat{d}_s$  with  $\tilde{l}$  for the 45° wing-wall and vertical-wall abutments in gravel-beds studied by **Raikar and Dey (2005b)**, is presented in Fig. 6.38(b)



## Effect of Approaching Flow Depth - Abutment Length Ratio on Scour Depth

- The dependency of  $\hat{d}_s$  at 45° wing-wall abutments for clear-water scour condition on approaching flow depth - abutment length ratio  $\hat{h}$  ( $= h_1/l$ ) for different  $\tilde{l}$  and  $d_{50} = 0.26$  mm is presented in Fig. 6.39 (**Dey and Barbhuiya 2004a**)

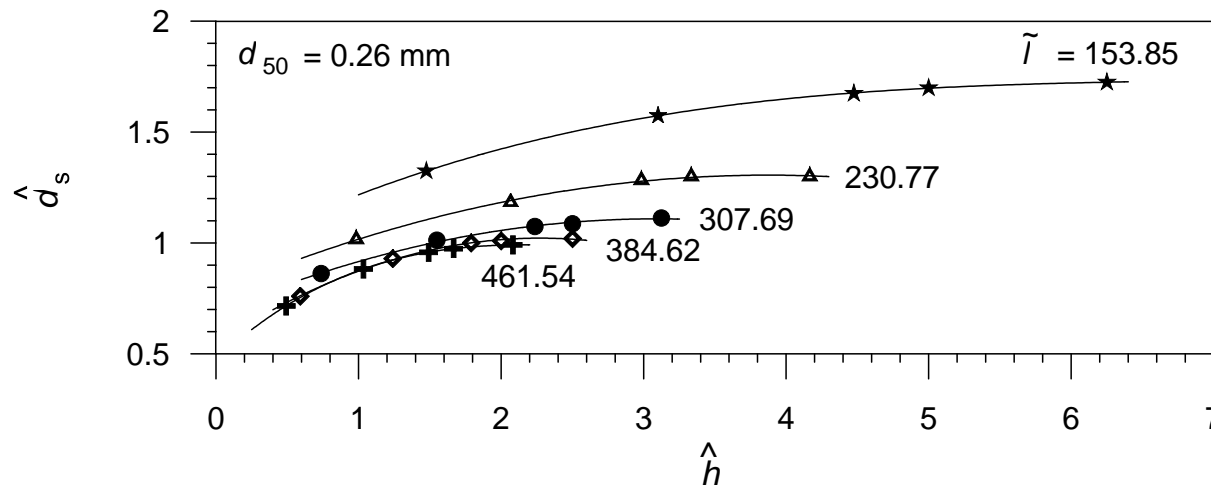


Fig. 6.39 Dependency of  $\hat{d}_s$  on  $\hat{h}$  for 45° wing-wall abutments for  $U_1/U_c \approx 1$  (after **Dey and Barbhuiya 2004a**)

- At small  $\hat{h}$ , the nondimensional equilibrium scour depth  $\hat{d}_s$  increases significantly with an increase in  $\hat{h}$
- As  $\hat{h}$  increases,  $\hat{d}_s$  becomes almost independent of  $\hat{h}$
- The variation of  $\hat{d}_s$  with  $\hat{h}$  has similar trend as that of pier scour case (see Fig. 6.28)
- For large  $l$ , scour depth  $d_s$  is essentially independent of flow depth at  $\hat{h}$  being two, while for small  $l$ ,  $\hat{h}$  is approximately six
- That is there is a little increase in strength of primary vortex due to an increase in flow depth beyond two and six times of abutment length for large and small abutment sizes, respectively
- It is also apparent that  $\hat{d}_s$  decreases with an increase in  $\tilde{l}$
- For shallow flow depths, the surface roller, termed bow wave, having a sense of rotation opposite to the primary vortex, helps to reduce the strength of primary vortex, resulting in a reduced scour depth

## Effect of Sediment Gradation on Scour Depth

- Similar to pier scour, the particle size distribution  $\sigma_g$  of sediments also has a pronounced influence on the scour depth at abutments
- Nonuniform sediments ( $\sigma_g > 1.4$ ) consistently produce lower scour depths than that in uniform sediments due to formation of armor-layer within the scour hole
- The equilibrium scour depth  $d_s(\sigma_g)$  at abutments embedded in nonuniform sediments can be obtained by multiplying the equilibrium scour depth at abutments in uniform sediments by the coefficient  $K_\sigma$  [as shown in Eq. (6.3)]
- The variations of  $K_\sigma$  with  $\sigma_g$  for vertical-wall, 45° wing-wall and semicircular abutments are given in Fig. 6.40
- For different abutments, scour depth in nonuniform sediment with  $\sigma_g = 3.5$  is drastically reduced to 20% of scour depth in uniform sediment

- For  $\sigma_g > 3.5$ , the reduction of scour depth is not influenced by the nonuniformity of sediments
- For a given  $\sigma_g$ , coefficient  $K_\sigma$  for vertical-wall abutment is slightly greater than that for other types of abutments

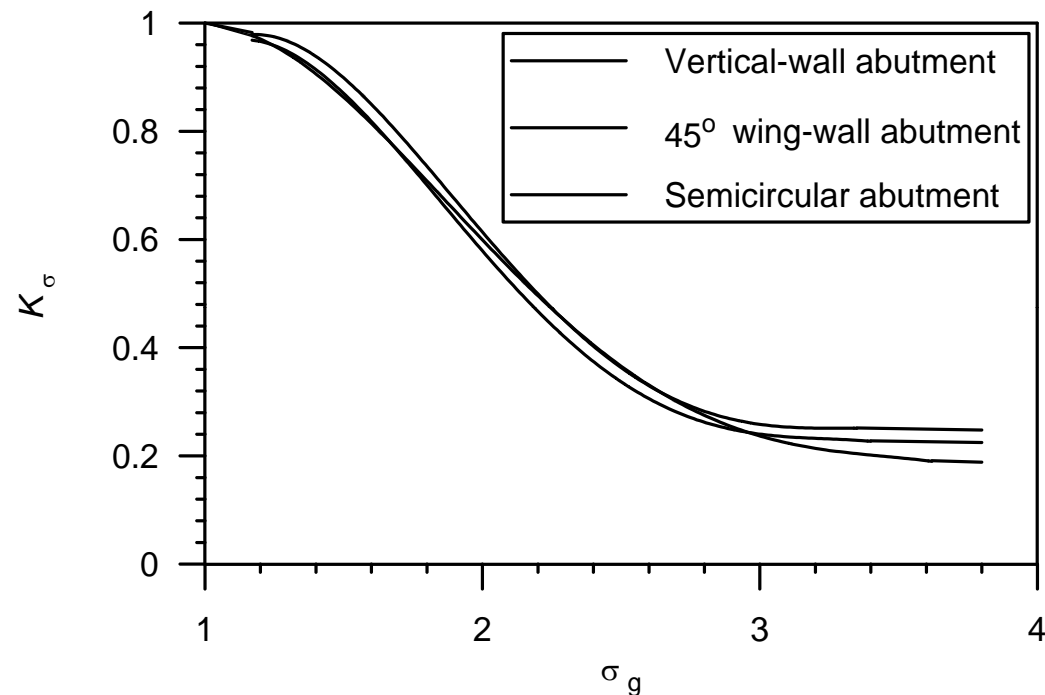


Fig. 6.40 Variation of  $K_\sigma$  as a function of  $\sigma_g$  for abutments under  $U_1/U_c \approx 1$  (after **Dey and Barbhuiya 2004a**)

## Time-Variation of Scour Depth

### Scour Depth in Uniform Sediments:

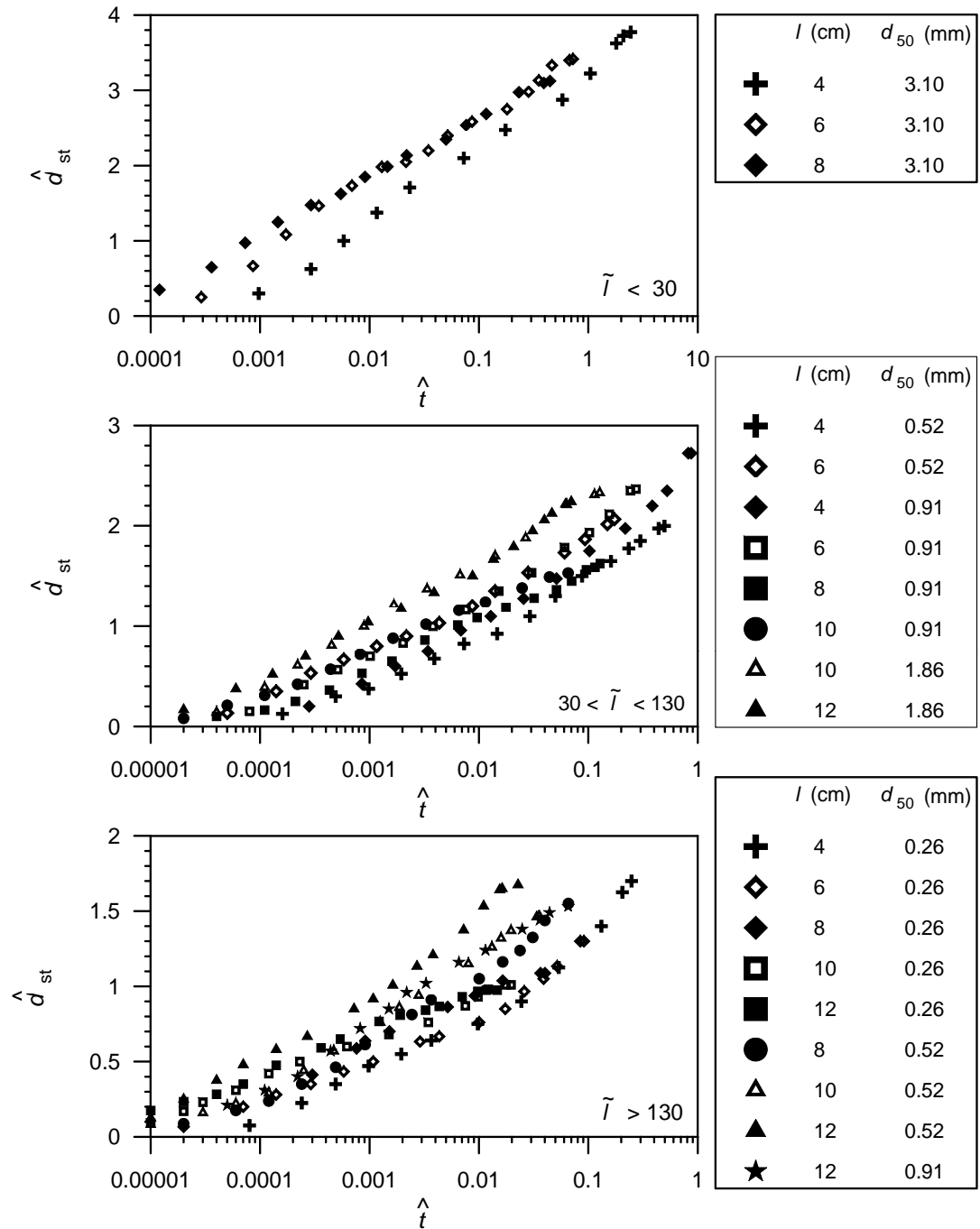
- **Dey and Barbhuiya (2004a)** studied the time-variation of clear-water scour at different sizes of vertical-wall, 45° wing-wall and semicircular abutments embedded in various uniform sediment sizes
- The nondimensional instantaneous scour depth  $\hat{d}_{st}$  at an abutment is represented in functional form as

$$\hat{d}_{st} = f(\hat{t}, \tilde{l}) \quad (6.84)$$

where  $\hat{d}_{st} = d_{st}/l$ ;  $d_{st}$  = instantaneous scour depth at time  $t$ ;  $\hat{t} = S/(R_l)$ , that is the nondimensional time;  $S_l = Ut/l$ , that is the Strouhal number; and  $R_l = Ul/\nu$ , that is the abutment Reynolds number

- The variation of nondimensional instantaneous scour depth  $\hat{d}_{st}$  with nondimensional time  $\hat{t}$  for 45° wing-wall of different  $\tilde{l}$  is presented in Fig. 6.41

Fig. 6.41 Variation of  $\hat{d}_{st}$  as a function of  $\hat{t}$  for 45° wing-wall abutments in uniform sediments for  $U_1/U_c \approx 1$  (after **Dey and Barbhuiya 2004a**)



• Density of sediment (given by  $\rho_s$ )

- In the initial stage, the rate of scouring is rapid

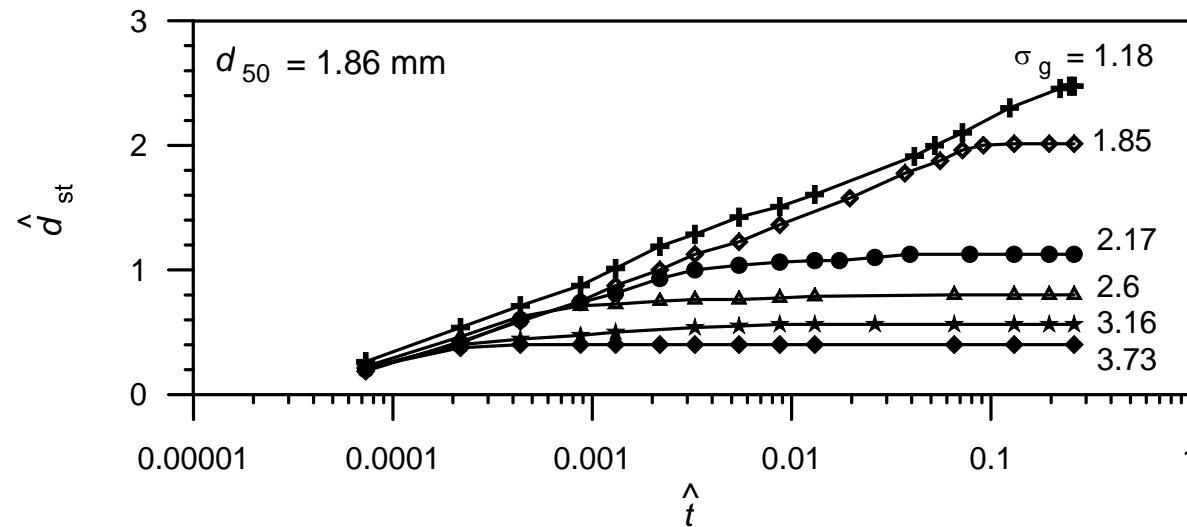


Fig. 6.42 Variation of  $\hat{d}_{st}$  with  $\hat{t}$  for different  $\sigma_g$  and  $d_{50} = 1.86$  mm for  $45^\circ$  wing-wall abutments under  $U_1/U_c \approx 1$  (after **Dey and Barbhuiya 2004a**)



## ***Equations of Equilibrium Scour Depth***

- Number of proposed equations for the estimation of maximum scour depth at abutments is overwhelming (**Barbhuiya and Dey 2004**)
- Their application is limited to the conditions similar to those for which they are valid
- The design approach recommended by **Melville and Coleman** (2000) for the estimation of maximum scour depth at abutments based on empirical relationship, called *K*-factors is given by

$$d_s = K_h K_I K_d K_s K_\alpha K_G K_t \quad (6.85)$$

where  $K_h$  = flow depth - foundation size factor;  $K_I$  = flow intensity factor;  $K_d$  = sediment size factor;  $K_s$  = abutment shape factor;  $K_\alpha$  = abutment alignment factor;  $K_G$  = channel geometry factor; and  $K_t$  = time factor

- The relationships for  $K$ -factors are given as follows:
- The *flow depth - foundation size factors*  $K_h$  for abutments scour are

$$K_h(l < h_1) = 2l \quad (6.86a)$$

$$K_h(h_1 \leq l < 25h_1) = 2(h_1 l)^{0.5} \quad (6.86b)$$

$$K_h(l < h_1) = 10h_1 \quad (6.86c)$$

- The *flow intensity factor*  $K_f$  given by Eqs. (6.76a) and (6.76b) for the case of pier scour is also applicable for the abutment scour
- The *sediment size factor*  $K_d$ , which is same as for the pier scour, given by Eqs. (6.77a) and (6.77b) is also applicable for the estimation of scour depth at abutments in sand-beds
- However, for the abutments in gravel-beds, **Raikar and Dey** (2005b) proposed new sediment size factors as

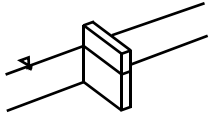
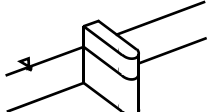
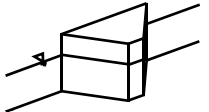

$$K_d(\tilde{l} \leq 10) = 0.514 \ln \tilde{l} - 0.273 \quad (6.87a)$$

$$K_d(10 < \tilde{l} \leq 25) = 0.098 \ln \tilde{l} + 0.682 \quad (6.87b)$$

$$K_d(\tilde{l} > 25) = 1 \quad (6.87c)$$

- The *shape factor*  $K_s$  is defined as the ratio of the scour depth for a particular abutment shape to that for the vertical-wall abutments. The values of shape factors  $K_s$  for different shapes of abutments are given in Table 6

Table 6. Shape Factors  $K_s$  for Abutments

Abutment model	Abutment shape	$K_s$
	Vertical-wall	1
	Semicircular ended	0.75
	45° wing-wall	0.75
	Spill-through with slope horizontal : vertical 0.5 : 1 1 : 1 1.5 : 1	0.6 0.5 0.45

- For long abutments (abutment length / upstream flow depth > 1), the values of *alignment factor*  $K_\alpha$  are given in Table 7

Table 7. Alignment Factors  $K_\alpha$  for Long Abutments

$\alpha$ (degree)	30	45	60	90	120	135	150
$K_\alpha$	0.9	0.95	0.98	1	1.05	1.07	1.08

- For short abutments, the values of alignment factor  $K_\alpha^*$  are

$$K_\alpha^*(l \geq 3h_1) = K_\alpha \quad (6.88a)$$

$$K_\alpha^*(h_1 < l < 3h_1) = K_\alpha + (1 - K_\alpha)(1.5 - 0.5b/h_1) \quad (6.88b)$$

$$K_\alpha^*(l \leq h_1) = 1 \quad (6.88c)$$

- The *channel geometry factor*  $K_G$  is defined as the ratio of the scour depth at an abutment to that at the same abutment in the equivalent rectangular channel
- In case of rectangular channels, the channel geometry factor  $K_G = 1$
- For abutments in compound channels,  $K_G$  depends on the position of the abutment in the compound channel
- The equation of  $K_G$  is

$$K_G = \sqrt{1 - \left(\frac{l^*}{l}\right) \left[ 1 - \left(\frac{h_1^*}{h_1}\right)^{5/3} \left(\frac{n}{n^*}\right) \right]} \quad (6.89)$$

where  $l^*$  = abutment length spanning the flood channel;  $h_1^*$  = flow depth in the flood channel; and  $n$  and  $n^*$  = Manning roughness coefficient in the main and flood channels, respectively

- The *time factor*  $K_t$  is the ratio of scour depth at a particular time  $t$  to the equilibrium scour depth. Its value depends on the scour condition
- For live-bed scour,  $K_t$  is unity
- For clear-water scour,  $K_t$  is given by

$$K_t = 0.1 \frac{U_c}{U_1} \ln \left( \frac{t}{t_e} \right) + 1 \quad (6.90)$$

where the expressions for  $t_e$  can be given by

$$t_e \text{ (days)} = 25h_1 / U_1 \quad (6.91)$$

$$t_e \text{ (days)} = 20.83 l / U_1 \quad (6.92)$$

- **HEC18 (Richardson and Davis 2001)** recommends **Froehlich's** (1989) equation of the live-bed scour at abutments for the estimation of maximum scour depth. It is

$$\frac{d_s}{h_1} = 2.27 K_s K_\alpha \left( \frac{l}{h_1} \right)^{0.43} F_r^{0.61} + 1 \quad (6.93)$$

where  $F_r = U_e / (gh_1)^{0.5}$ ;  $U_e = Q_e / A_e$ ;  $Q_e$  = flow rate obstructed by the abutment and approach embankment; and  $A_e$  = flow area of the approaching cross-section obstructed by the embankment

- The values of shape factors  $K_s$  are furnished in Table 8, while the alignment factor  $K_\alpha$  can be obtained from Fig. 6.43



Table 8. Shape Factors  $K_s$  for Abutments

Abutment shape	$K_s$
Vertical-wall abutment	1
Vertical-wall abutment with wing walls	0.82
Spill-through abutment	0.55

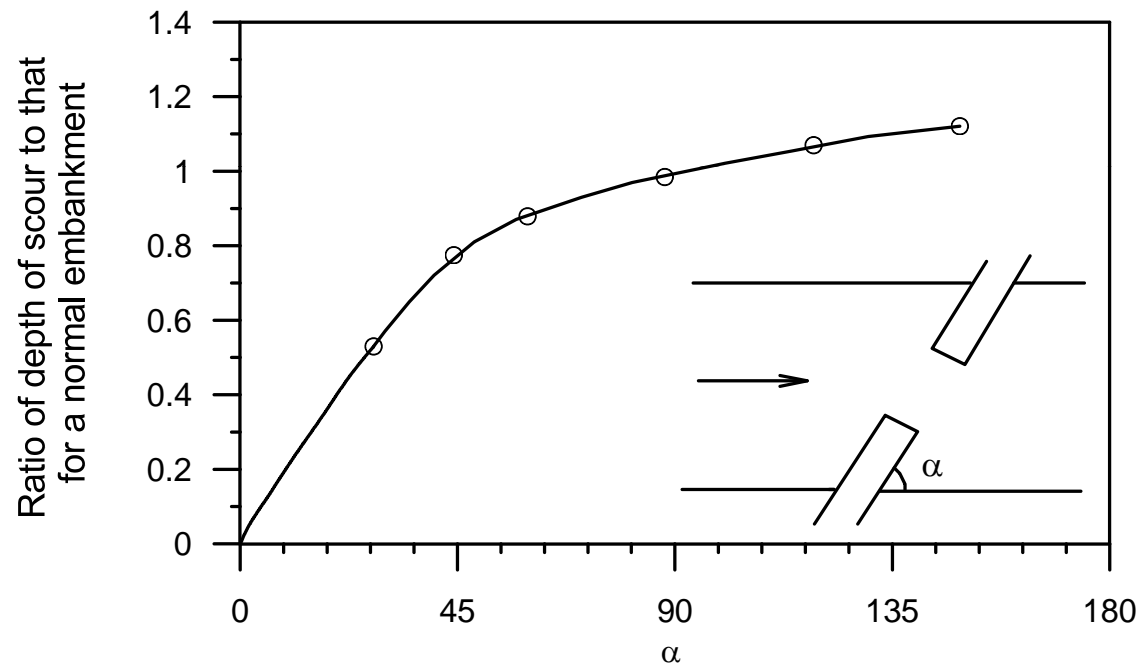


Fig. 6.43 Alignment factors  $K_\alpha$  for abutments (after **HEC18**)

## Example

- Determine the maximum equilibrium scour depth at an abutment for the following data:
  - Wing-wall abutment having  $l = 12.5$  m inclined at  $60^\circ$  to the approaching flow direction
  - Approaching flow velocity,  $U_1 = 1.1$  m/s
  - Approaching flow depth,  $h_1 = 8$  m
  - Median size of bed sediment,  $d_{50} = 2.3$  mm
  - Geometric standard deviation of sediment,  $\sigma_g = 1.14$
  - Manning roughness coefficient,  $n = 0.02$  SI units
  - Channel geometry,  $l^* = 110$  m,  $h_1^* = 2$  m and  $n^* = 0.04$

- For  $d_{50} = 2.3$  mm, the critical shear velocity  $u_{*c}$  is calculated from Eq. (2.30a) – (2.30e) as 0.0397 m/s
- Using the equation of semi-logarithmic average velocity [ $U_c/u_{*c} = 5.75\log(0.5h_1/d_{50}) + 6$ ] the critical flow velocity  $U_c$  corresponding to  $h_1 = 8$  m is obtained as 0.98 m/s
- The  $K$ -factors are:
  1. For  $l/h_1 = 12.5/8 = 1.563 > 1$  (that is a long abutment), using Eq. (6.86b),  $K_h = 2(12.5 \times 8)^{0.5} = 20$  m
  2. For  $U_1/U_c = 1.1/0.98 = 1.125 > 1$  (live-bed scour condition), using Eq. (6.76b)  $K_l = 1$  and corresponding  $K_t = 1$
  3. For  $\tilde{l} = l/d_{50} = 12.5/(2.3 \times 10^{-3}) = 5434.78 > 25$ , using Eq. (6.77b)  $K_d = 1$
  4. For wing-wall abutment,  $K_s = 0.75$  (from Table 6)

5. For  $\alpha = 60^\circ$ ,  $K_\alpha = 0.98$  (from Table 7)
  6. From Eq. (6.89),  $K_G = 0.405$
  7. For  $\sigma_g = 1.14 < 1.4$  (that is uniform sediment),  $K_\sigma = 1$
- Using **Melville and Coleman's** (2000) equation [Eq. (6.85)], the maximum scour depth at wing-wall abutment in uniform sediments is:  $d_s = K_h K_l K_d K_s K_\alpha K_G K_t = 20 \times 1 \times 1 \times 0.75 \times 0.98 \times 0.405 \times 1 = 5.95$  m

## Scour in Armored Beds

- In the upper reaches, riverbeds are commonly composed of a mixture of different sizes of sands and gravels
- Under the varied stream flow velocities, a process of armoring on the riverbeds commences resulting in an exposure of coarser particles due to washing out of the finer fraction
- The armor-layers of concern are those where the structure is embedded in a sand-bed overlain by a layer of gravels, formed owing to the sorting of riverbed sediments
- The armor-layer extends the magnitude of critical flow velocity for the motion of bed particles, sustaining an extended clear-water scour condition up to the limiting stability of surface particles, as shown in Fig. 6.44

- As a consequence of the surface particles at critical condition, a considerably larger scour depth develops in an armored bed (unless a secondary armor-layer developed within the scour hole is compact enough to prevent further scouring) than in a bed of uniform sediments

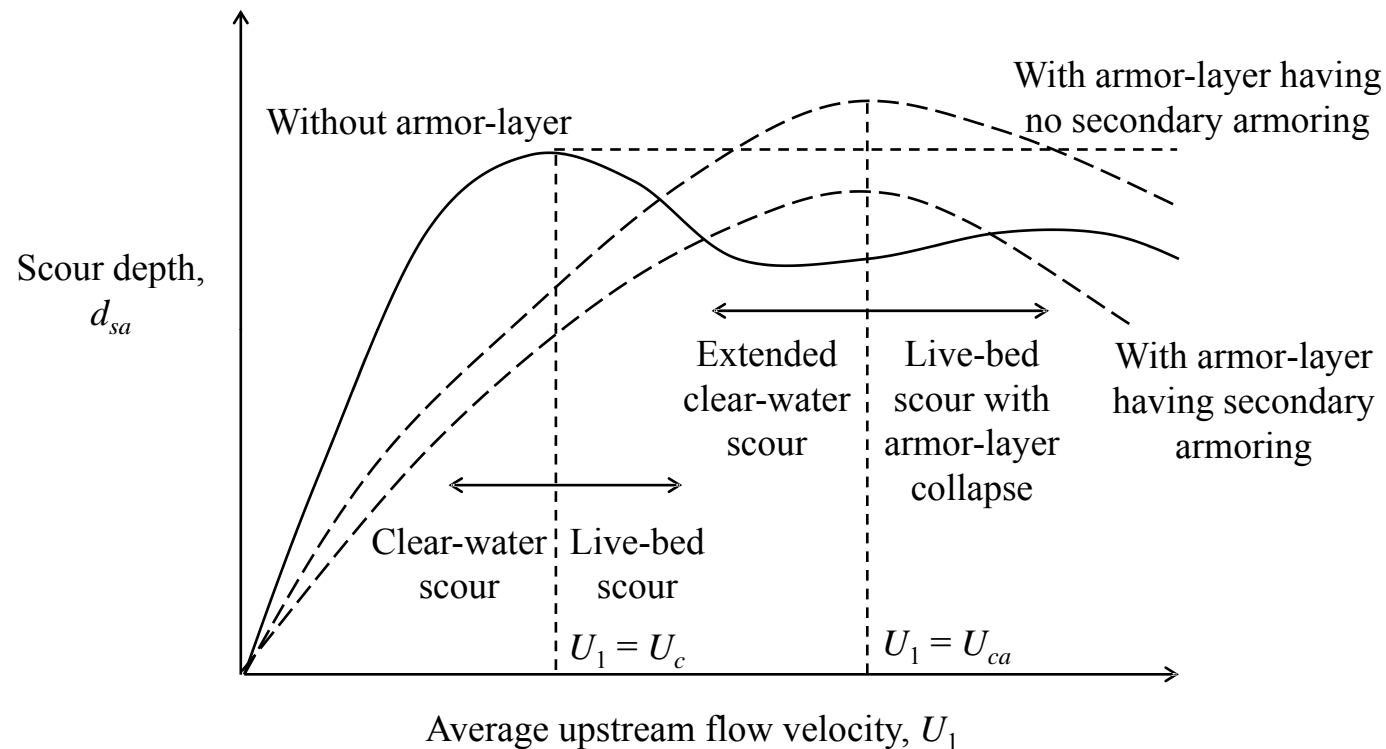


Fig. 6.44 Effect of armor-layer on scour depth as a function of upstream flow velocity

## ***Scour within Channel Contractions in Armored Beds***

- **Raikar and Dey** (2006) [also in **Raikar** (2006)] investigated scour within channel contractions in sand-bed with a thin surface-layer of gravels
- They reported that the scour depth (relative to the approaching flow depth) within long contractions with surface-layers increases
  - with an increase in surface-gravel to bed-sand size ratio  $\tilde{d}_g$  ( $= d_g/d_{50}$ ; where  $d_g$  = median size of surface-gravels; and  $d_{50}$  = median size of bed-sand) and
  - with a decrease in channel opening ratio  $\hat{b}$
- The scour depth within a channel contraction with a surface-layer of gravels is greater than that without surface-layer for the same bed sediments and flow condition

- When the flow velocity in the contracted zone of channel reaches the critical velocity  $U_{ca}$  for the gravels in the surface-layer, the gravel-layer is scoured
- Bed-sand is exposed to the flow velocity, which is far greater than the critical velocity  $U_c$  of bed-sand
- The bed-sand in the contracted zone scours significantly
- With an increase in scour depth in the contracted zone, the flow velocity in the contracted zone decreases
- As the flow velocity approaches the value of critical velocity for the bed-sand, scour within the contraction ceases and the equilibrium of the scour hole is attained
- At equilibrium, the original surface-layer of gravels remains intact in the upstream bed of uncontracted channel



- In the contracted zone, the scoured gravel particles of the surface-layer are distributed in a scattered and loose manner
- Fig. 6.45 displays the photograph of the equilibrium scour hole within a long contraction with a gravel-layer



Fig. 6.45 Photograph showing equilibrium scour within a long contraction with a thin gravel-layer

- The variation of nondimensional scour depth  $\hat{d}_{sa}$  ( $= d_{sa}/h_1$ ; where  $d_{sa}$  = equilibrium scour depth in armored bed) versus  $\tilde{d}_g$  for the bed-sand of  $d_{50} = 1.86$  mm under  $U_1/U_{ca} \approx 1$  (that is maximum limit of clear-water scour) is shown in Fig. 6.46(a)

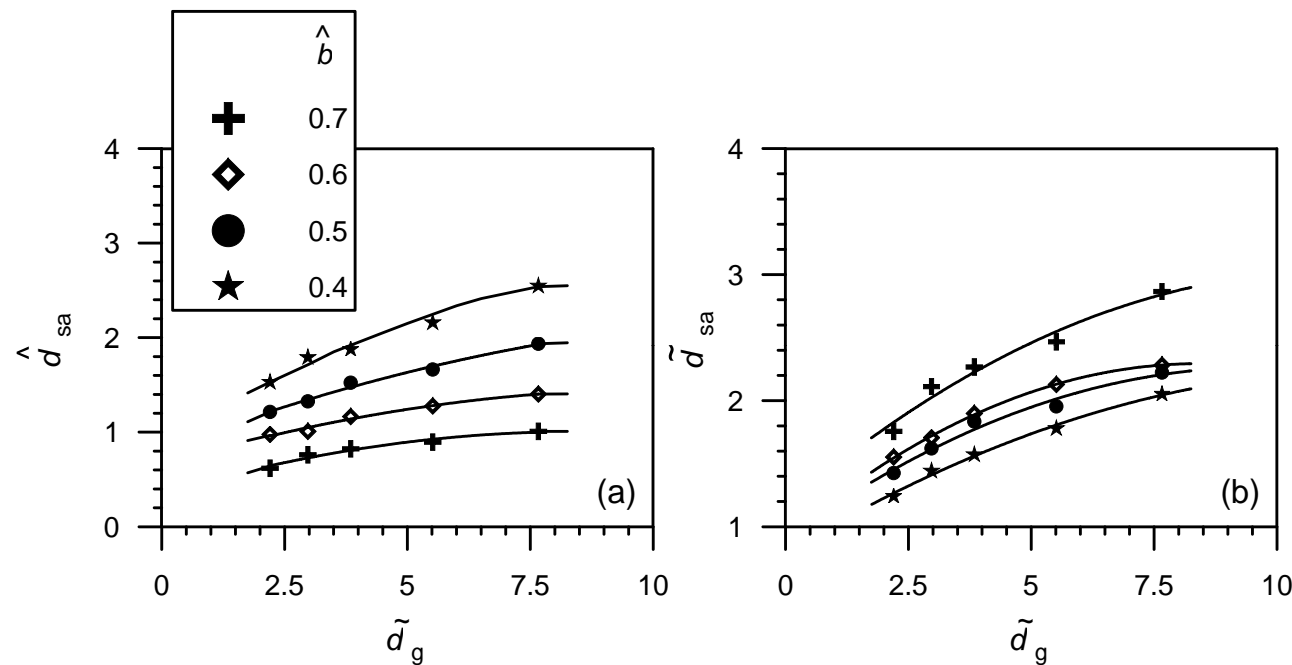


Fig. 6.46 (a) Variations of scour depth  $\hat{d}_{sa}$  with  $\tilde{d}_g$  for different  $\hat{b}$  and  $d_{50} = 1.86$  mm and (b) Variations of scour depth  $\tilde{d}_{sa}$  with  $\tilde{d}_g$  for different  $\hat{b}$  and  $d_{50} = 1.86$  mm (after **Raikar and Dey 2006**)

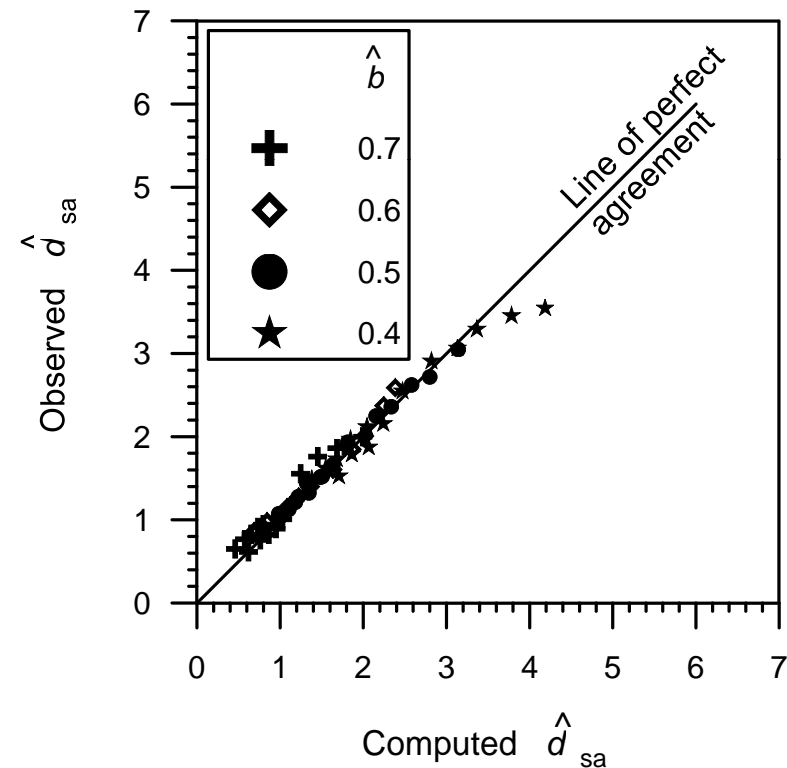
- $\hat{d}_{sa}$  increases with an increase in  $\tilde{d}_g$
- Also,  $\hat{d}_{sa}$  increases significantly with a decrease in channel opening ratio  $\hat{b}$
- Fig. 6.46(b) displays the variations of  $\tilde{d}_{sa}$  with  $\tilde{d}_g$  for different values of  $\hat{b}$  and  $d_{50} = 1.86$  mm under approaching flow close to the maximum limit of clear-water scour

where  $\tilde{d}_{sa} = d_{sa}/d_s$ , that is the ratio of scour depth within long contractions with surface-layers to those of scour depth within long contractions in un-layered bed-sands; and  $d_s$  = scour depth within long contractions in un-layered uniform sands

- $\tilde{d}_{sa}$  increases with an increase in  $\tilde{d}_g$
- As  $\tilde{d}_{sa} > 1$ , scour depths within long contractions with surface-layers of gravels are always greater than those in uniform bed sediments (un-layered beds)

- The maximum equilibrium scour depth within a long contraction with gravel-layer  $d_{sa}$  was computed using the energy and continuity equations [using **Dey and Raikar's** (2005) clear-water scour model without sidewall correction]
- The comparison of  $\hat{d}_{sa}$  computed using the model with the experimental data is shown in Fig. 6.47

Fig. 6.47 Comparison between the equilibrium scour depths  $\hat{d}_{sa}$  computed using clear-water scour model (**Dey and Raikar** 2005) and the experimental data of **Raikar and Dey** (2006)



## ***Scour at Bridge Piers in Armored Beds***

- **Ettema** (1980) and **Raudkivi and Ettema** (1985) studied scour at piers in thin armor-layer and stratified beds
- Thickness of stratified bed was more than that of natural armor-layer thickness
- **Froehlich** (1995) reported that the natural armor-layer thickness being one to three times the armor particle sizes
- **Raikar** (2006) studied the scour at piers embedded in a bed of uniform sands of median size  $d_{50}$  overlain by a thin armor-layer of uniform gravels of size  $d_g$
- The thickness of armor-layers was twice the armor-gravel size
- The influences of various parameters on scour depth along with the design equation for maximum scour depth at bridge piers embedded in armor-layers was reported **Raikar** (2006)

## Classification of Scour Hole and Scouring Process

- For the approaching flow velocities  $U_1$  nearly equaling the critical velocity  $U_{ca}$  for armor particles ( $U_1/U_{ca} \approx 0.9$ ), three different cases of idealized topography of scour holes were identified [Figs. 6.48(a) – 6.48(c)], depending on the pier width, flow depth and ratio of armor-gravel to bed-sand size  $\tilde{d}_g$
- The salient features of three cases of scour hole are:

- Case 1: The scour hole in the vicinity of a pier develops through the armor-layer removing the sand from the bed underneath. The armor-layer remains intact around the perimeter of the scour hole [Fig. 6.48(a)]

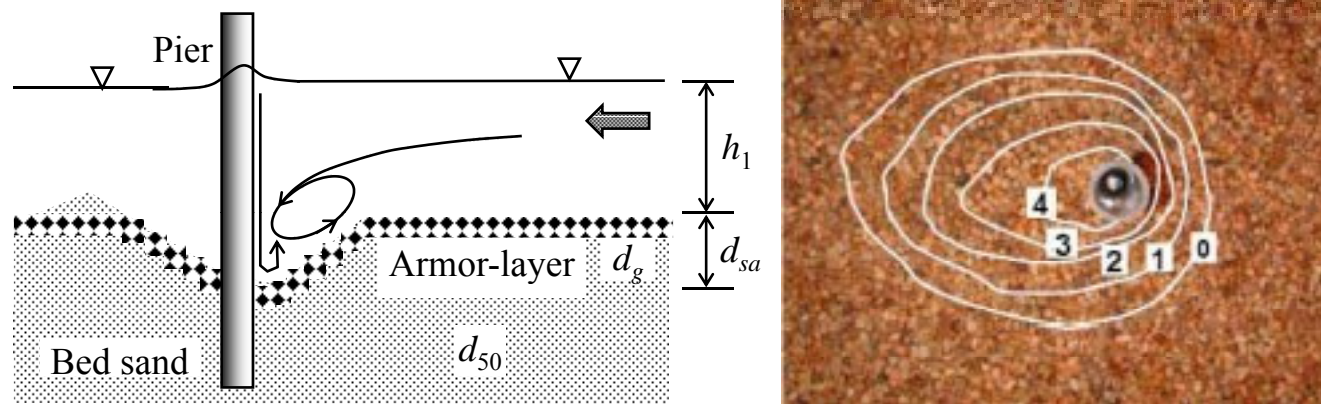


Fig. 6. 48(a) Schematic of scour holes at pier in armored beds: case 1

- Case 2: The scour hole in the vicinity of a pier forms through the armor-layer having relatively more extension of scour hole in the upstream. The armor-layer disintegrates over a short distance downstream. However, the armor-layer remains intact around the upstream perimeter of the scour hole [Fig. 6.48(b)] [same as “case b” in Raudkivi and Ettema (1985)]

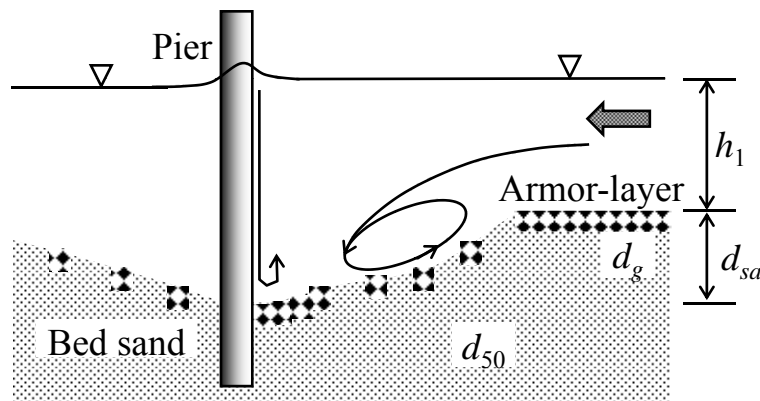


Fig. 6. 48(b) Schematic of scour holes at pier in armored beds: case 2



- Case 3: The scour hole in the vicinity of a pier develops collapsing the armor-layer over a considerable distance upstream. On the other hand, the armor-layer washed out completely downstream. However, the armor-layer exists in the far upstream perimeter of the scour hole in the form of a large arc [Fig. 6.48(c)] [same as “case c” in **Raudkivi and Ettema (1985)**]

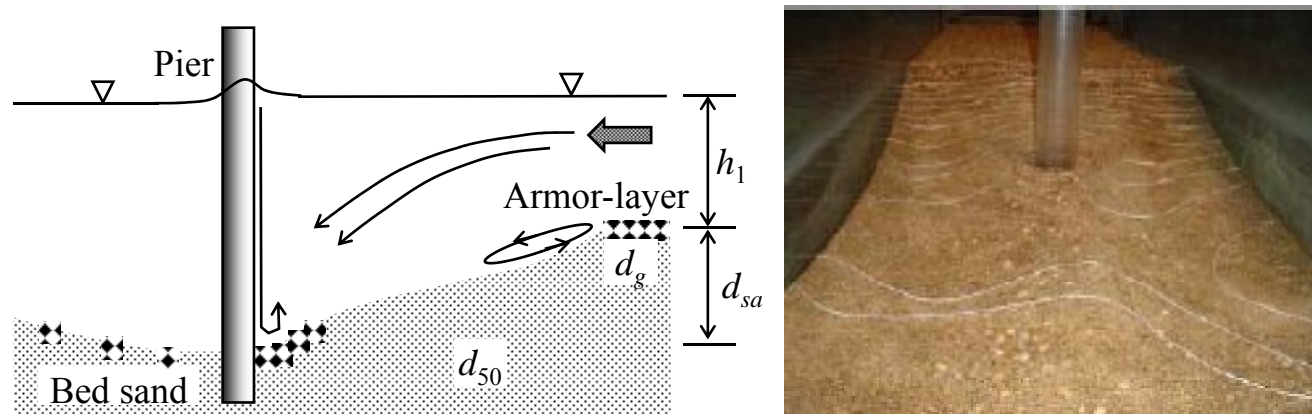


Fig. 6. 48(c) Schematic of scour holes at pier in armored beds: case 3

- In case 1, at the initial stage the scour took place through the armor-layer removing the bed-sands rapidly
- A compact secondary armor-layer having one-grain thickness of gravel, which covered the scour hole almost fully, was gradually developed within the scour hole
- This secondary armor-layer offers resistance towards the entrainment of bed-sands and inhibits the progress of further scour
- The original armor-layer remained unbroken around the perimeter of the scour hole
- This case prevailed for a small pier width and for smaller flow depths
- Small pier width was unable to induce strong downflow and horseshoe vortex in front of the pier to disintegrate and entrain the armor-gravels to downstream of the pier

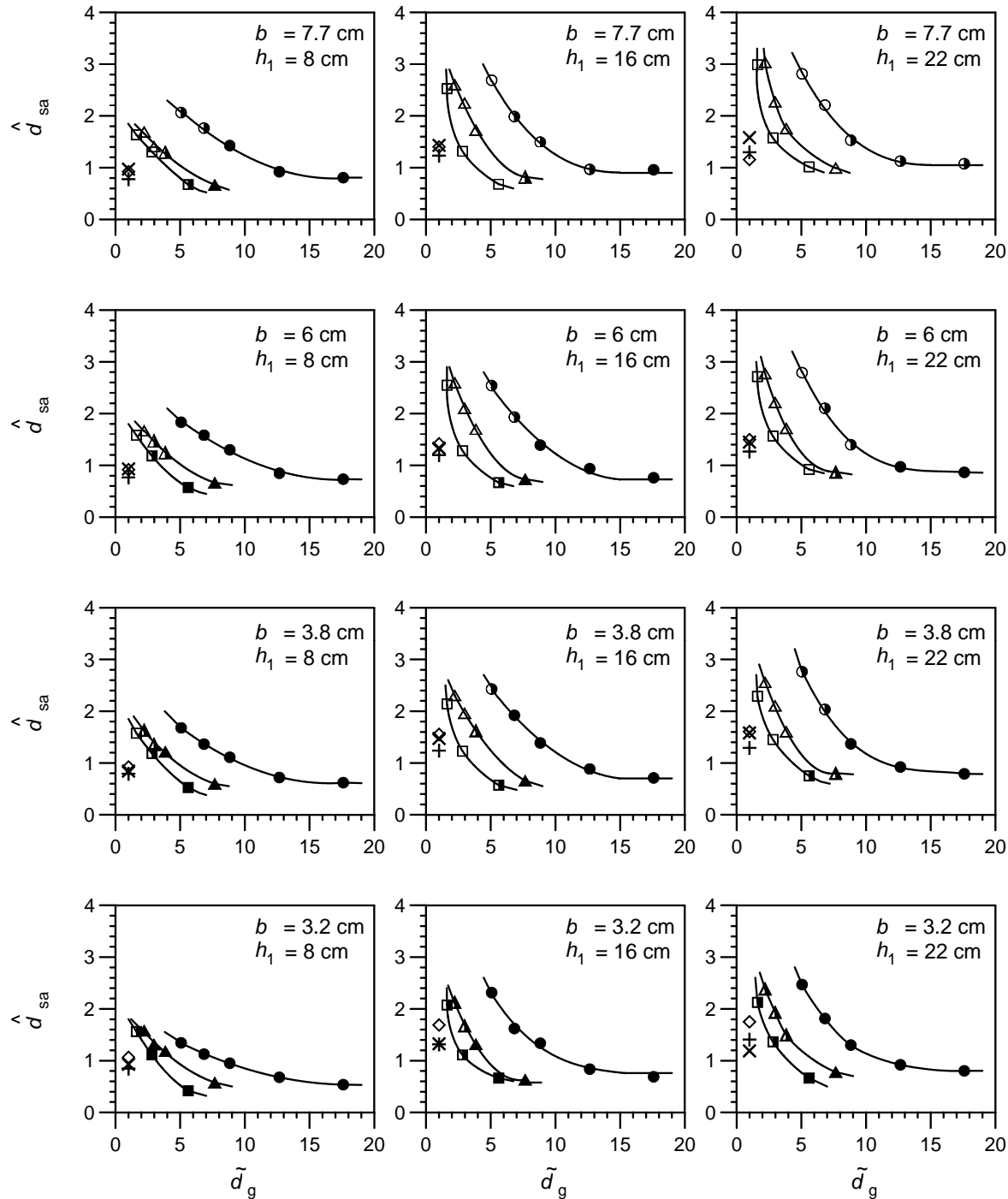
- In case 2, the scour hole in the vicinity of a pier formed through the armor-layer having an extension of scour hole in the upstream
- This was the stage when armor-layer started collapsing in the upstream by the joint action of the downflow and the horseshoe vortex
- The upstream portion of the scour hole shifted further upstream as a result of flow separation at the upstream edge of the scour hole forming a vortex flow
- The scour at the pier base took place due to the downflow along the upstream face of the pier
- In the upstream, the secondary armor-layer was rather loose in general; though adjacent to the pier it was well compact
- In the downstream, the original armor-layer disintegrated over a short distance without noticeable secondary armoring within the scour hole
- The original armor-layer remained intact around the upstream perimeter of the scour hole

- In case 3, when the scour hole was developed disintegrating the armor-layer up to some distance in the upstream and completely in the downstream
- The secondary armor-layer was mainly concentrated to the lower portion of the scour hole at the upstream base of the pier
- The scour hole extended over a considerable distance upstream, where the original armor-layer existed in the form of a large arc at the extremity of the scour hole
- Instead of a conical shaped scour hole, a streamwise curved shaped scour hole (almost two-dimensional, as an effect of flume side-walls) prevailed in this case
- In the field, the influence of the scour hole on that at neighboring piers may result in a curved shaped scour hole with an overlapping of scour holes at the pier sides

- At the far upstream of the scour hole, scour took place as if the sand-bed were scoured downstream of a rigid platform
- However, scour near pier occurred solely by the action of downflow along the upstream face of the pier
- A large pier width was capable to induce sufficiently strong downflow and horseshoe vortex to dislodge the armor-gravels to the pier downstream
- A relatively large flow depth helped to occur case 3
- Case 2 is the transition of case 1 and case 3

## Effect of Armor-Layer on Scour Depth

- The variations of nondimensional equilibrium scour depth  $\hat{d}_{sa}$  ( $= d_{sa}/b$ ) with  $\tilde{d}_g$  for different flow depths  $h_1$  and widths  $b$  of circular piers is shown in Fig. 6.49
- $\hat{d}_{sa}$  decreases with an increase in  $\tilde{d}_g$
- The decreasing rate of scour depth  $\hat{d}_{sa}$  is very rapid for  $\tilde{d}_g < 5, 7$  and 12 for bed-sands of  $d_{50} = 2.54$  mm, 1.86 mm and 0.81 mm, respectively
- The influence of  $\tilde{d}_g$  on  $\hat{d}_{sa}$  is less prominent for  $\tilde{d}_g > 5, 7$  and 12 in bed-sands of  $d_{50} = 2.54$  mm, 1.86 mm and 0.81 mm, respectively, due to the secondary armor-layer within the scour hole, which controls the development of scour hole
- $\hat{d}_{sa}$  decreases with an increase in bed-sand size  $d_{50}$  and with a decrease in upstream flow depth  $h_1$  and pier width  $b$



Case 1	Case 2	Case 3
		$d_{50}$ (mm)
●	◐	○ 0.81
▲	◑	△ 1.86
■	◒	□ 2.54

Uniform sand	
$d_{50}$ (mm)	
+	0.81
◇	1.86
X	2.54

Fig. 6.49 Variation of scour depth  $\hat{d}_{sa}$  with  $\tilde{d}_g$  for different  $h_1$  and  $b$  of circular piers under  $U_1/U_{ca} \approx 1$  (after Raikar 2006)

- For particular values of  $\tilde{d}_g$ ,  $d_{50}$  and  $h_1$ , the scour depth  $\hat{d}_{sa}$  increases with an increase in pier width  $b$
- For a given value of  $\tilde{d}_g$ , case of scour changes depending on flow depth  $h_1$  and pier width  $b$
- The data plots at  $\tilde{d}_g = 1$  corresponds to  $\hat{d}_{sa}$  in un-layered bed-sands
- Fig. 6.49 shows that the nondimensional scour depth  $\hat{d}_{sa}$  increases with a sequence of case 1, case 2 and case 3
- Greater nondimensional scour depths occur in cases 2 and 3 as there is no sediment supply from upstream
- When the armor-gravel size is marginally larger than the bed-sand size, larger scour depth is developed due to the bed-sand having a smaller  $U_c$  than  $U_{ca}$  of armor-gravels, resulting in case 3 of scour



- If the armor-gravel size is considerably larger than the bed-sand size (case 1), in the beginning of scour process, the secondary flow induced by the pier dislodges the armor-gravels in the form of a shear failure
- After a while, a secondary armor-layer within the scour hole develops and the secondary flow is then unable to entrain the secondary armor-gravels
- But the winnowing of bed-sands through the interstices of secondary armor-gravels increases the scour depth slightly
- The comparison of the scour depth reveals that in case 1, the scour depth in armored beds is lesser than that in un-layered beds, as the surface of the scour hole is shielded by the secondary armor gravels
- In contrast, in case 3, the scour depth in armored beds is greater than that in un-layered beds, since the secondary armor gravels are scattered within the scour hole

## Maximum Equilibrium Scour Depth

- It is recognized that case 2 and case 3 are the major threat of scour at piers in armored beds
- The equations of maximum equilibrium scour depth  $d_{sa}$  at a pier in an armored bed for case 2 and case 3, obtained using the experimental data of **Raikar** (2006), can be given by

$$\hat{d}_{sa} = 0.16K_s F_{ca}^{1.33} \tilde{b}^{1.14} \hat{h}^{0.52} \tilde{d}_g^{-0.93} \quad \text{for case 2} \quad (6.94a)$$

$$\hat{d}_{sa} = 0.14K_s F_{ca}^{0.78} \tilde{b}^{1.07} \hat{h}^{0.6} \tilde{d}_g^{-0.95} \quad \text{for case 3} \quad (6.94b)$$

where  $F_{ca} = U_{ca}/(\Delta gb)^{0.5}$ ;  $\tilde{b} = b/d_{50}$ ; and  $\hat{h} = h_1/b$

- The classification of the different cases of scour holes can be determined from Table 9

Table 9. Classification of Scour Holes in Armored Beds  
(after **Raikar** 2006)

$\beta$	Circular pier			Square pier		
	Case 1	Case 2	Case 3	Case 1	Case 2	Case 3
0.128	$\eta \geq 6.25$	$2.78 < \eta < 6.25$	$\eta \leq 2.78$	$\eta \geq 8.33$	$1.33 < \eta < 8.33$	$\eta \leq 3.33$
0.1	$\eta \geq 2.56$	$1.54 < \eta < 2.56$	$\eta \leq 1.54$	$\eta \geq 3.57$	$1.96 < \eta < 3.57$	$\eta \leq 1.96$
0.063	$\eta \geq 1.35$	$0.71 < \eta < 1.35$	$\eta \leq 0.71$	$\eta \geq 1.70$	$0.97 < \eta < 1.70$	$\eta \leq 0.97$
0.053	$\eta \geq 0.60$	$\eta < 0.60$		$\eta \geq 0.79$	$\eta < 0.79$	

Note:  $\beta = b/B$  and  $\eta = \tilde{d}_g / \hat{h}$

### Determination of Maximum Equilibrium Scour Depth:

- For the given values of pier width  $b$ , pier spacing  $B$ , armor-gravel size  $d_g$ , bed-sand size  $d_{50}$  and flow depth  $h_1$ , the appropriate case of scour hole can be determined from Table 9
- Using Eqs. (6.94a) and (6.94b) for the appropriate case, the maximum equilibrium scour depth  $d_{sa}$  can be evaluated

## ***Scour at Bridge Abutments in Armored Beds***

- **Dey and Barbhuiya** (2004b) studied the development of clear-water scour at short abutments ( $l/h_1 < 1$ ), namely vertical-wall, 45° wing-wall and semicircular, embedded in a bed of relatively fine uniform sediment overlain by an armor-layer of coarser sediment

### **Classification of Scour Hole and Scouring Process**

- Depending on the approaching flow conditions, three topography of scour holes are classified [Figs. 6.50(a) – 6.50(c)]

- Case 1: The scour hole at an abutment develops through the armor-layer in the upstream mainly. The scour hole does not extend beyond the downstream edge of the abutment. The armor-layer remains intact in the downstream of the abutment and around the upstream perimeter of the scour hole [Fig. 6.50(a)]

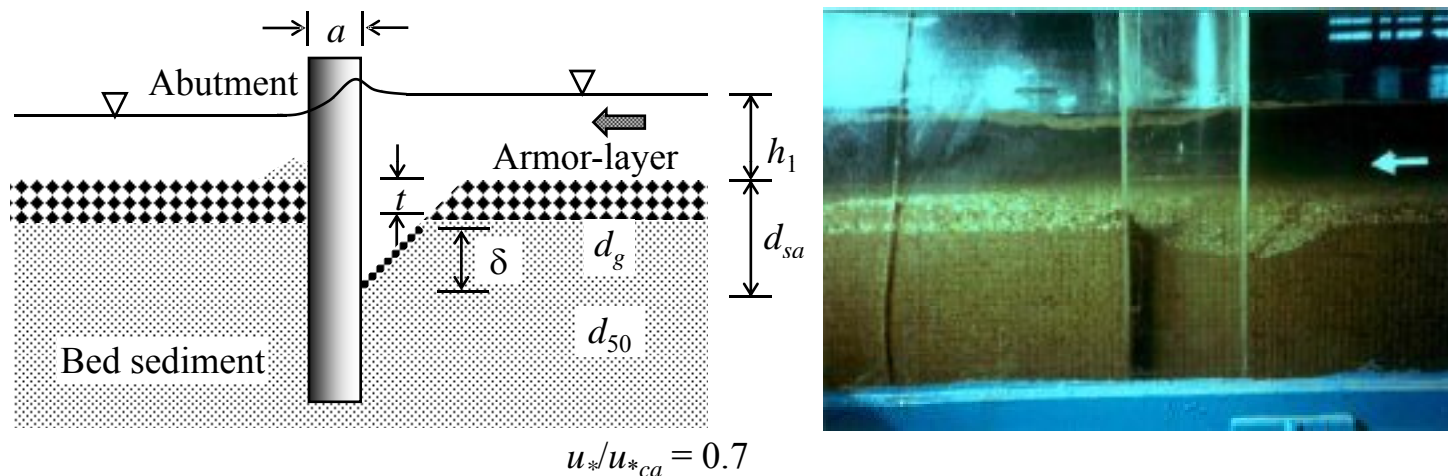


Fig. 6. 50(a) Schematic of scour holes at abutments in armored beds: case 1 (after **Dey and Barbhuiya 2004b**)

- Case 2: The scour hole at an abutment forms through the armor-layer in the upstream and downstream. The armor-layer remains intact in the downstream of the scour hole and around the upstream perimeter of the scour hole [Fig. 6.50(b)]

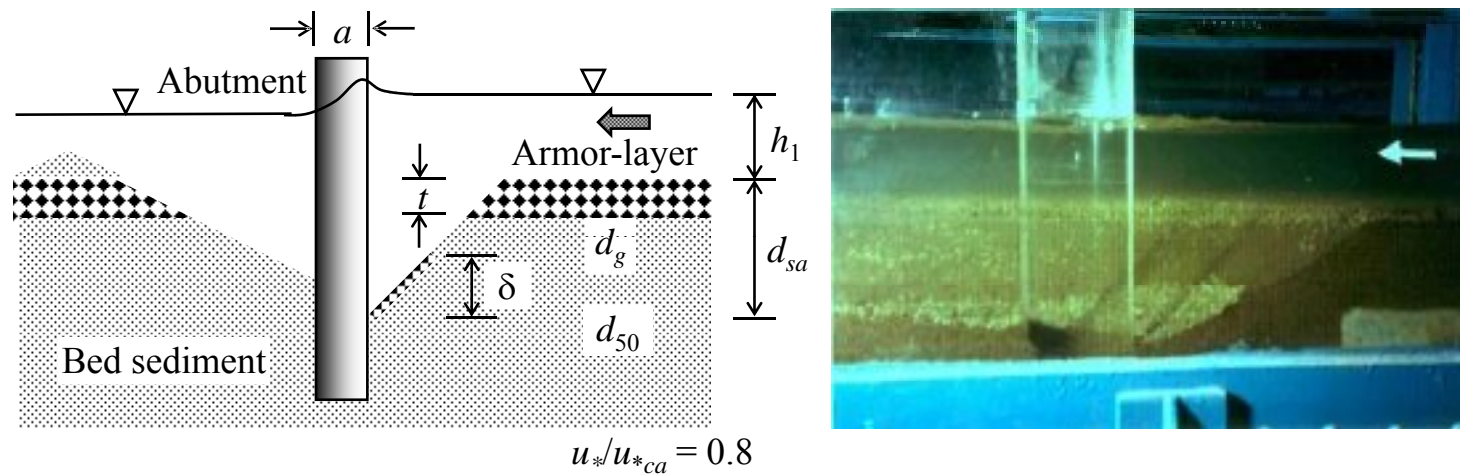


Fig. 6. 50(b) Schematic of scour holes at abutments in armored beds: case 2 (after **Dey and Barbhuiya 2004b**)

- Case 3: The armor-layer disintegrates over a long distance downstream but remains intact around the upstream perimeter of the scour hole [Fig. 6.50(c)]

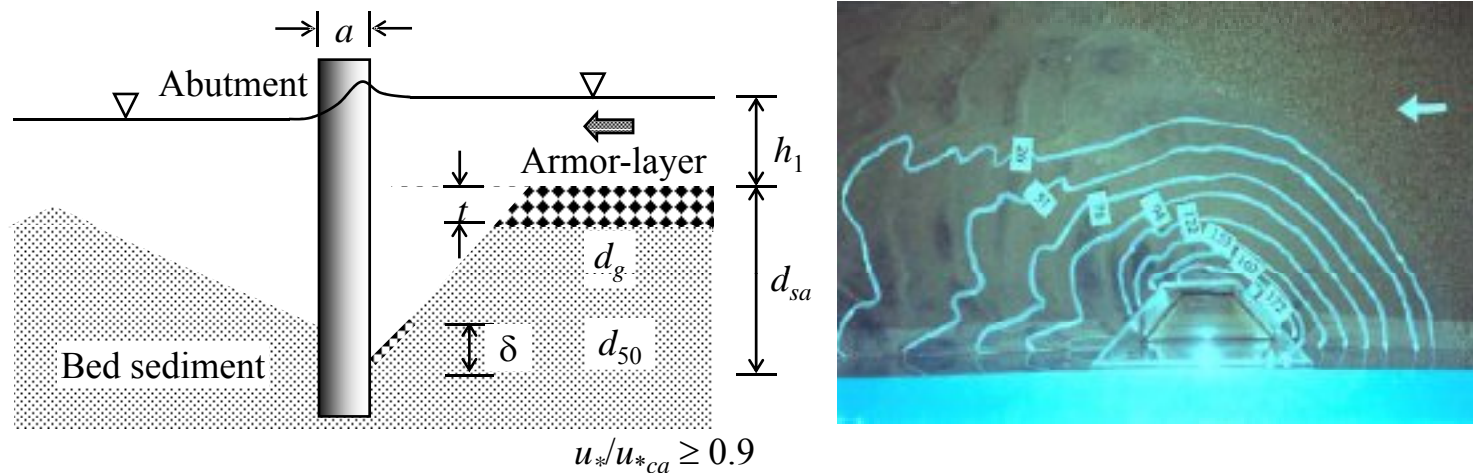


Fig. 6. 50(c) Schematic of scour holes at abutments in armored beds: case 3 (after **Dey and Barbhuiya 2004b**)



- Case 1 was observed for the approaching flow condition  $u_*/u_{*ca} = 0.7$
- For  $d_g > 2$  mm, a secondary armor-layer, which covered the scour hole either fully or partially, developed offering resistance towards the entrainment of bed sediment and restricting the progress of further scouring to a great extent
- No significant secondary armor-layer was found for  $d_g < 2$  mm
- With an increase in magnitude of approaching flow velocity, the scour hole extended beyond the downstream edge of abutments without disintegrating armor-layer in the downstream of the scour hole

- Case 2 prevailed for the approaching flow condition  $u_*/u_{*ca} = 0.8$
- For  $d_g > 2$  mm, a secondary armor-layer, which covered almost half portion of the scour hole, developed posing relatively less resistance to the progress of scouring
- When the approaching flow condition became close to the critical condition of the armor-layer particles, that is  $u_*/u_{*ca} \geq 0.9$ , case 3 was observed with completely disintegrating armor-layer in the downstream of the scour hole
- The secondary armor-layer, for  $d_g > 2$  mm, was mainly concentrated to the lower portion of the scour hole near the upstream base of abutments

## Effect of Armor-Layer on Scour Depth

- Fig. 6.51 depicts the variations of scour depth  $\hat{d}_{sa}$  ( $= d_{sa}/l$ ) at 45° wing-wall abutments with  $\tilde{d}_g$  for different  $\hat{h}$  ( $= h_1/l$ ),  $u_*/u_{*ca}$ , and  $\hat{t}$  ( $= t/d_g$ ; where  $t$  = thickness of armor-layer)
- In Fig. 6.51, two points are plotted in some plots for the same value of  $\tilde{d}_g$  due to different  $\hat{t}$  resulting in different values of  $\hat{d}_{sa}$
- The scour depth  $\hat{d}_{sa}$  for  $\hat{t} < 2$  (shown by the broken line curves) is greater than that for  $\hat{t} > 2$  (shown by the firm line curves)
- Because more sediment particles are supplied by a relatively thick armor-layer into the scour hole to form a secondary-armor layer resulting in a lesser scour depth for the same value of  $\tilde{d}_g$
- The scour depth  $\hat{d}_{sa}$  decreases with an increase in  $\tilde{d}_g$  up to  $\tilde{d}_g = 4-5$ , and then  $\hat{d}_{sa}$  increases with further increase in  $\tilde{d}_g$  to form a second peak of the curve at  $\tilde{d}_g = 6-7$

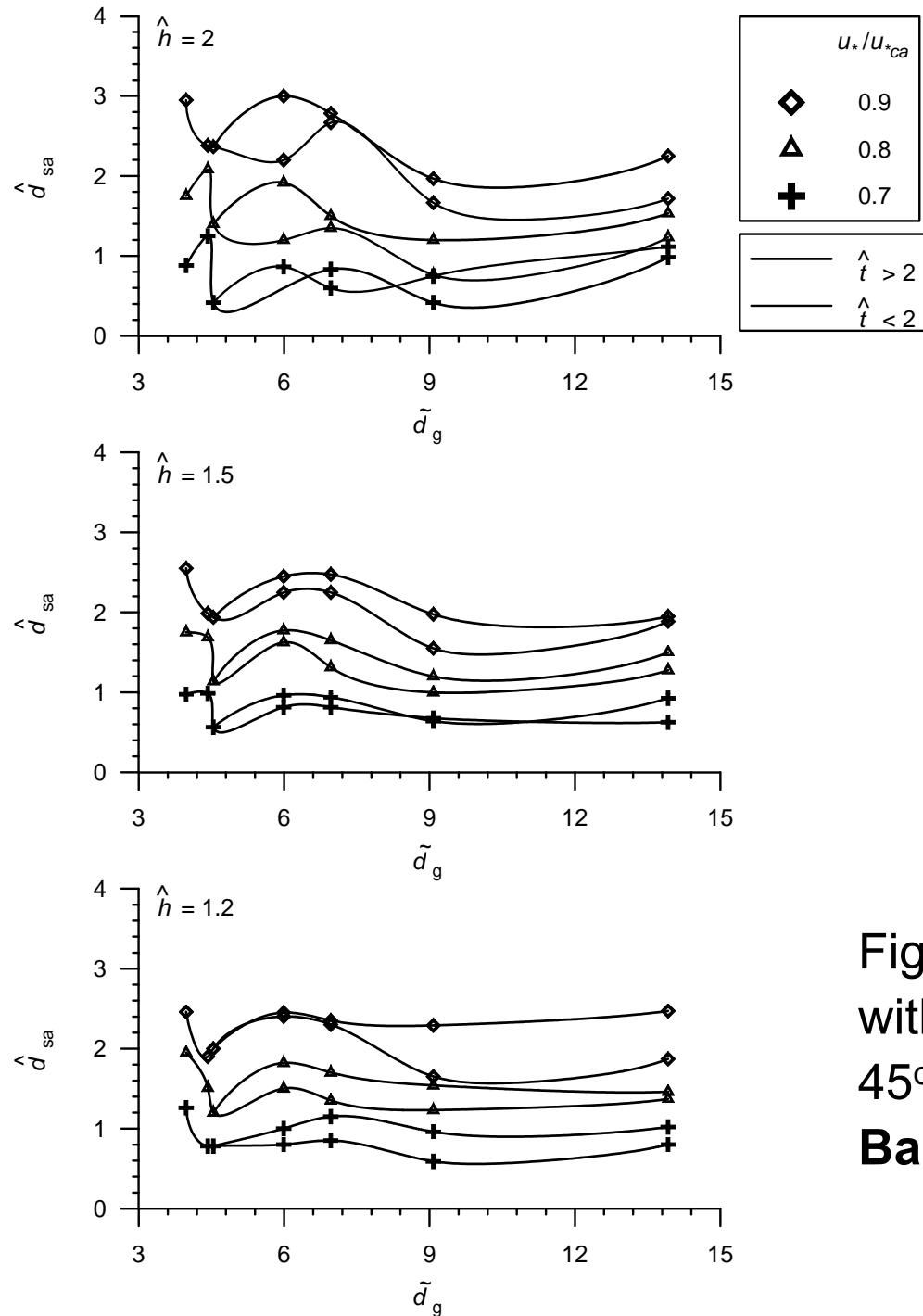


Fig. 6.51 Variations of scour depth  $\hat{d}_{sa}$  with  $\tilde{d}_g$  for different  $\hat{h}$ ,  $\hat{t}$ , and  $u_*/u_{*ca}$  for 45° wing-wall abutments (after **Dey and Barbhuiya 2004b**)

- Thereafter,  $\hat{d}_{sa}$  again decreases up to  $\tilde{d}_g = 9$ , and then  $\hat{d}_{sa}$  gradually increases at a feeble rate
- In general, scour depths  $\hat{d}_{sa}$  for  $\tilde{d}_g > 9$  (ripple forming sediments) are less than that for  $\tilde{d}_g < 9$
- This confirms that the clear-water scour depth in ripple forming sediments is less than that in non-ripple forming sediments [**Ettema** (1980), and **Raudkivi and Ettema** (1983, 1985)]
- The formation of secondary armor-layer resists the rate of increase of  $\hat{d}_{sa}$  with an increase in  $\tilde{d}_g$  for  $\tilde{d}_g > 9$
- The increase in scour depth  $\hat{d}_{sa}$  with an increase in  $\hat{h}$  and  $u_*/u_{*ca}$  is observed
- The scour depth in armored beds is significantly greater than that in uniform sediments

## Maximum Equilibrium Scour Depth

- The equations for maximum equilibrium scour depths for different abutments obtained by regression analysis of the experimental data of **Dey and Barbhuiya (2004b)** are

$$\hat{d}_{sam} = 4.42 F_{ca}^{0.266} \hat{h}^{0.195} \hat{t}^{-0.147} \hat{d}_g^{-0.117} \quad \text{for vertical-wall} \quad (6.95a)$$

$$\hat{d}_{sam} = 5.28 F_{ca}^{0.266} \hat{h}^{0.207} \hat{t}^{-0.306} \hat{d}_g^{-0.211} \quad \text{for } 45^\circ \text{ wing-wall} \quad (6.95b)$$

$$\hat{d}_{sam} = 3.582 F_{ca}^{0.185} \hat{h}^{0.165} \hat{t}^{-0.151} \hat{d}_g^{-0.135} \quad \text{for semicircular} \quad (6.95c)$$

where  $\hat{d}_{sam} = d_{sam}/l$ ; and  $F_{ca} = U_{ca}/(\Delta g l)^{0.5}$ , that is the critical abutment Froude number

**Thank You**